Plasma accelerator applications II: photon science, medical

Olle Lundh

Department of Physics, Lund University, Sweden

Bad Honnef Physics School on Plasma Acceleration

5-10 February 2023

LUND UNIVERSITY

LLC

LUND LASER CENTRE

WALLENBERG ACADEMY FELLOWS

Development of particle acceleration

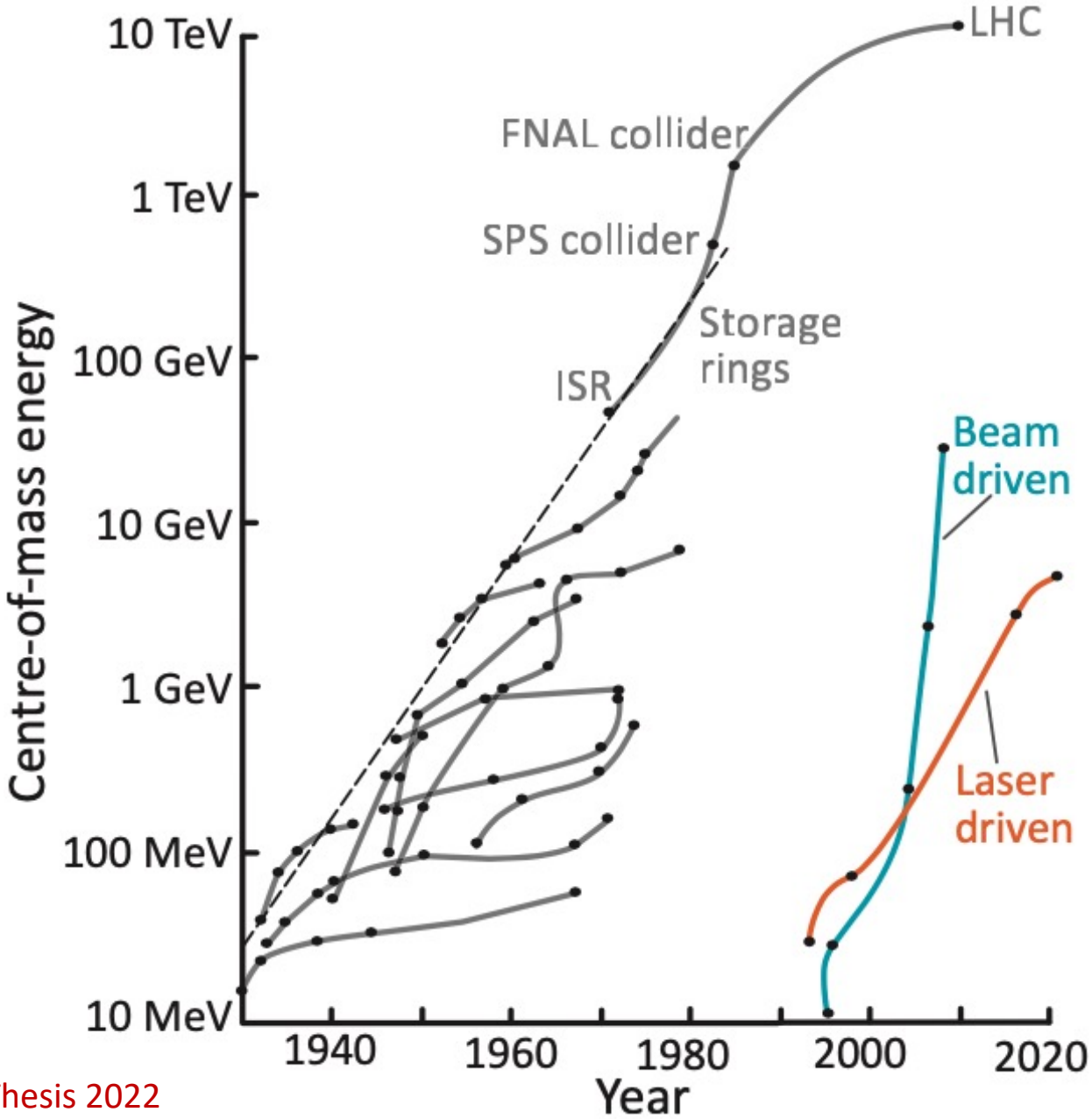

K Svendsen, PhD Thesis 2022

Why particle accelerators matter

Discovery Science

Particle accelerators are essential tools of discovery for particle and nuclear physics and for sciences that use x-rays and neutrons.

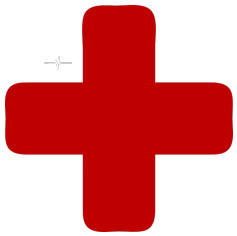

Medicine

Tens of millions of patients receive accelerator-based diagnoses and therapy each year in hospitals and clinics around the world.

Industry

Worldwide, hundreds of industrial processes use particle accelerators – from the manufacturing of computer chips to the cross-linking of plastic for shrink wrap and beyond.

Security

Particle accelerators play an important role in ensuring security, including cargo inspection and materials characterization.

Laser-plasma acceleration and X-ray generation

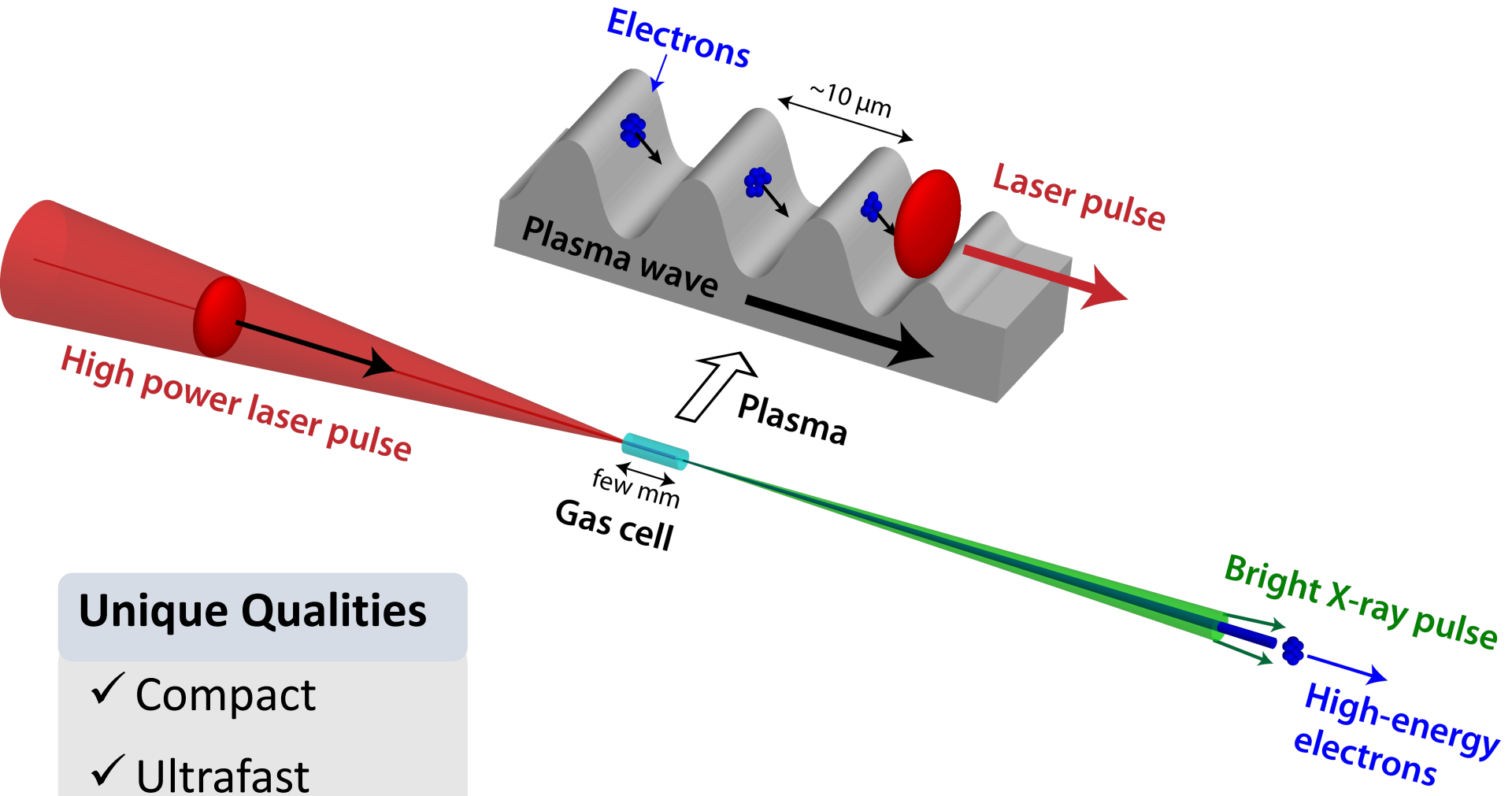

Unique Qualities

- ✓ Compact
- ✓ Ultrafast
- ✓ Tunable

O Lundh *et al*, Nature Physics **7**, 219–222 (2011)
J B Svensson *et al*, Nature Physics **17**, 639–645 (2021)

Outline

Laser-accelerated electron beams for radiotherapy

Betatron X-rays for imaging and spectroscopy

Other light sources based on plasma accelerators

Number of deaths in 2020, both sexes, all ages

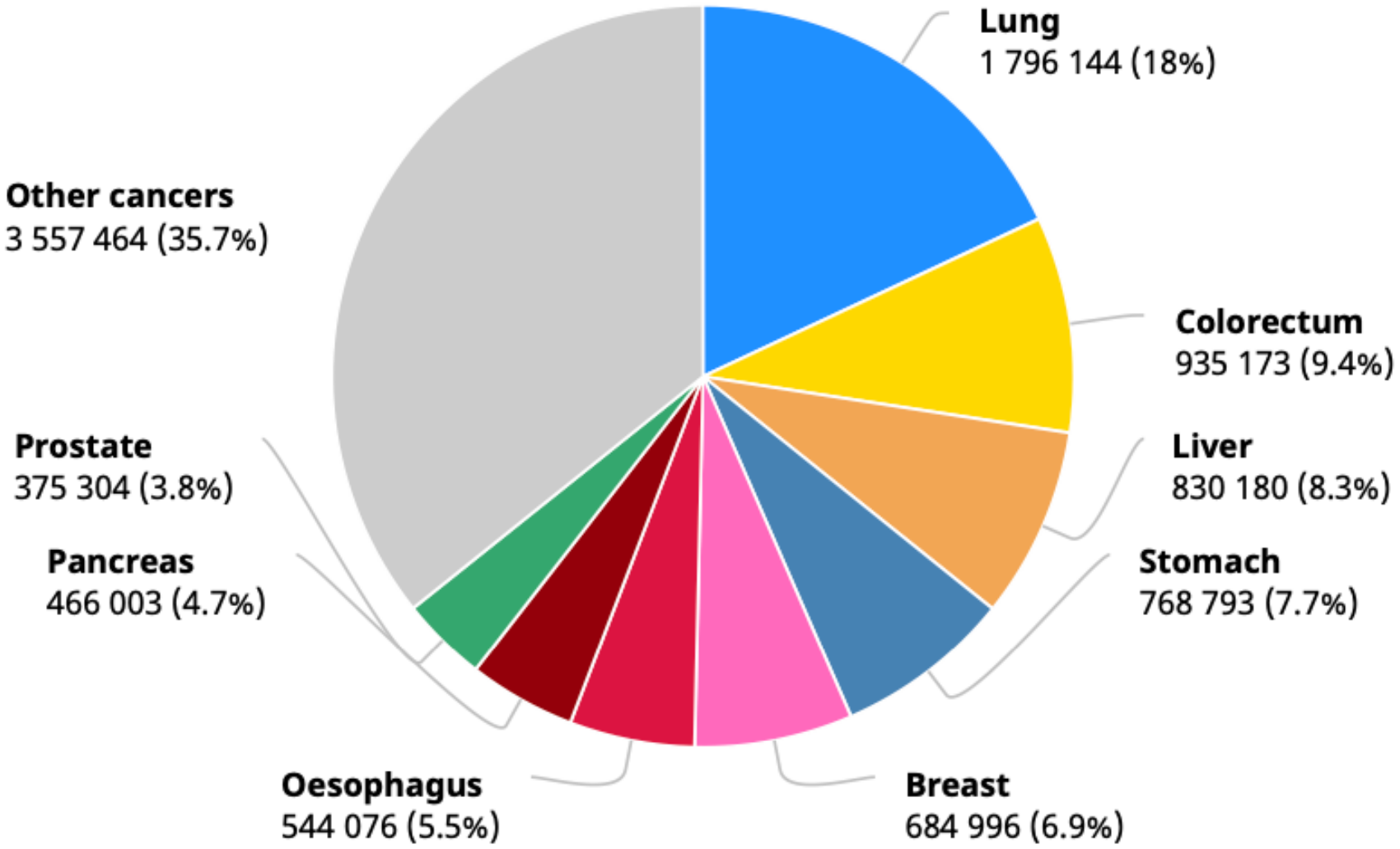

Total: 9 958 133 deaths

Number of radiotherapy machines per million citizens

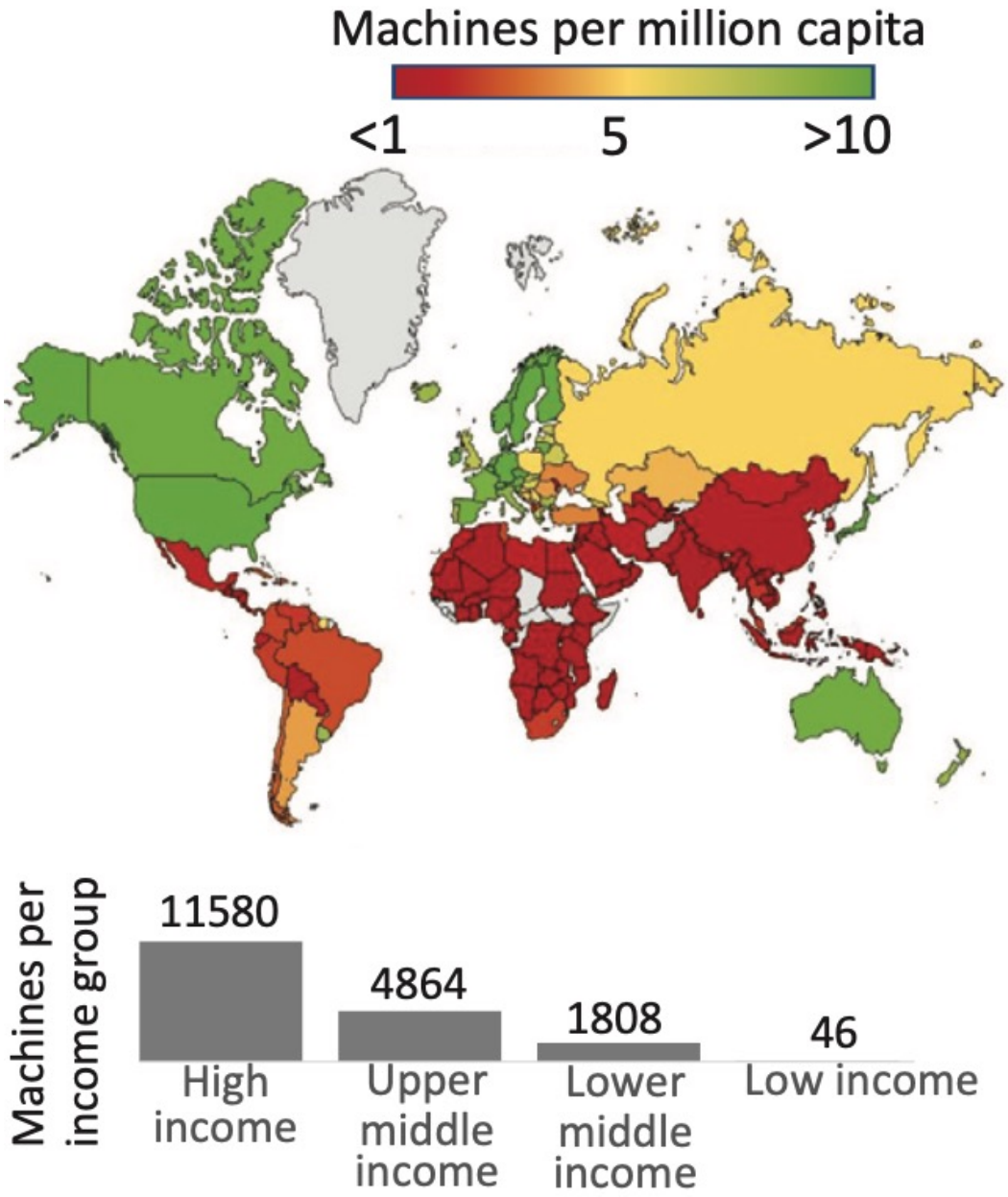

External beam radiotherapy

Clinical oncology machine

- 5-20 MeV electron beam
- X-rays by bremsstrahlung

Direct electron irradiation

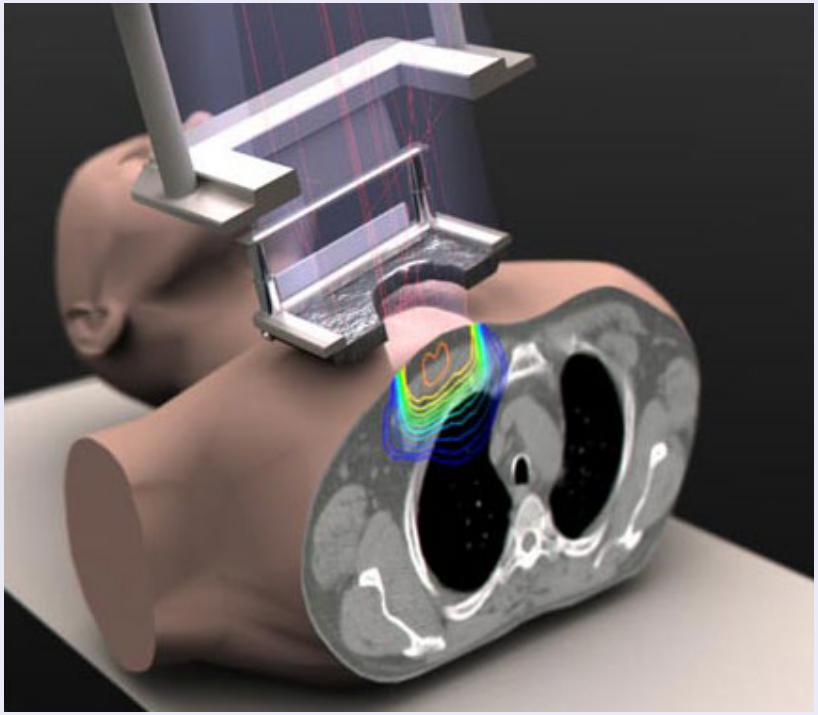

- Electrons have limited range
- Underlying structures spared

Stopping power and dose

Low energy electrons primarily lose energy through **collisions** which leads to **ionization** and **excitation**. Contributes to the dose **near the track**.

High-energy electrons primarily lose energy by **radiation** (**bremsstrahlung).** Energy spent is **carried away** from the track by photons.

The stopping power is the mean rate of energy loss $S(x) = -\frac{dE}{dx}$

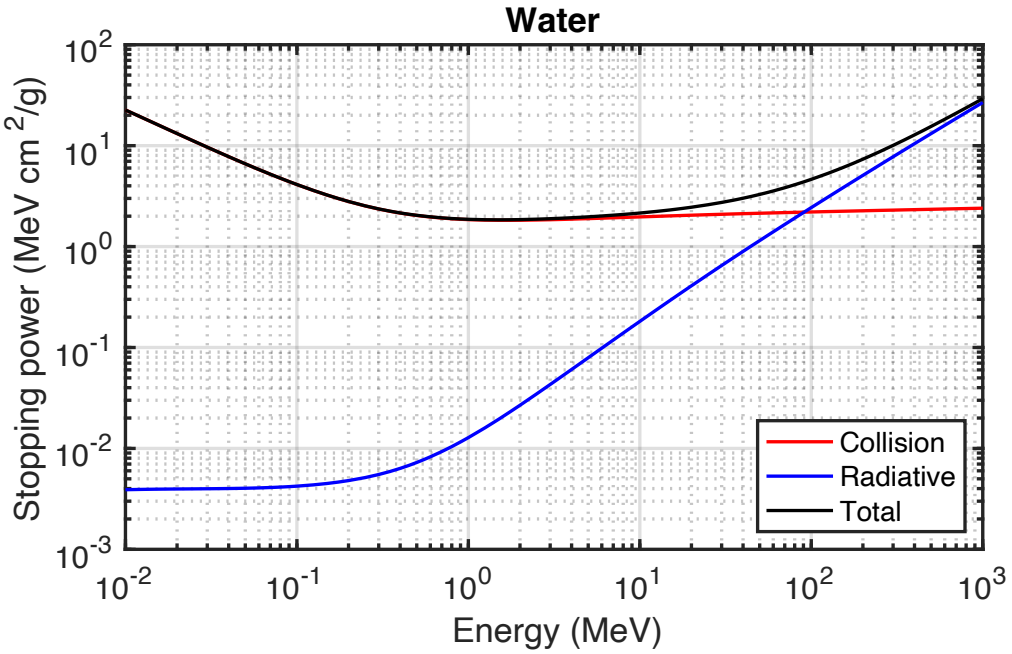

The locally deposited dose is

$$D(x) = \Phi \frac{S_{col}(x)}{\rho}$$

where Φ is the particle flux density

The databases ESTAR, PSTAR, and ASTAR calculate stopping-power and range tables for electrons, protons, or helium ions for many different materials: https://www.nist.gov/pml/stopping-power-range-tables-electrons-protons-and-helium-ions

Multiple scattering

Multiple collisions and radiative interactions lead to

1. Secondary low-energy particles
2. Multiple scattering

of the primary particles. Multiple scattering leads to an increased beam divergence and a wider dose distribution

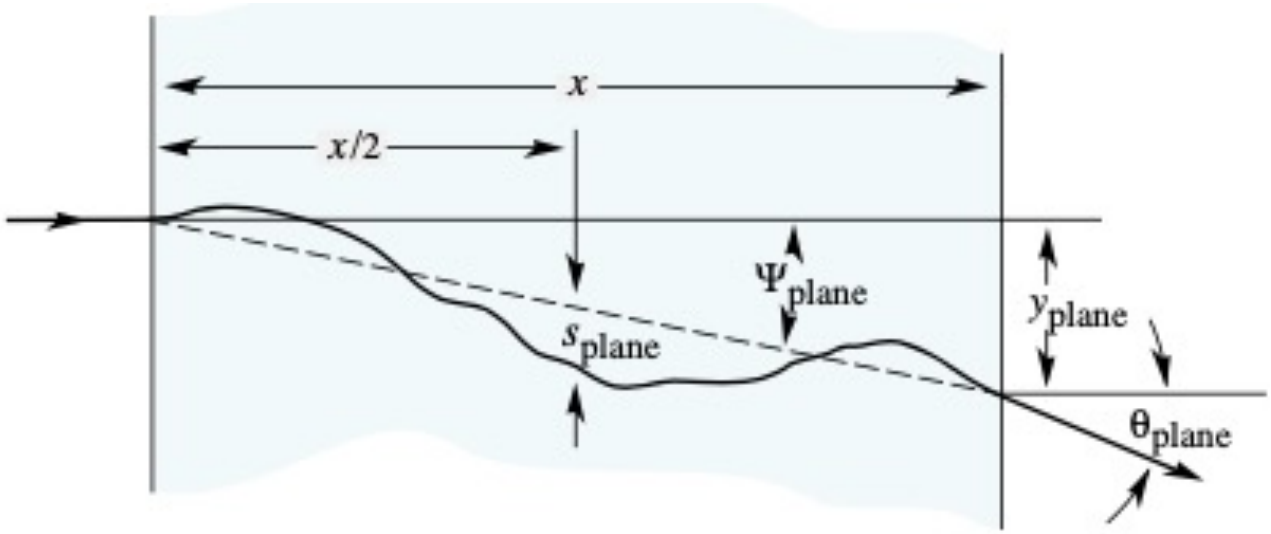

Monte-Carlo simulations

Simulates the passage of particles through matter invoking relevant physics

Particles and interaction physics are modelled using probability distributions

Used in radiotherapy and dosimetry to model the interactions between radiation and human tissue, and to predict the distribution of radiation dose within the patient's body.

Examples of codes

- PENELOPE (Physically-Based Simulation of Electron and Photon Transport)
- GEANT4 (Simulation toolkit for particle physics)
- MCNP (Monte Carlo N-Particle)
- FLUKA (Fluctuation and Transport of High Energy Particles in Matter).

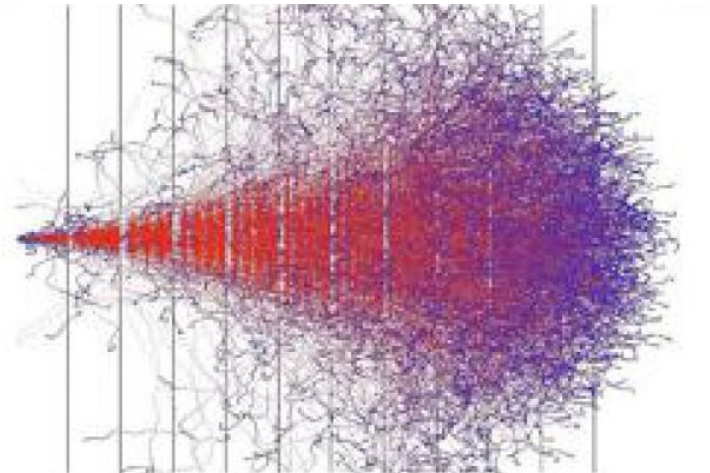

Dose deposition for different particles

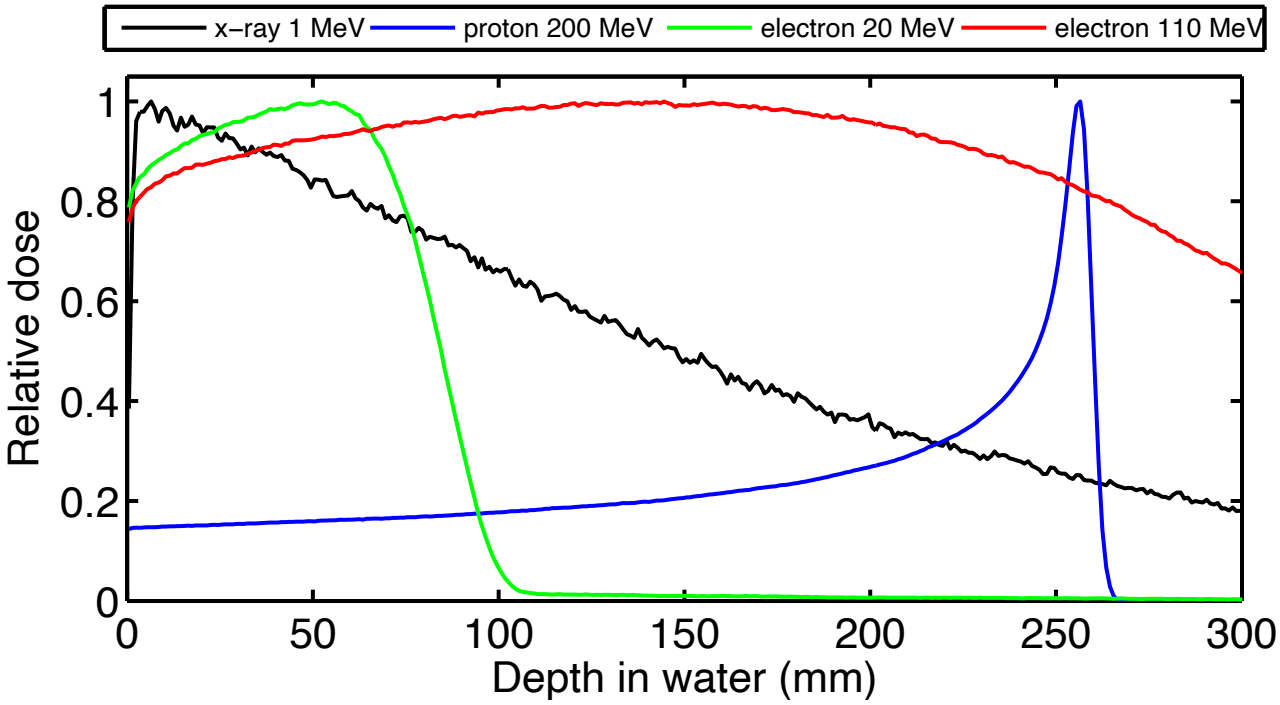

Low energy electrons < 20 MeV widely used for superficial tumours

High energy electrons > 100 MeV not yet available in hospitals

Can high-energy electrons be useful for radiotherapy?

Potential advantage of high energy electrons

Schüler *et al*, Med. Phys. **44**, 2544-2555 (2017)

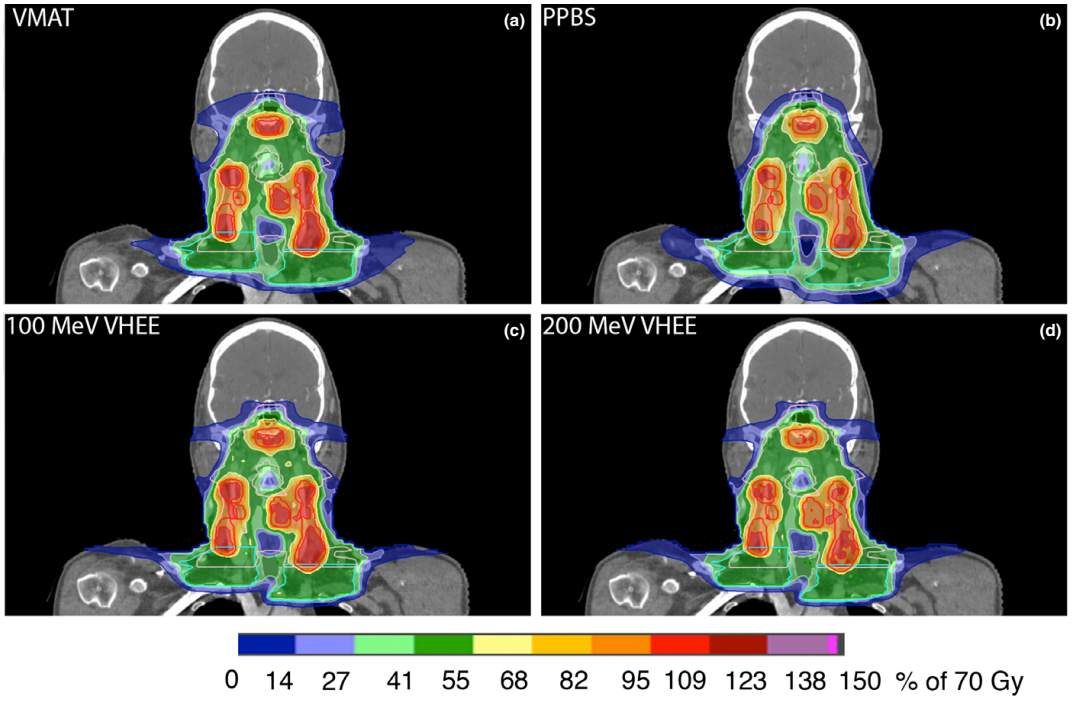

VHEE Very High Energy Electrons

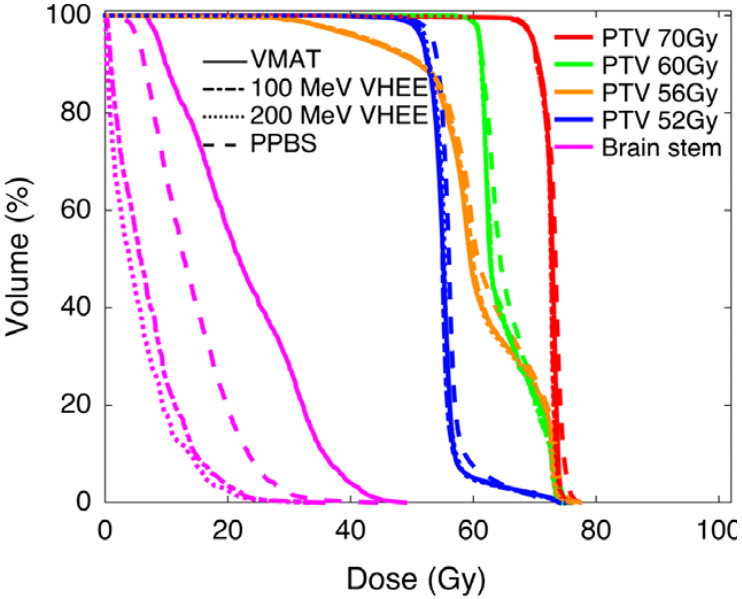

Compared to X rays (IMRT, VMAT), high-energy electrons (100-200 MeV) can give

- Similar coverage of the target volume
- Better sparing of critical structures and organs at risk

Can plasma accelerators provide such beams?

Isodose curves for laser-accelerated electrons

Monte-Carlo simulation study in GEANT4
Dose deposition by 170 MeV electrons

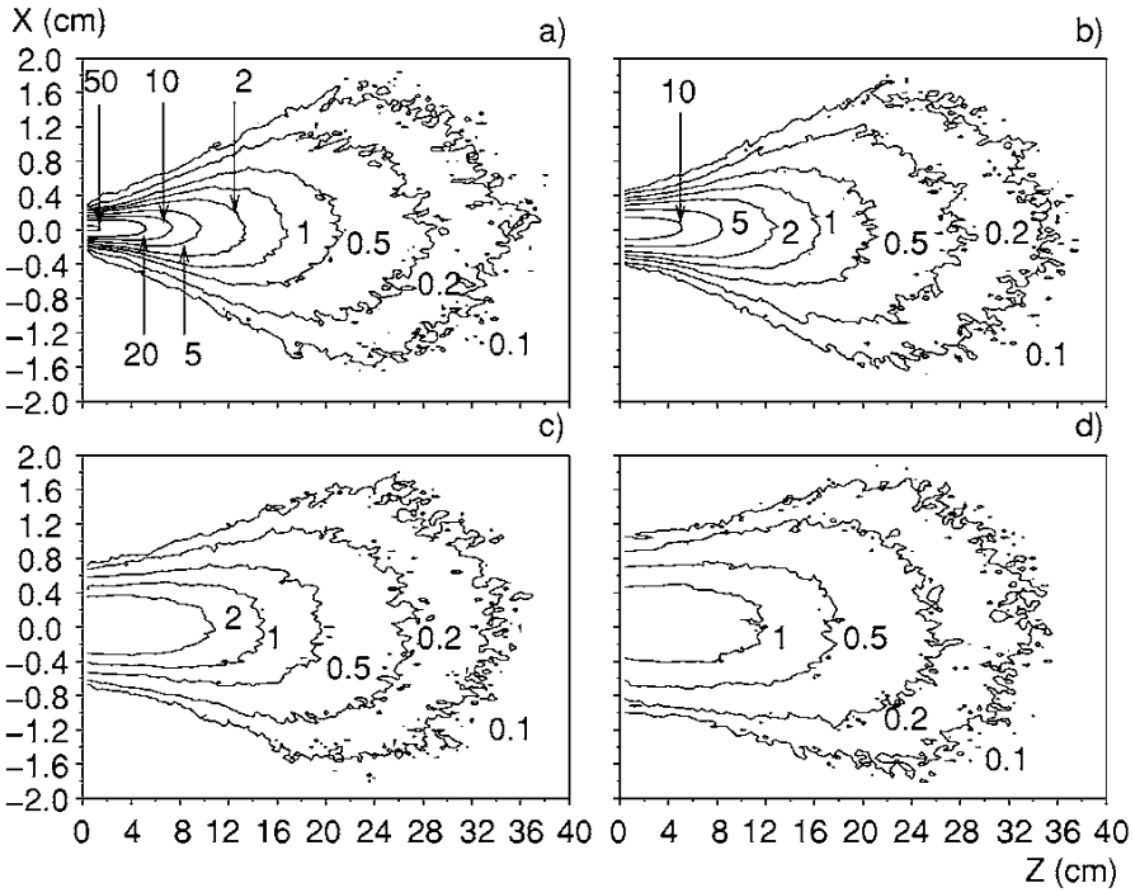

[Gy/nC]

Y. Glinec *et al.,* Med. Phys. **33**, 155-162 (2006)

Experimental setup

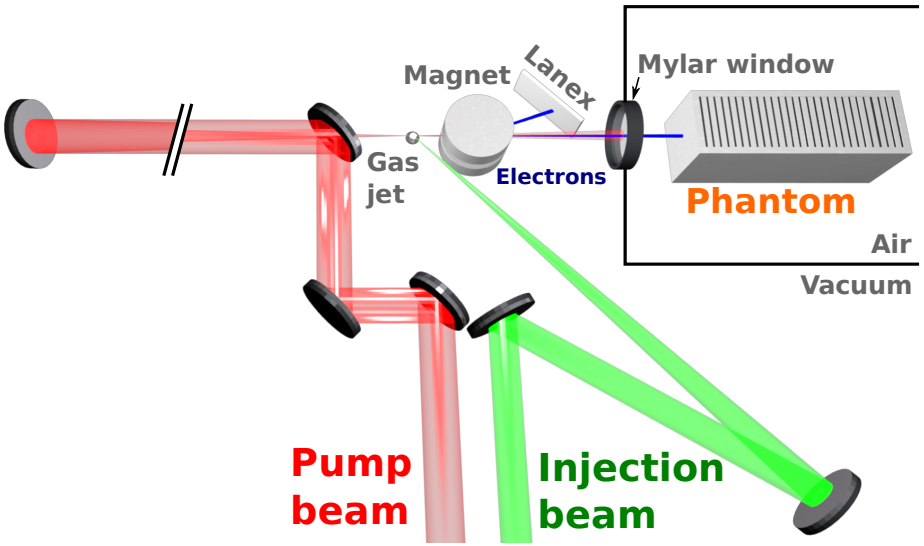

Electron beam: 120 MeV; 30 pC

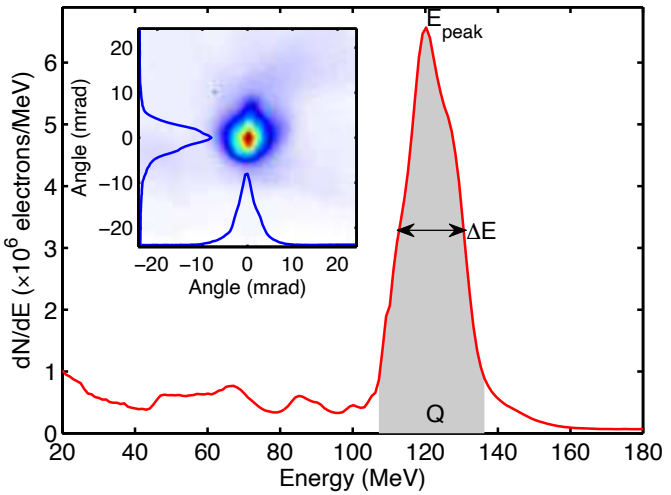

Blocks of polystyrene (10 mm) + Fuji film detectors (40x40 mm²)

loa

Lundh *et al*, Medical Phys. 39, 3501-3508 (2012)

Measured dose profiles

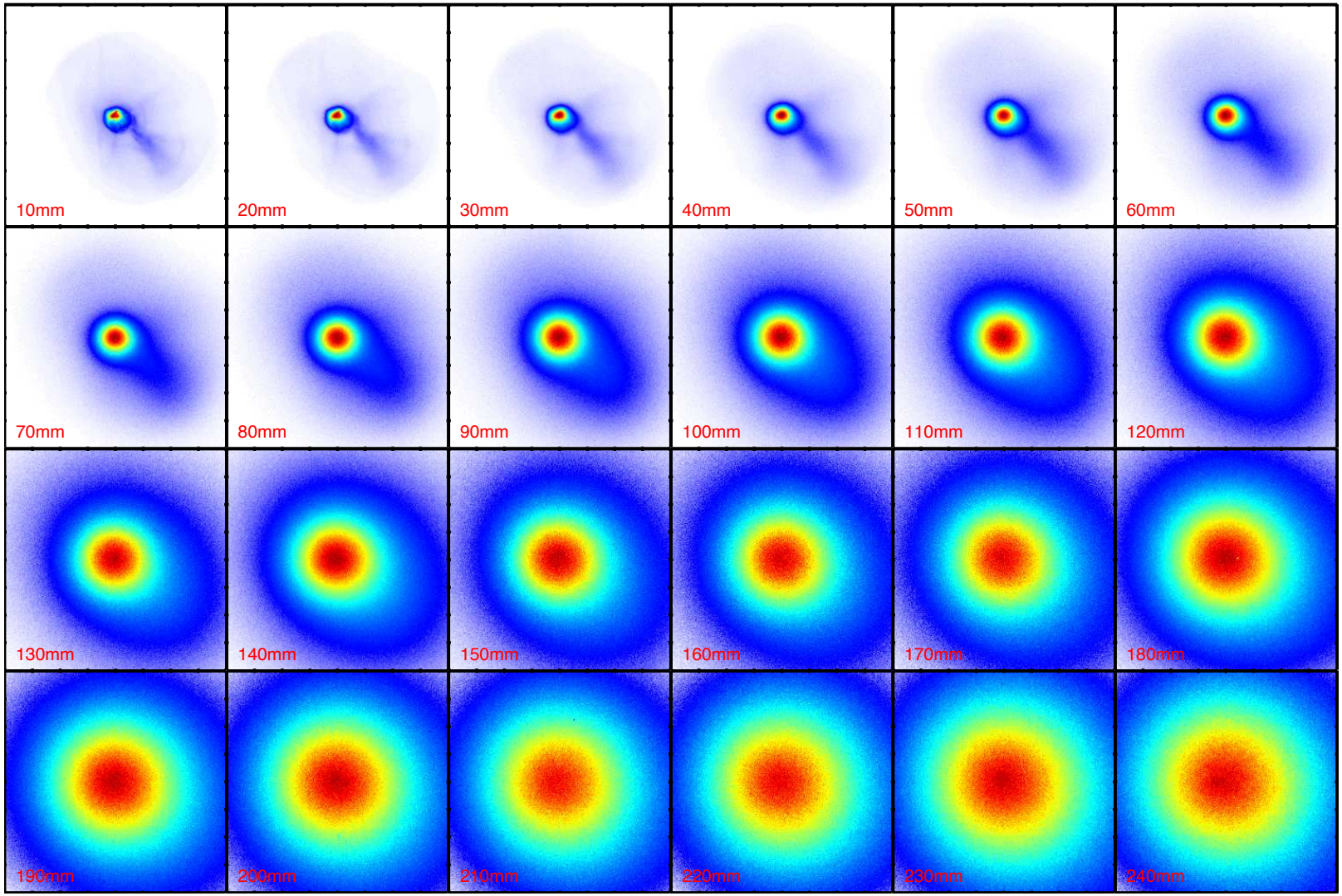

Lundh *et al*, Medical Phys. 39, 3501-3508 (2012)

Comparison to simulation

Experiment

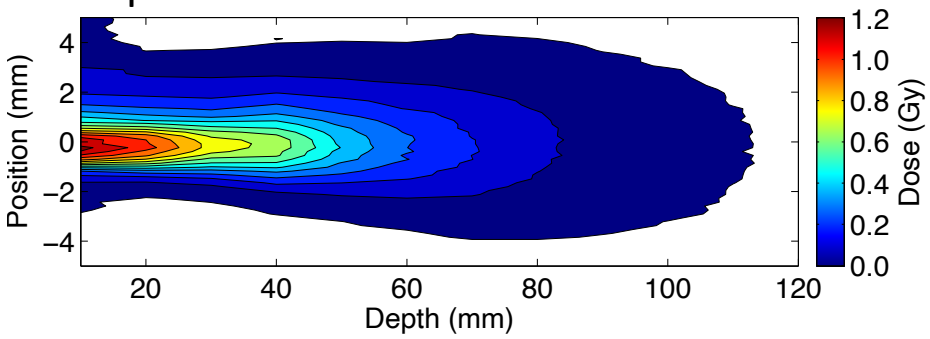

Simulation (Geant4)

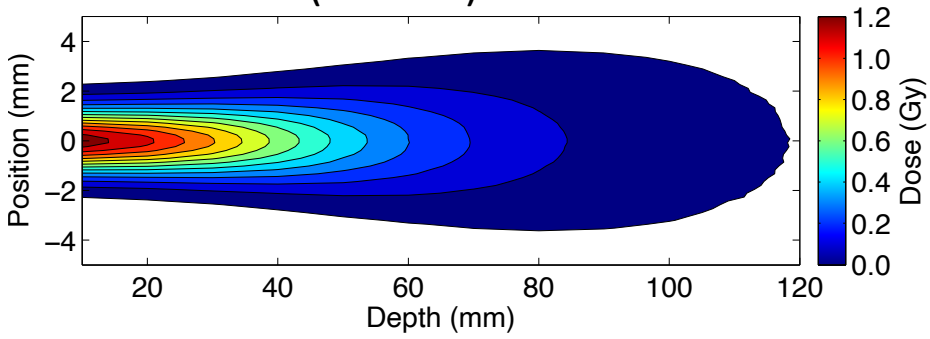

Beam size

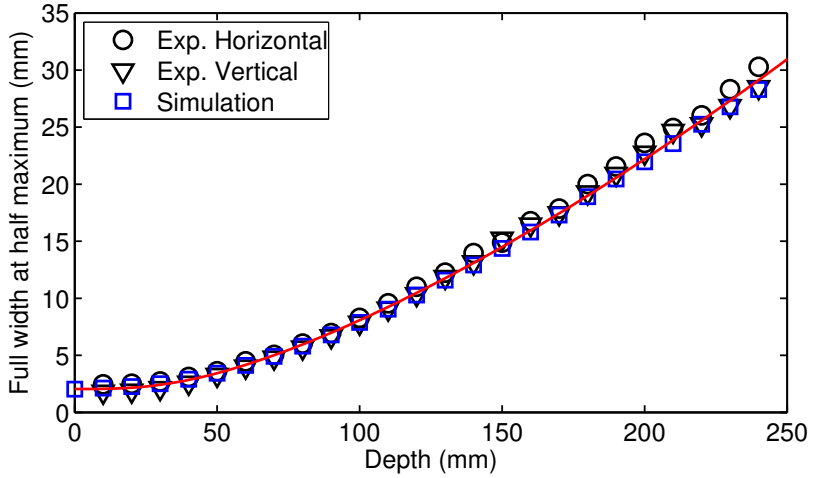

Peak dose

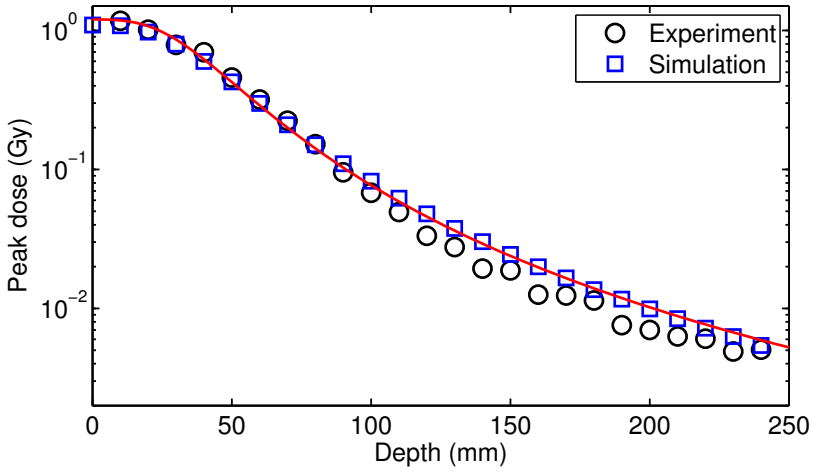

Lundh *et al*, Medical Phys. 39, 3501-3508 (2012)

Laser-accelerated VHEE's for radiotherapy?

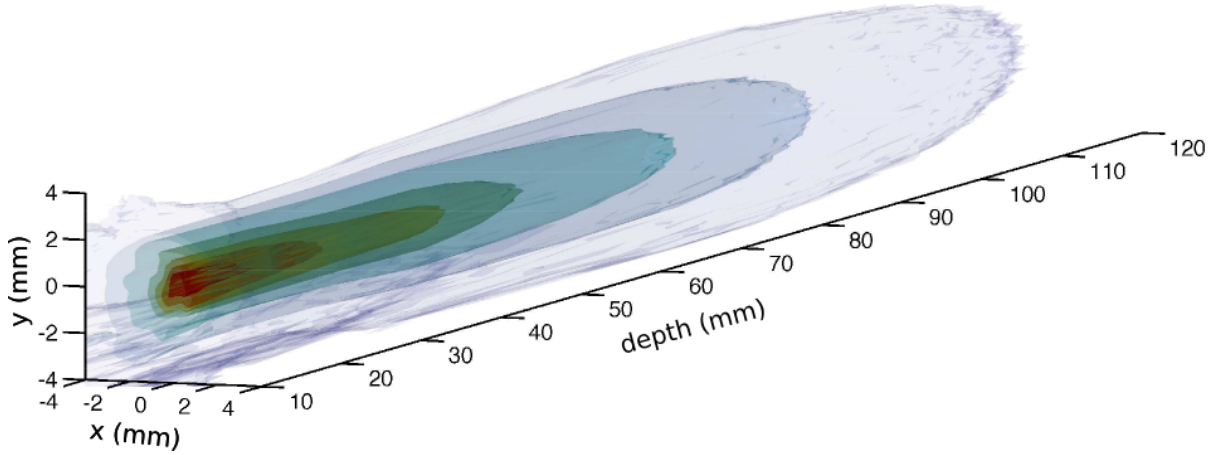

Treatment plan

Total treatment dosage: 20-80 Gy

Fractional daily dosage: 2 Gy/day

Laser-plasma beam

1 Gy/shot over 2x2 mm^2

200 shots (20 s): 2 Gy over 20x20 mm^2

Reasonable numbers

Broad irradiation field

Lateral scattering is mitigated when using a broad irradiation field

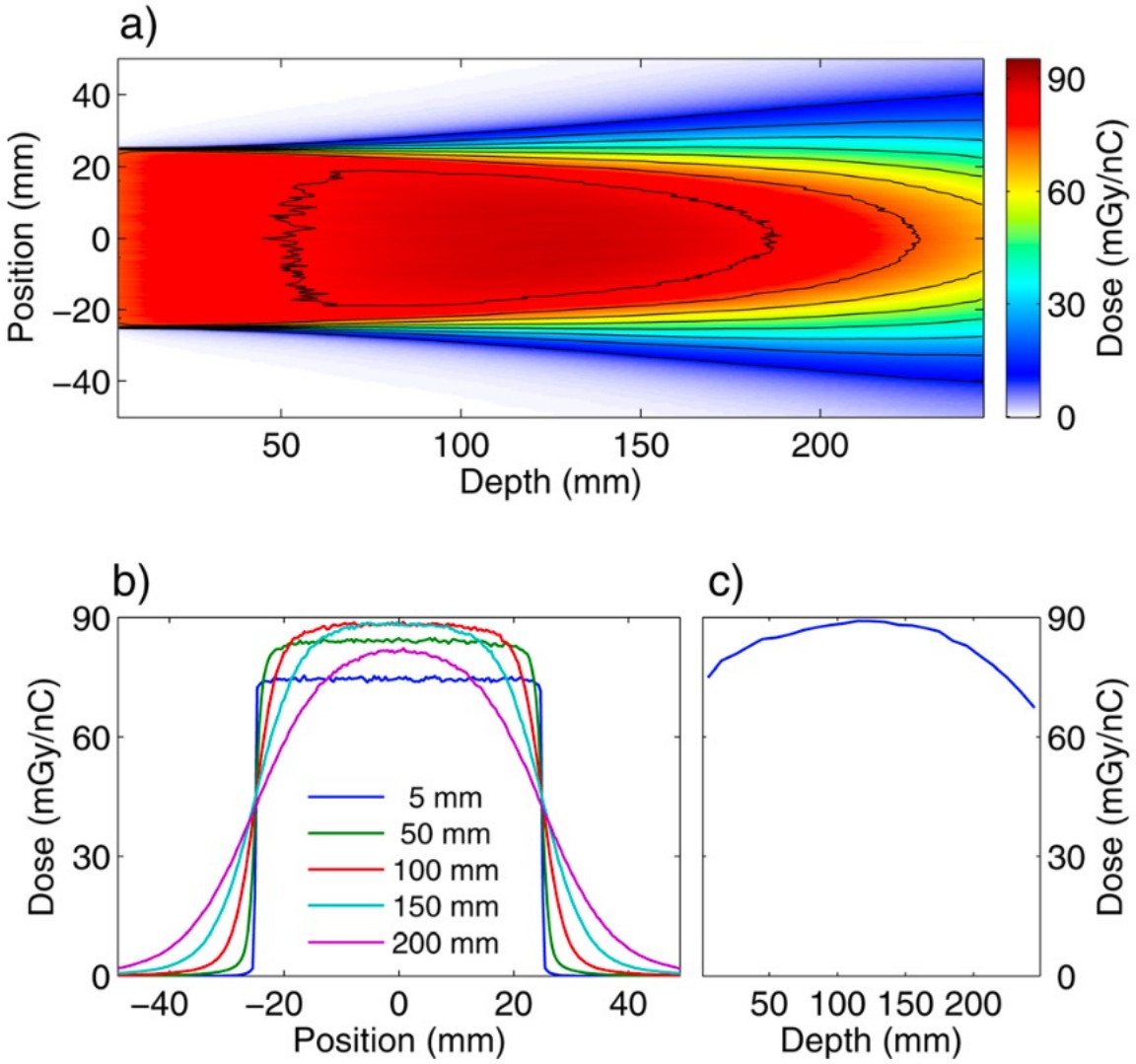

Simulation in GEANT4

Impact of inhomogeneities

- Inhomogeneities (air bubbles, bone, etc.) can negatively impact the dose delivered compared to the dose plan.
- This simulation study shows that the dose deposition by high-energy electrons is less sensitive to inhomogeneities when compared to protons and x-rays. This effect is also confirmed by dose measurements.

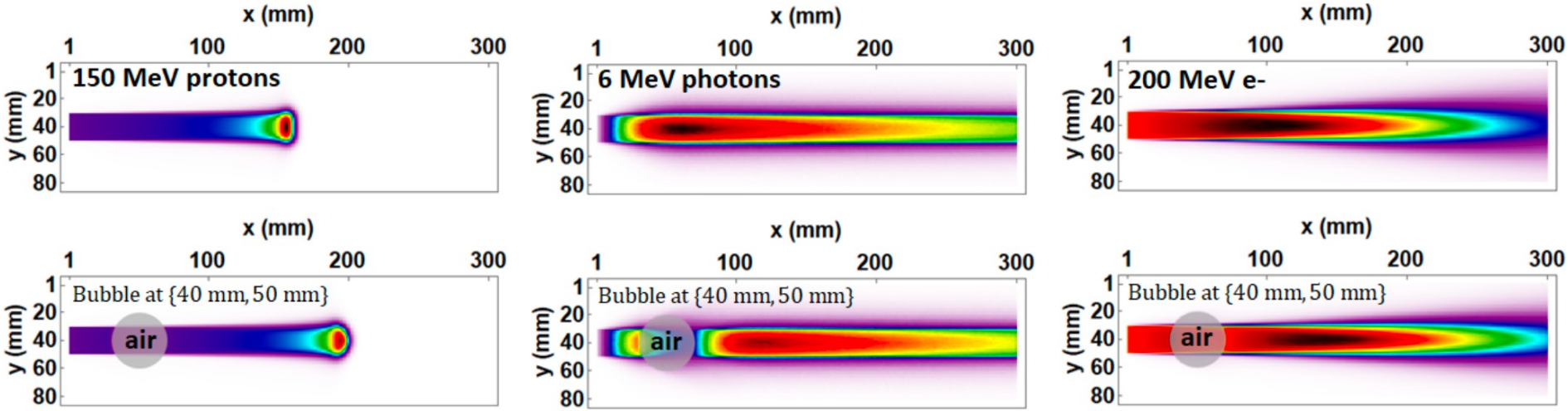

A. Lagzda, Ph.D. Thesis, 2019

Focused electron beams

Contrary to X-rays, electrons can be magnetically focused to increase the dose at depth.

In this simulation study, the influence of the focusing geometry and focusing depth is explored.

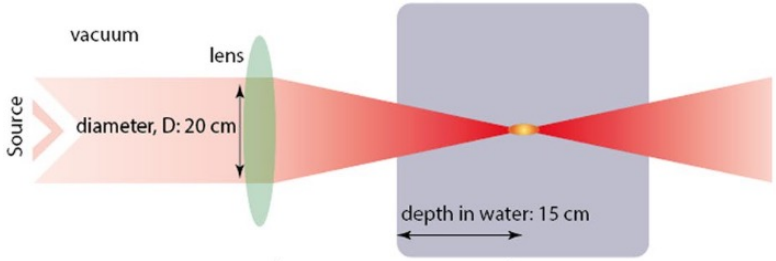

Focusing depth, 200 MeV

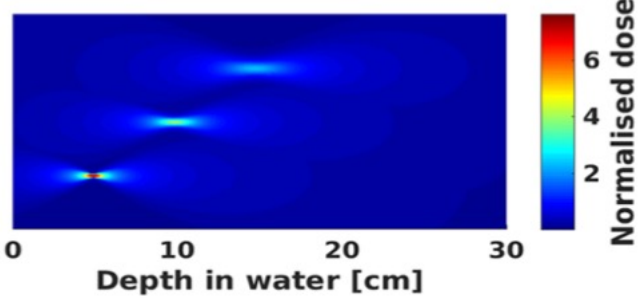

Focusing geometry, 200 MeV

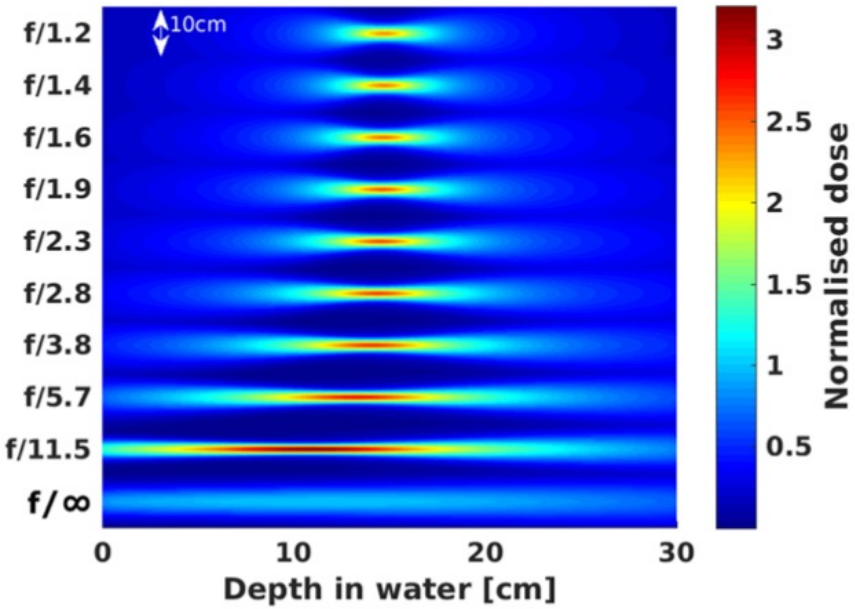

K. Kokurewicz *et al.*, Sci Rep **9**, 10837 (2019)

Beam shaping using EMQ magnets

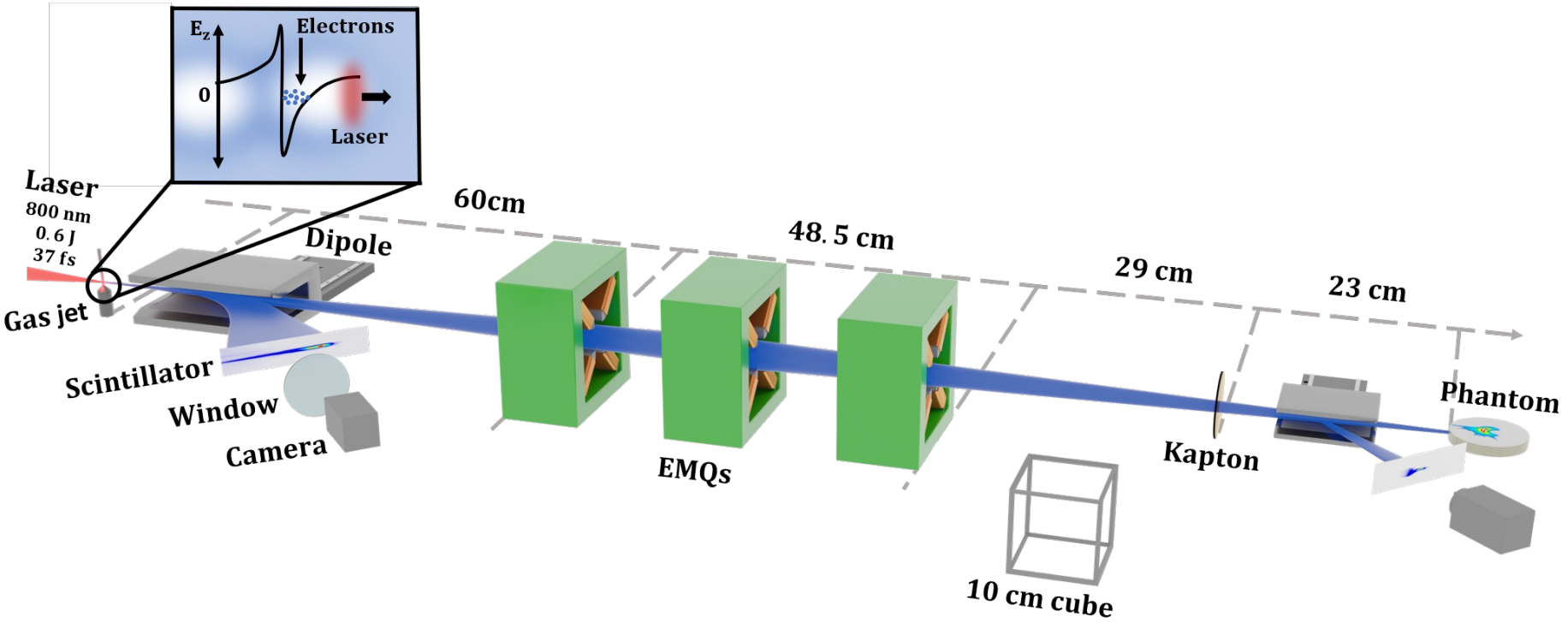

Focusing the beam at depth

✓ Mitigates lateral spread

✓ Gives more uniform dose

LUND UNIVERSITY

Dose deposition by focused beams

Changing focal plane changes the dose depth distribution

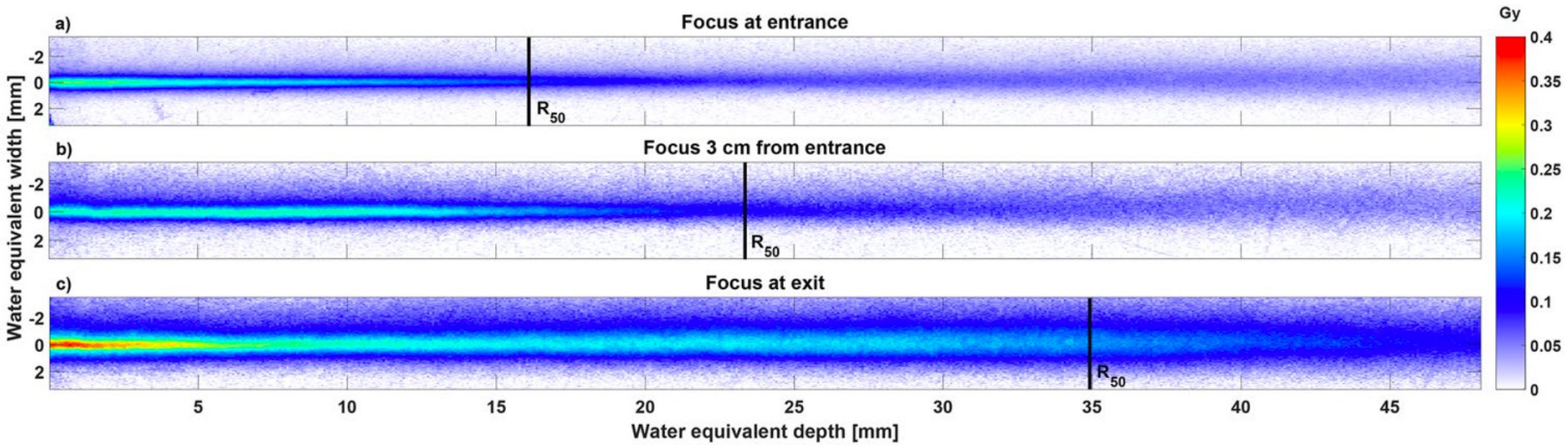

LUND UNIVERSITY

Multiple irradiation angles

Phantom stack

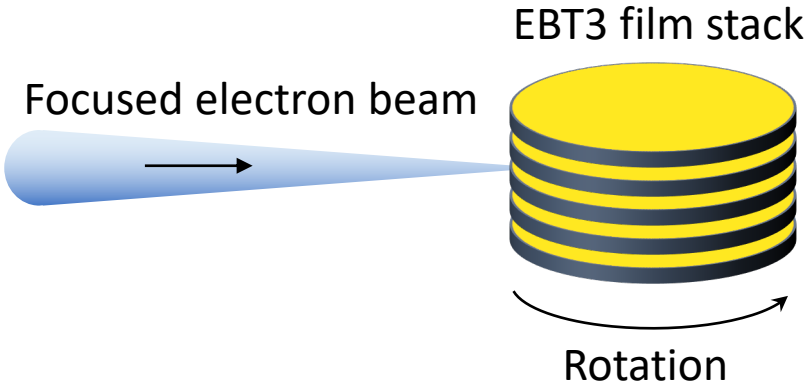

Simulation

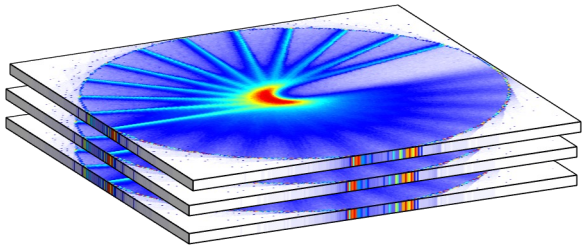

Simulation using Fluka

Measurement – concave volume

36 angles, 10 pulses/angle

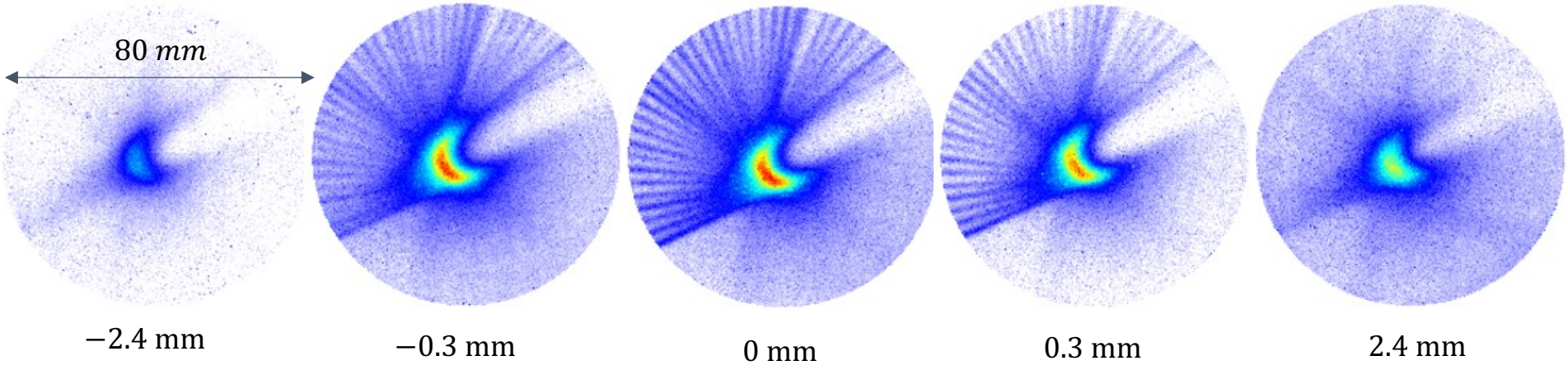

Layers at different heights from beam center

K. Svendsen *et al*, Sci Reports **11**, 5844 (2021)

Towards stereotactic radiotherapy

Purpose of stereotactic radiotherapy is very precise delivery of the dose to the target volume

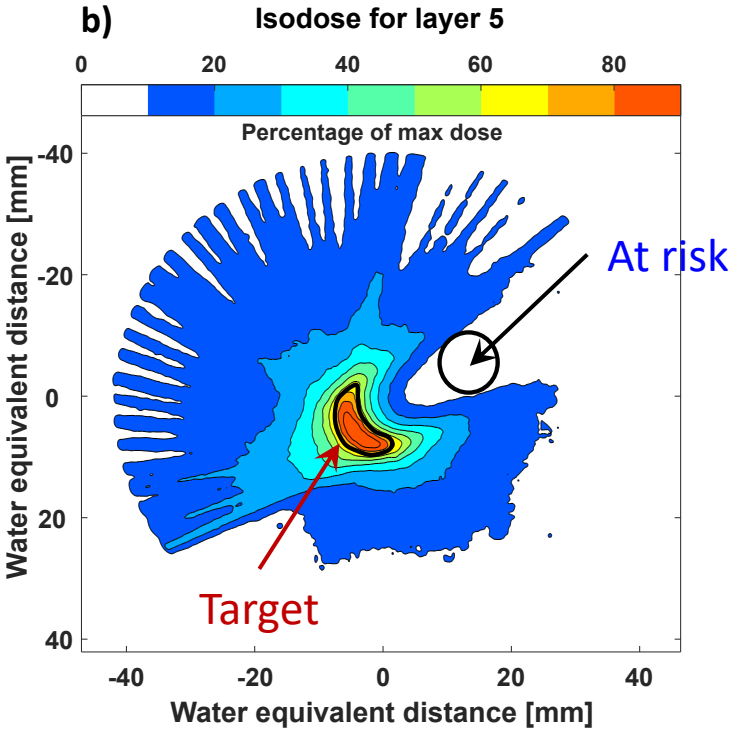

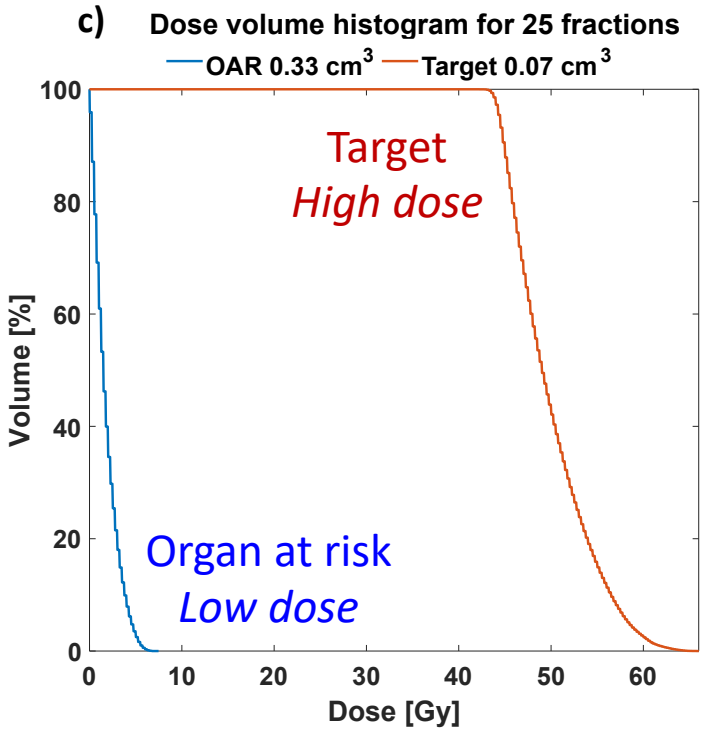

K. Svendsen *et al*, Sci Reports **11**, 5844 (2021)

LUND UNIVERSITY

Multi-field irradiation and intensity modulation

- Multi-field irradiation provides precise dose delivery in the target volume
- Intensity-modulated radiation field by controlled exposure at different locations

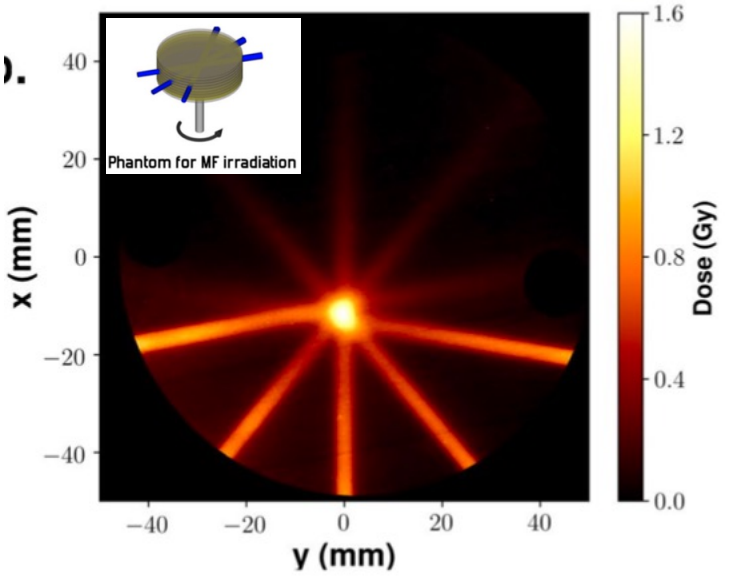

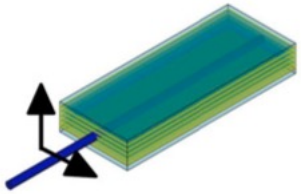

Number of shots at position

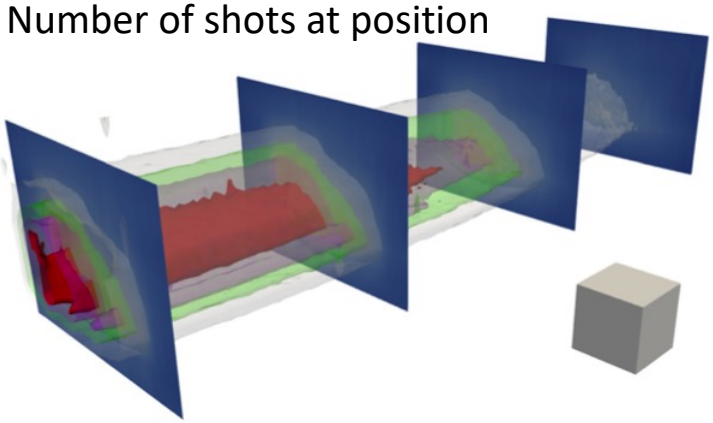

Measured isodose distribution

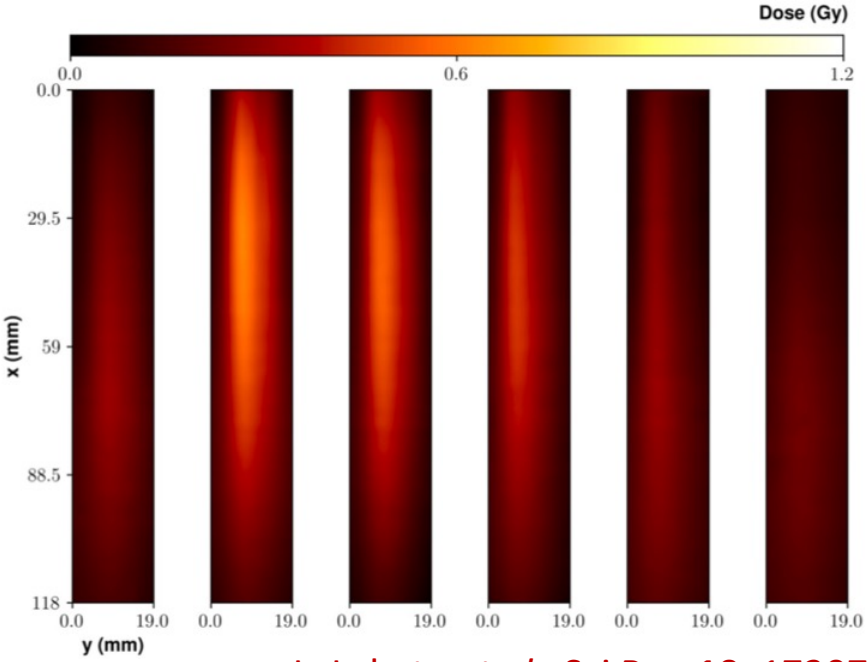

L. Labate *et al.*, Sci Rep **10**, 17307 (2020)

Direct and indirect action of radiation

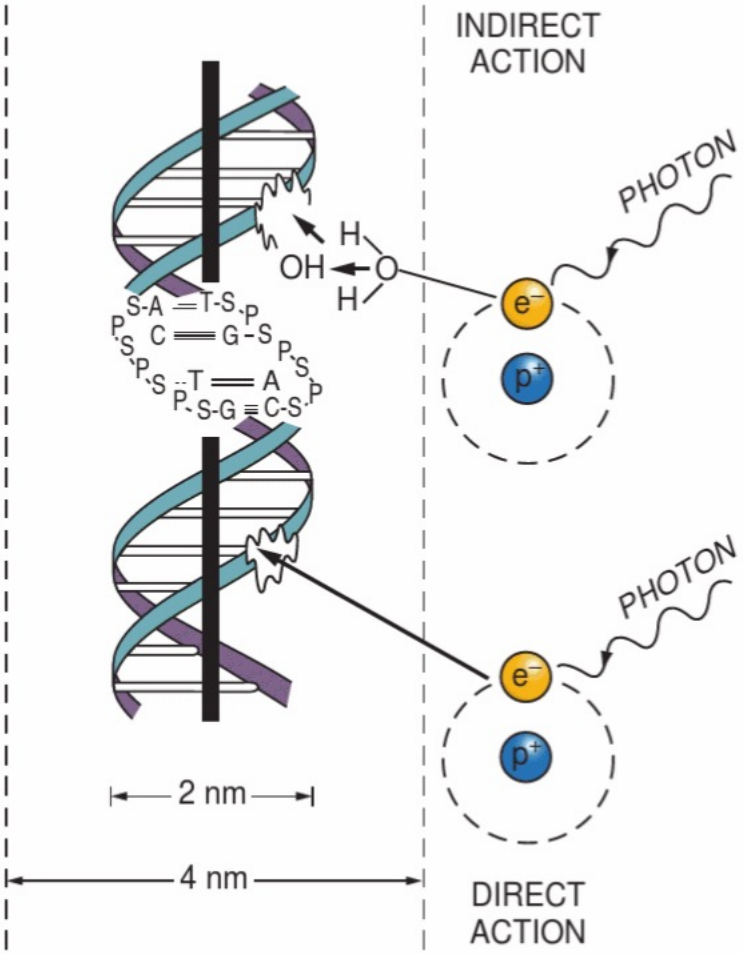

Radical cylinder

Direct action: a secondary electron resulting from absorption of an x-ray photon interacts with the DNA to produce an effect.

Indirect action: a secondary electron interacts with, for example, a water molecule to produce a hydroxyl radical (OH-), which in turn produces the damage to the DNA.

Towards ultrafast radiation biology

- Evaluation of DNA damage by comet assay
- 5×10^5 human skin cancer cells (A431) exposed to 1 Gy in a single shot (duration few fs)
- Measurable assessment of immediate and *reversible* DNA damage in carcinoma cells can be explored at the single-cell level.

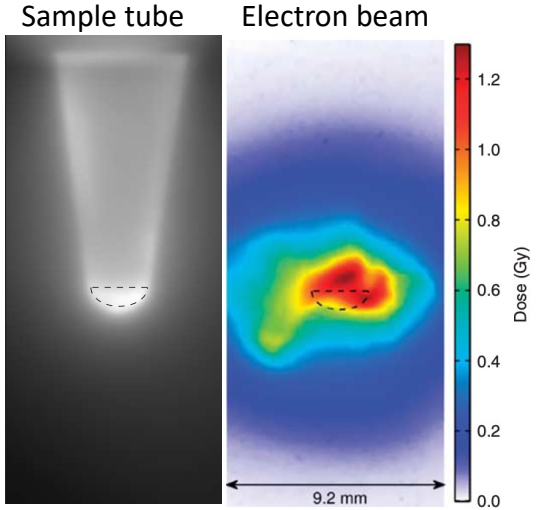

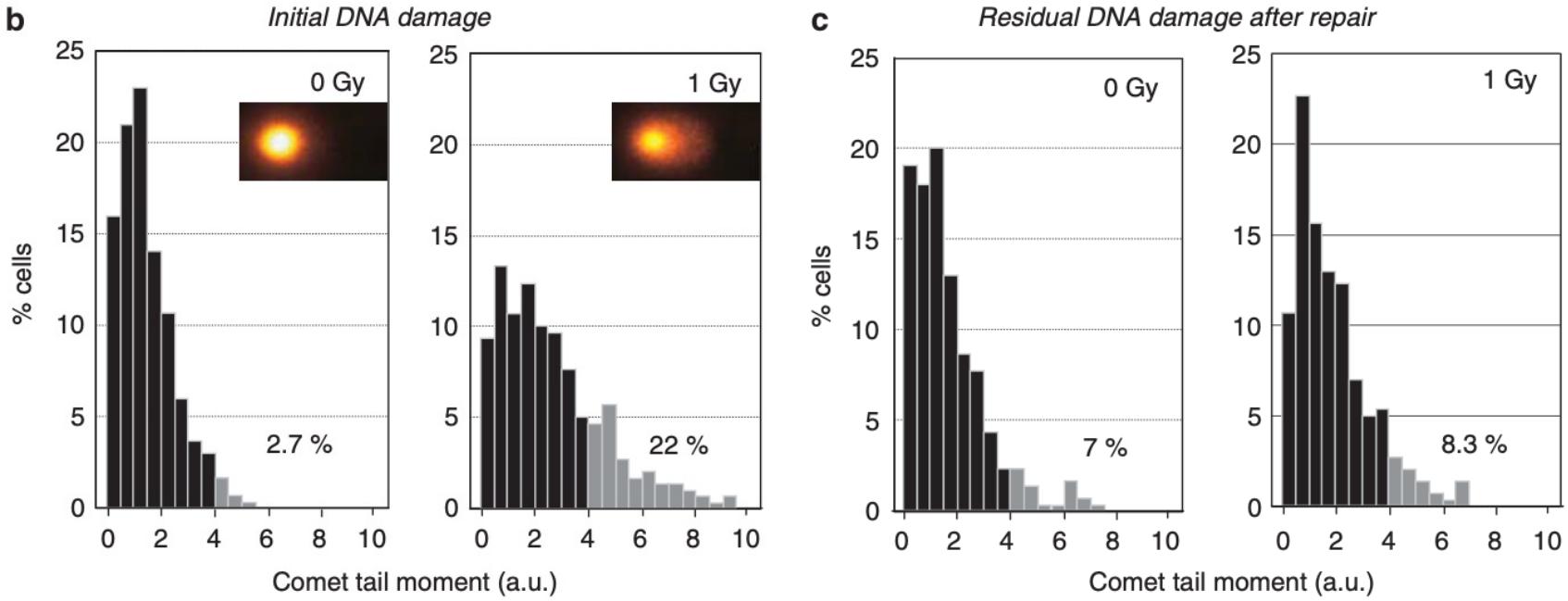

O Rigaud *et al*, Cell Death and Disease **1**, e73 (2010)

Radiobiological response to pulsed radiation

Results reveal that ultra-high pulse dose rates of 10^{10} Gy/min and the low repetition rate of laser accelerated electrons have **no statistically significant influence** (within the 95% confidence intervals) on the radiobiological effectiveness of megavoltage electrons.

Radiation quality	$\alpha \pm$ SE/Gy^{-1}	$\beta \pm$ SE/Gy^{-2}	R^2	$RBE_{0.1} \pm$ SE
200 kVp X-ray	0.394 ± 0.041	0.030 ± 0.007	0.951	
ELBE: Quasi-continuous	0.405 ± 0.038	0.021 ± 0.005	0.831	0.95 ± 0.11
ELBE: UHPDR-HF	0.397 ± 0.021	0.018 ± 0.003	0.943	0.92 ± 0.09
ELBE: UHPDR-LF	0.334 ± 0.046	0.023 ± 0.006	0.913	0.86 ± 0.12

	20 MeV ELBE electron beam		
		Ultra-high pulse dose rate	
Beam Parameter	Quasi-continuous	High frequency	Low frequency
Pulse frequency	13 MHz	13 MHz	2.5 Hz
Pulse length	~ 5 ps	~ 5 ps	~ 5 ps
Dose per pulse	~ nGy	~ mGy	~ mGy
Irradiation time	~ min	≤ 1 ms	≤ 30 min
Mean dose rate/Gy min^{-1}	4.1 ± 0.2	$(0.54 \pm 0.05) \times 10^6$	0.38 ± 0.03
Pulse dose rate/Gy min^{-1}	~ 10^4	~ 10^{10}	~ 10^{10}

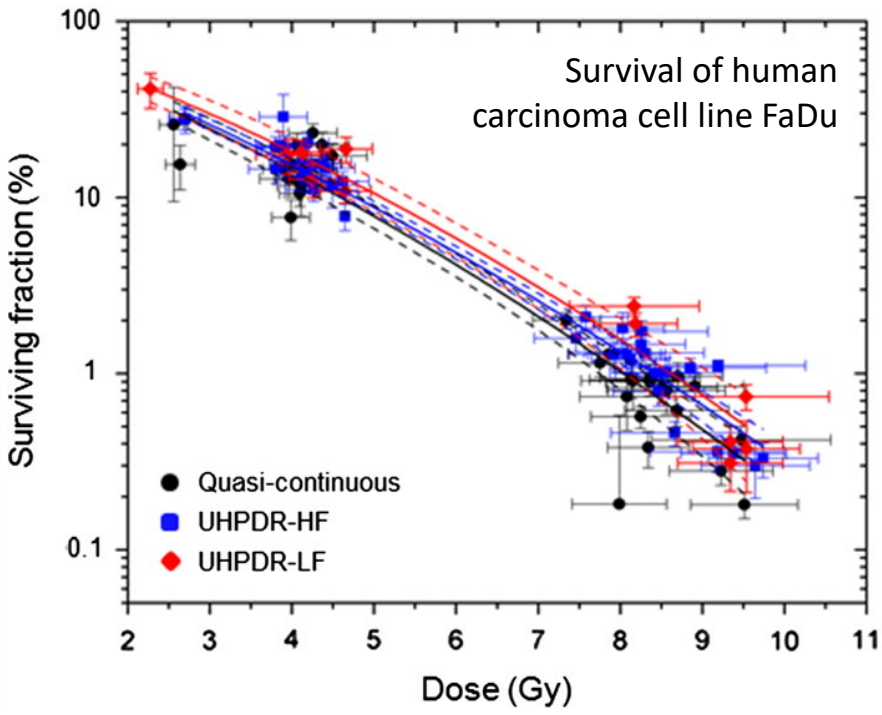

E Beyreuther *et al*, Cell Death and Disease **1**, e73 (2010)

The therapeutic window

The therapeutic window in radiotherapy refers to the delicate **balance** between the **dose required to effectively treat** a cancerous tumor and the **dose that can cause harm** to normal, healthy cells in the surrounding tissue.

Increasing the therapeutic window improves the treatment

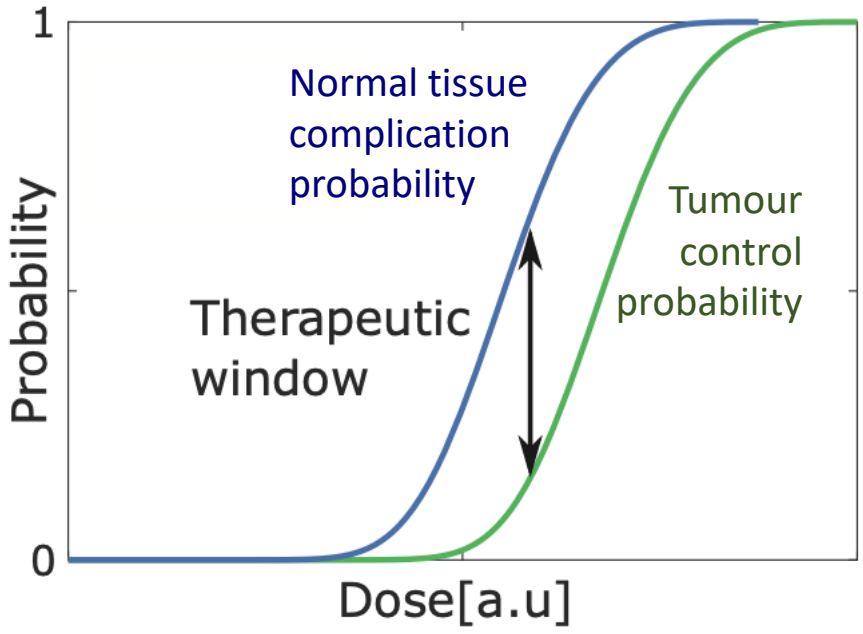

Perspectives for FLASH therapy

FLASH therapy is the delivery of very high dose rates (>40 Gy/s)

FLASH effect provides better sparing of healthy tissue

not yet completely understood

Femtosecond electron bunches from LWFA

- Allow radiobiological studies at ultra-high dose rates
- High repetition rate (>10 Hz) is also needed for delivering the high total dose (~1-10 Gy) in very short time (~100 ms)

Seminal paper

V Favaudon *et al., "Ultrahigh dose-rate FLASH irradiation increases the differential response between normal and tumor tissue in mice"*, Science Transl. Med. **6** (2014)

Review articles

M Kim *et al*, IEEE Transactions on Radiation and Plasma Medical Sciences **6** (2021)

Hughes and Parsons, Int. J. Molecular Sciences **5** (2020)

Conclusions

- VHEE-RT is attracting more and more interest from medical community
- VHEE-RT could be the next important societal application
- LPAs are offering several advantages over conventional accelerators

Outline

Laser-accelerated electron beams for radiotherapy

Betatron X-rays for imaging and spectroscopy

Other light sources based on plasma accelerators

Light sources based on LWFA

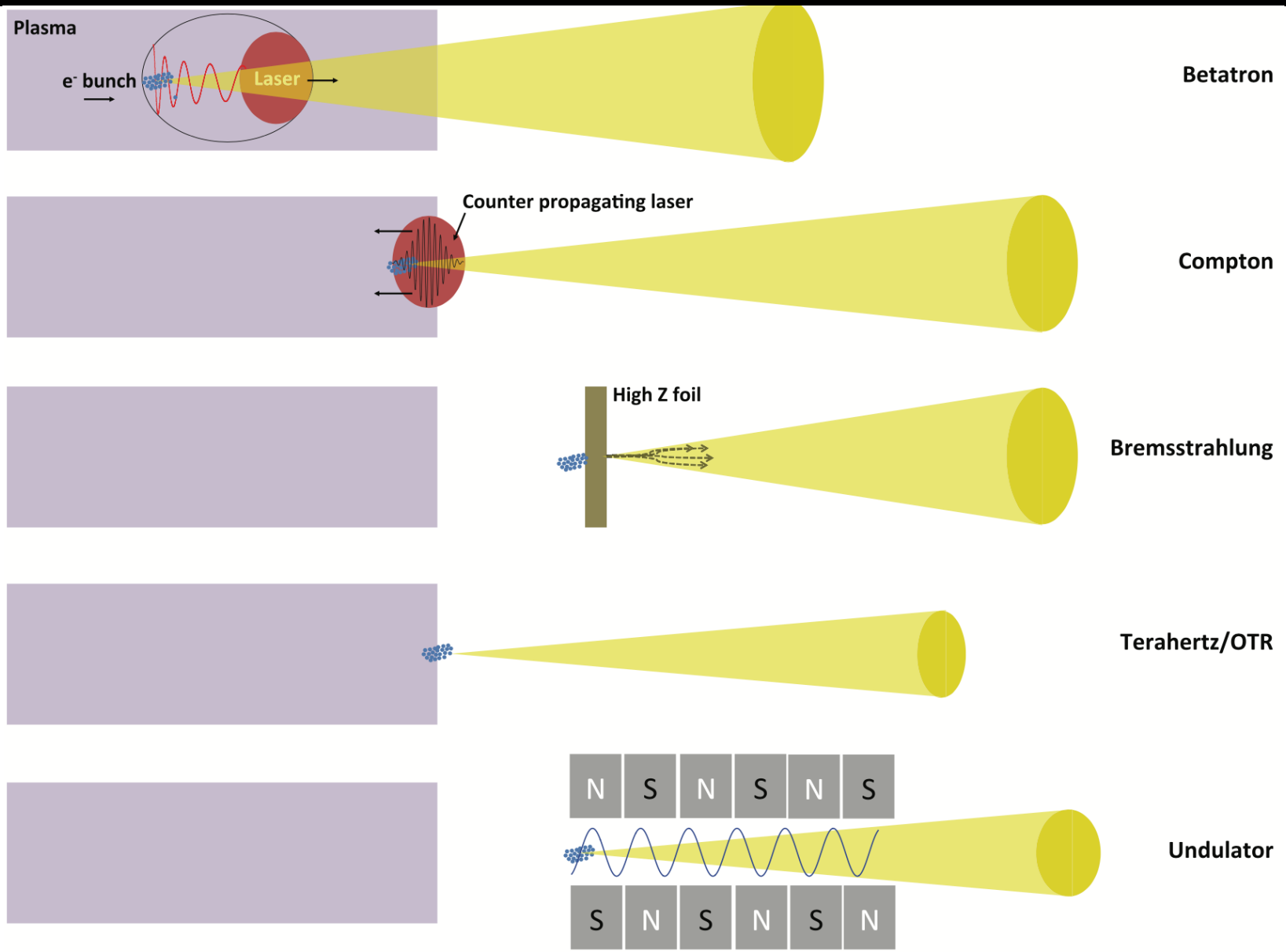

F Albert and AGR Thomas, Plasma Phys. Control. Fusion **58,** 103001 (2016)

Betatron oscillations in an ion cavity

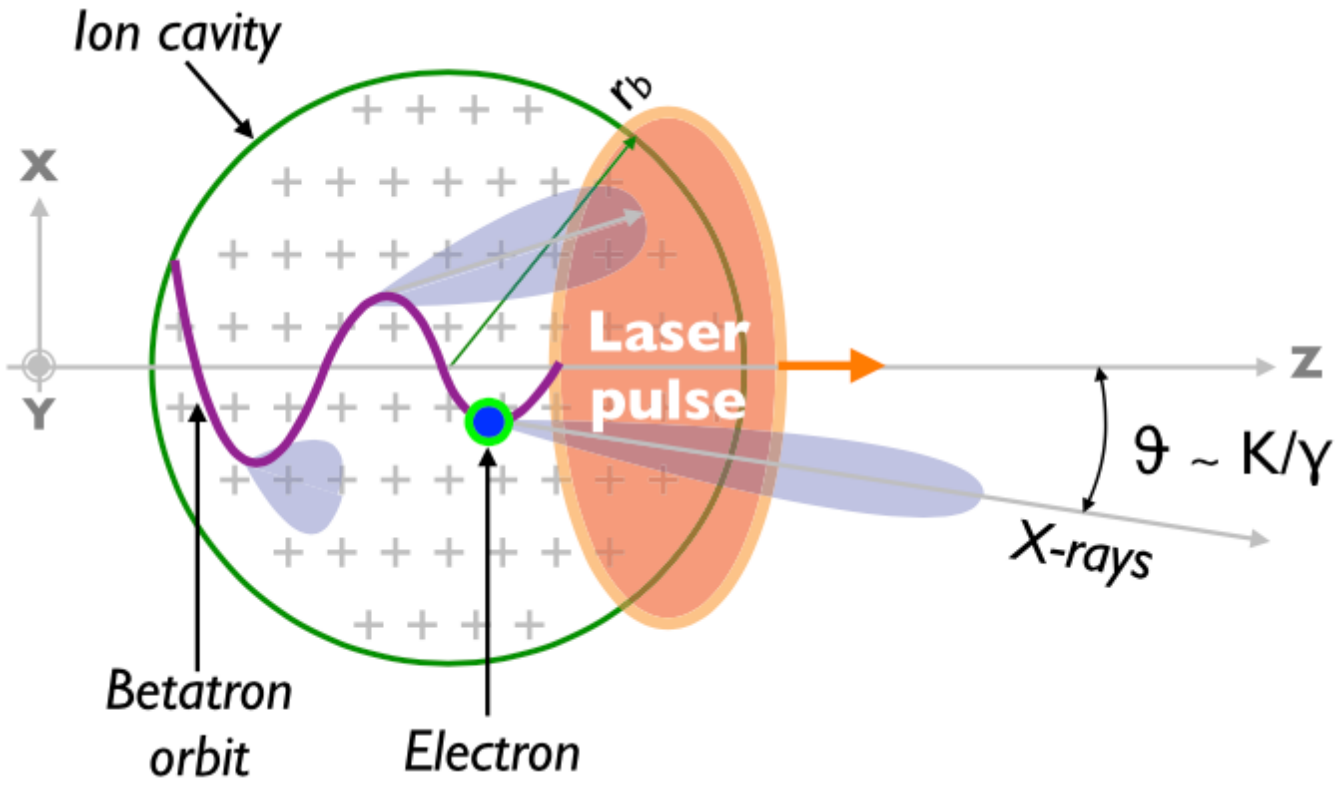

Review article

S Corde *et al*, *"Femtosecond x rays from laser-plasma accelerators",* Rev Mod Phys **85**, (2013)

Betatron oscillation in an ion channel

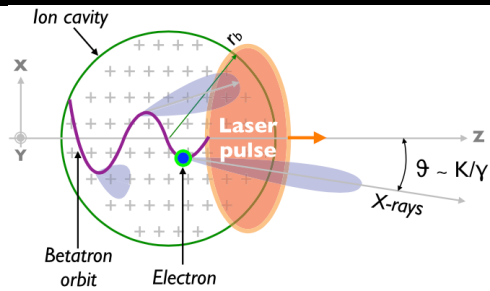

Gauss's law and assuming cylindrical symmetry

$$\nabla \cdot \boldsymbol{E} = \frac{\rho}{\epsilon_0}$$

$$\Rightarrow \frac{1}{r}\frac{d}{dr}(rE_r) = \frac{q_e n_e}{\epsilon_0} \Rightarrow E_r = \frac{q_e n_e}{\epsilon_0}\frac{r}{2}$$

Assuming transverse motion is small and does not change the total energy of the particle ($p_\perp \ll p_z$ and $\gamma \simeq \gamma_{z0} \simeq const$)

$$\frac{dp_\perp}{dt} = -q_e E_r \Rightarrow \frac{d}{dt}(\gamma m_e v) = -\frac{m_e \omega_p^2}{2} r \Rightarrow \frac{d^2 r}{dt^2} = -\frac{\omega_p^2}{2\gamma} r$$

Which is the equation of motion of a harmonic oscillator with frequency

$$\boxed{\omega_\beta = \frac{\omega_p}{\sqrt{2\gamma}}}$$

The transverse motion is sinusoidal: $r = r_\beta \cos \omega_\beta t$

Maximum angle of the trajectory

$$\psi = \left(\frac{dr}{cdt}\right)_{\max} = \frac{r_\beta \omega_\beta}{c} = \frac{K}{\gamma} \Rightarrow \boxed{K = \gamma r_\beta \omega_\beta / c}$$

Undulator and wiggler regimes

$\psi \ll \Delta\theta$

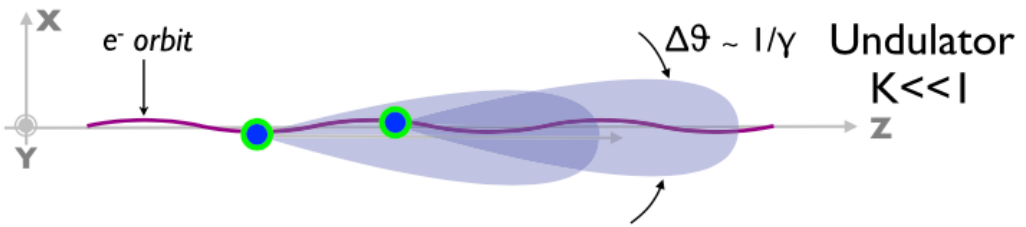

$\psi \gg \Delta\theta$

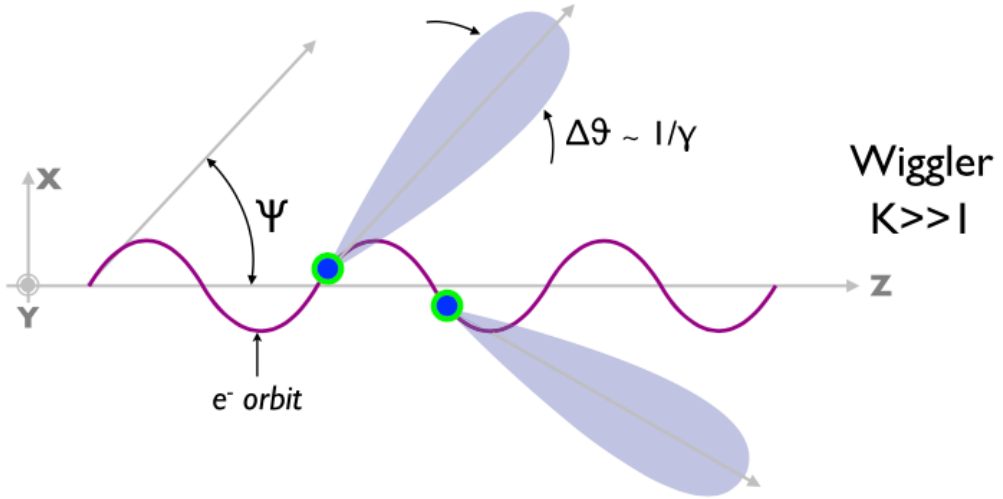

ψ	Maximum angle of the electron velocity vector
$\Delta\theta = 1/\gamma$	Opening angle of the radiation cone
$K = \gamma\psi$	Dimensionless parameter separating the regimes

S Corde *et al*, Rev Mod Phys **85**, (2013)

Radiation from a relativistic electron

Energy radiated within a spectral band $d\omega$ centered on the frequency ω and within a solid angle $\mathrm{d}\Omega$:

$$\frac{d^2I}{d\omega d\Omega} = \frac{q_e^2}{16\pi\epsilon_0 c}\left|\int_{-\infty}^{\infty} e^{i\omega[t-\vec{n}\cdot\vec{r}(t)/c]}\frac{n\times\left[\left(\vec{n}-\vec{\beta}\right)\times\dot{\vec{\beta}}\right]}{\left(1-\vec{\beta}\cdot\vec{n}\right)^2}dt\right|$$

$\vec{r}(t)$ is electron position at time t

$\vec{\beta}$ is electron velocity normalized to c

$\dot{\vec{\beta}} = d\vec{\beta}/dt$ is electron acceleration normalized to c

$\vec{n}$ is the observation direction

J D Jackson, 2001

Synchrotron radiation

The radiation emitted over N_β betatron periods

$$\frac{d^2I}{d\omega d\Omega} = N_\beta \frac{3hq_e^2}{\pi^3 c} \frac{\gamma^2\zeta^2}{1+\gamma^2\theta^2}\left[\frac{\gamma^2\theta^2}{1+\gamma^2\theta^2}\mathcal{K}_{1/3}^2(\zeta) + \mathcal{K}_{2/3}^2(\zeta)\right]$$

$$\zeta = \frac{E}{2E_c}(1+\gamma^2\theta^2)^{3/2}$$

$$E_c = \frac{3\hbar}{2c}\gamma^3\omega_\beta^2 r_\beta$$

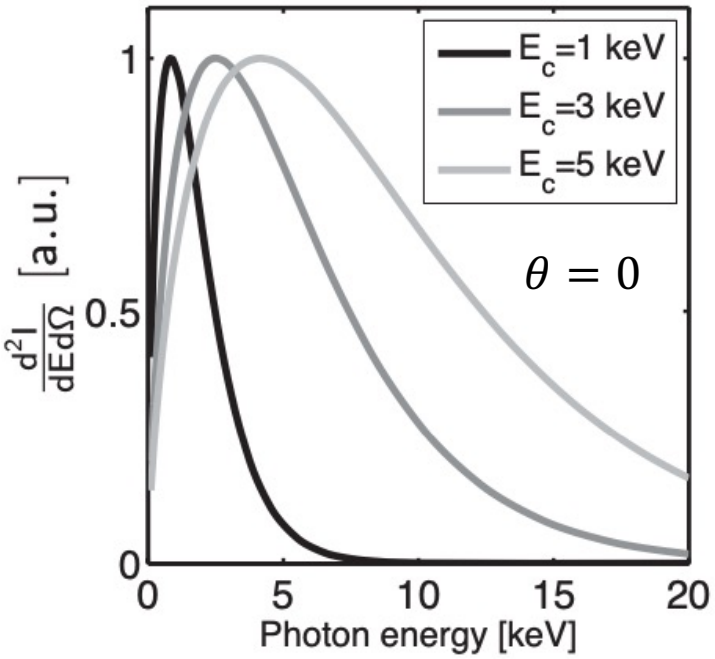

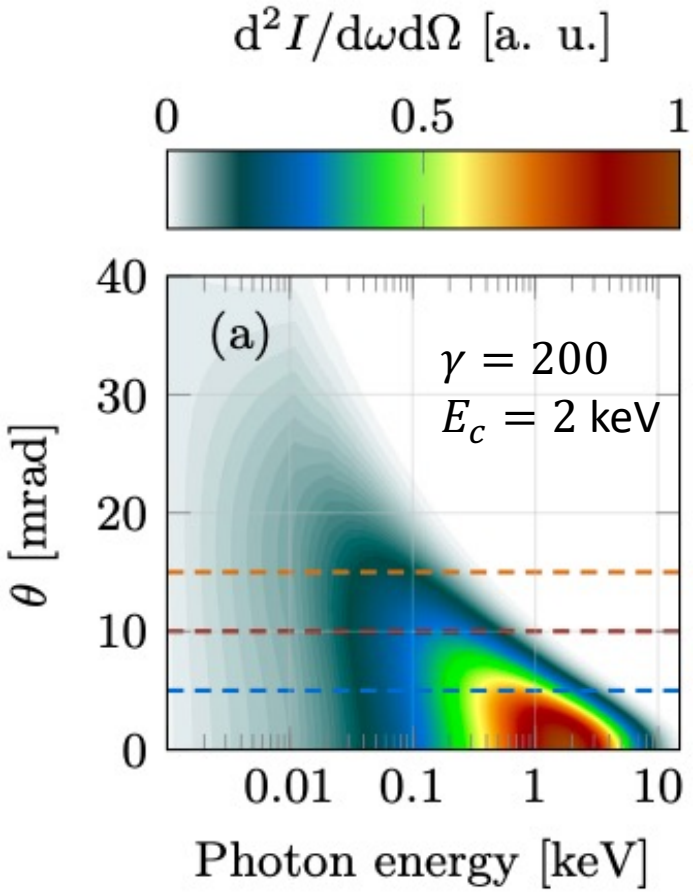

E Esarey *et al*, Phys Rev E 65, 056505 (2002)

I Gallardo-Gonzalez, PhD Thesis, 2018

First measurements of betatron X-rays

Beam-driven

VOLUME 88, NUMBER 13 PHYSICAL REVIEW LETTERS 1 APRIL 2002

X-Ray Emission from Betatron Motion in a Plasma Wiggler

Shuoqin Wang,[1] C. E. Clayton,[1] B. E. Blue,[1] E. S. Dodd,[1] K. A. Marsh,[1] W. B. Mori,[1] C. Joshi,[1] S. Lee,[2] P. Muggli,[2] T. Katsouleas,[2] F. J. Decker,[3] M. J. Hogan,[3] R. H. Iverson,[3] P. Raimondi,[3] D. Walz,[3] R. Siemann,[3] and R. Assmann[4]

[1]*University of California, Los Angeles, California 90095*
[2]*University of Southern California, Los Angeles, California 90089*
[3]*Stanford Linear Accelerator Center, Stanford, California 94309*
[4]*CERN, Switzerland*

(Received 8 October 2001; published 19 March 2002)

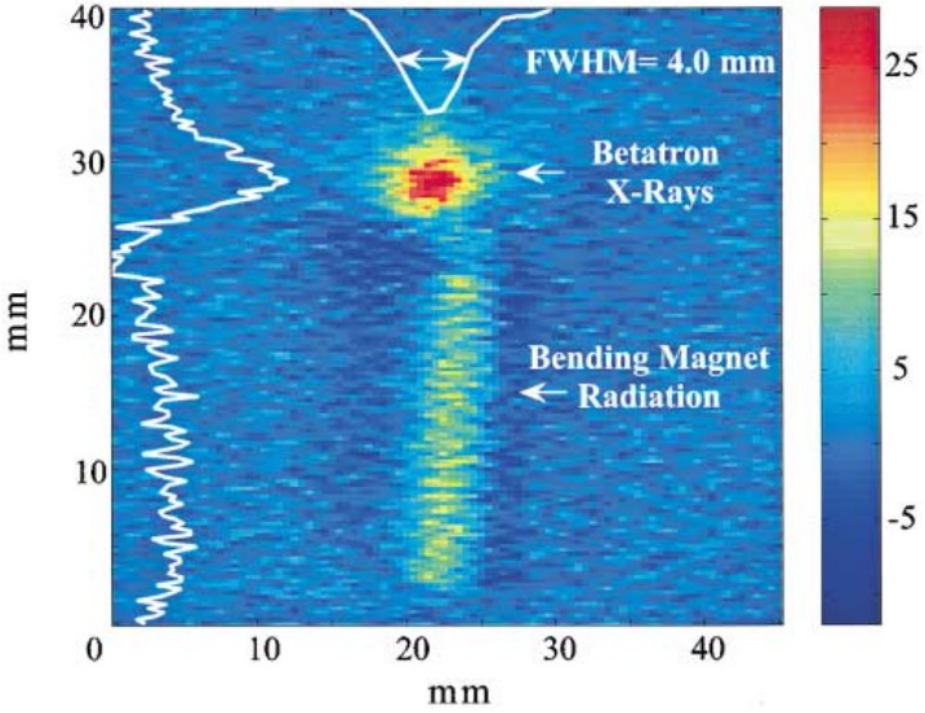

Laser-driven

VOLUME 93, NUMBER 13 PHYSICAL REVIEW LETTERS week ending 24 SEPTEMBER 2004

Production of a keV X-Ray Beam from Synchrotron Radiation in Relativistic Laser-Plasma Interaction

Antoine Rousse,[1] Kim Ta Phuoc,[1,2,*] Rahul Shah,[2] Alexander Pukhov,[3] Eric Lefebvre,[4] Victor Malka,[1] Sergey Kiselev,[3] Fréderic Burgy,[1] Jean-Philippe Rousseau,[1] Donald Umstadter,[2] and Daniéle Hulin[1]

[1]*Laboratoire d'Optique Appliquée, ENSTA, CNRS UMR7639, Ecole Polytechnique, Chemin de la Hunière, 91761 Palaiseau, France.*
[2]*Center for Ultrafast Optical Science, University of Michigan, 2200 Bonisteel Blvd, Ann Arbor, Michigan, 48109, USA.*
[3]*Insitut fuer Theoretische Physik I, Heinrich-Heine-Universitaet, Duesseldorf, 40225 Duesseldorf, Germany.*
[4]*Département de Physique Théorique et Appliquée, CEA/DAM Ile- de-France, BP 12, 91680 Bruyéres-le-Châtel, France*

(Received 22 January 2004; published 23 September 2004)

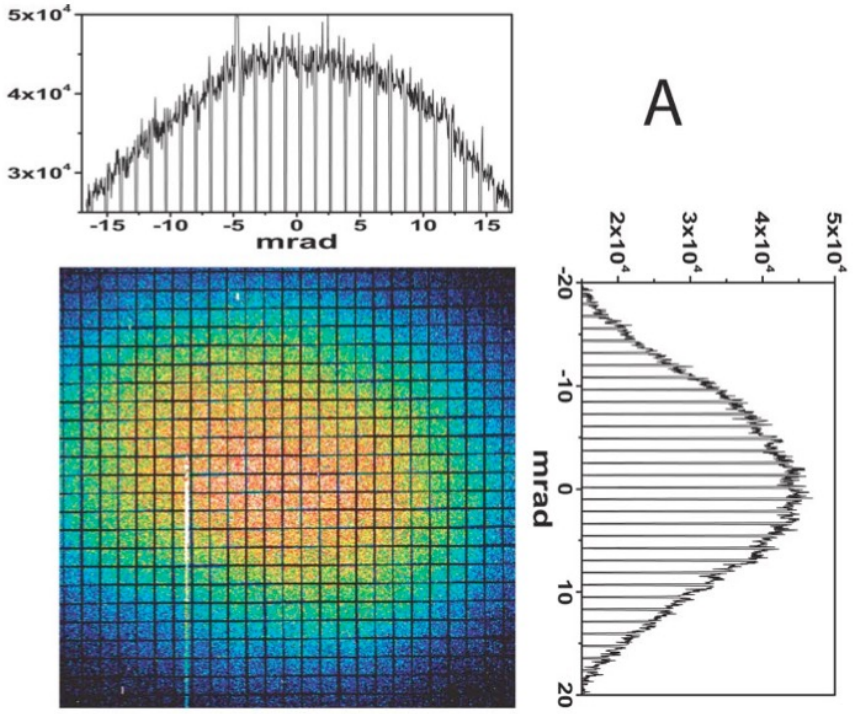

Electron trajectories shapes radiation

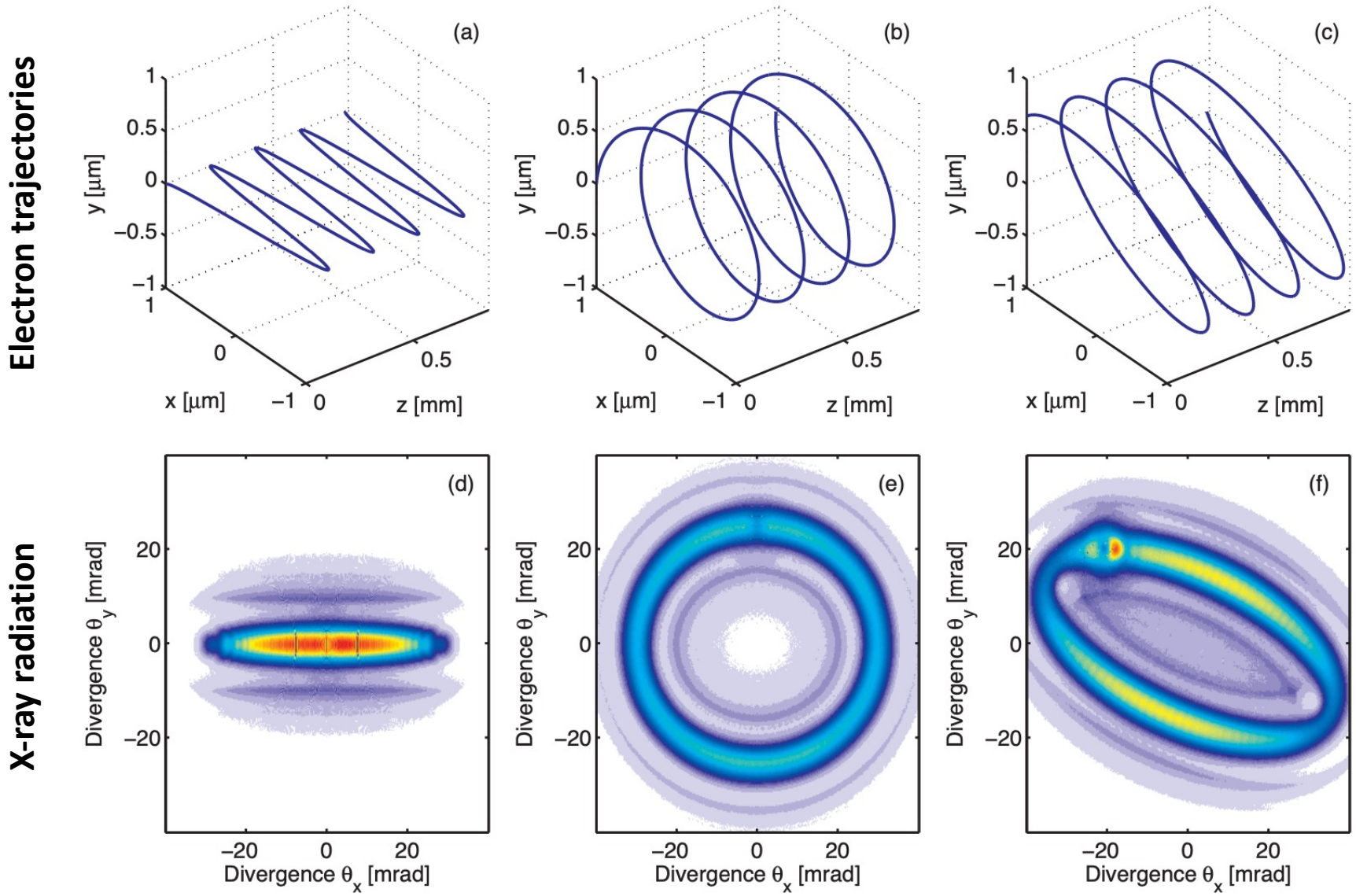

G Genoud, PhD Thesis, 2011

Electron trajectories shapes radiation

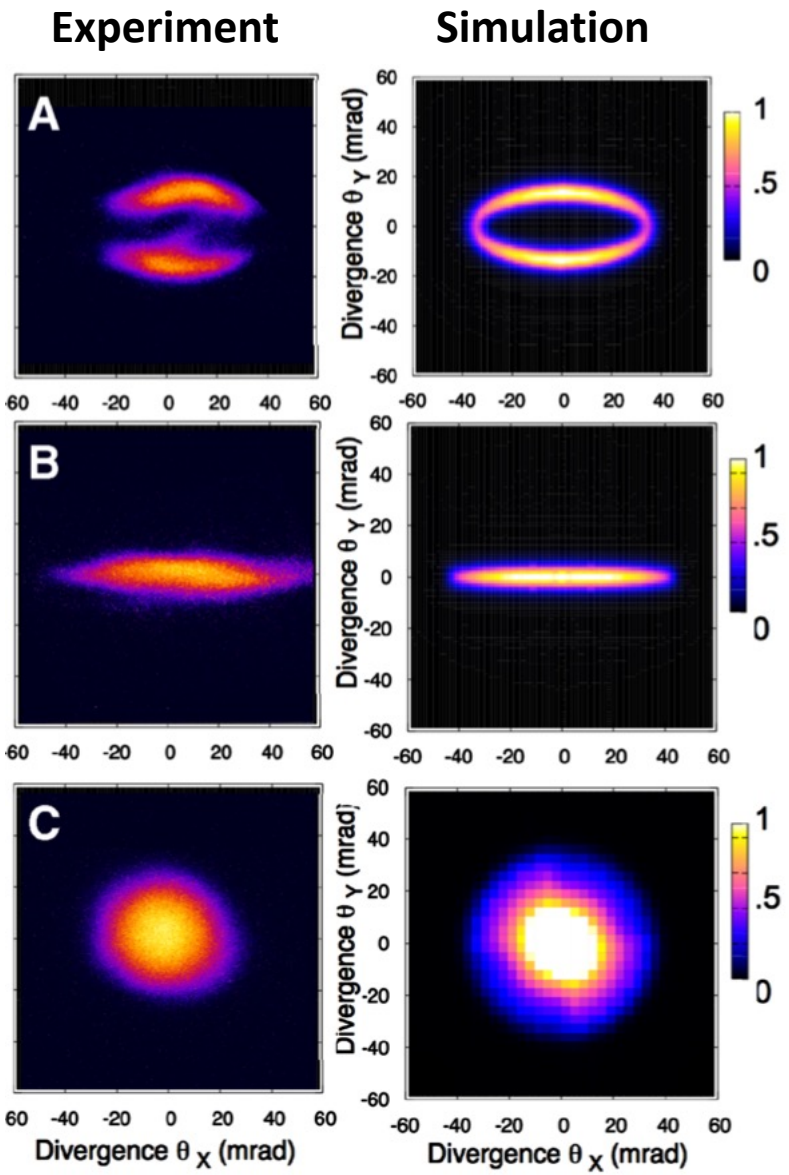

K Ta Phuoc *et al*, Phys Rev Lett **97**, 225002, 2006

Tunable X-ray polarization

Elliptical X-ray beams rotate with laser polarization

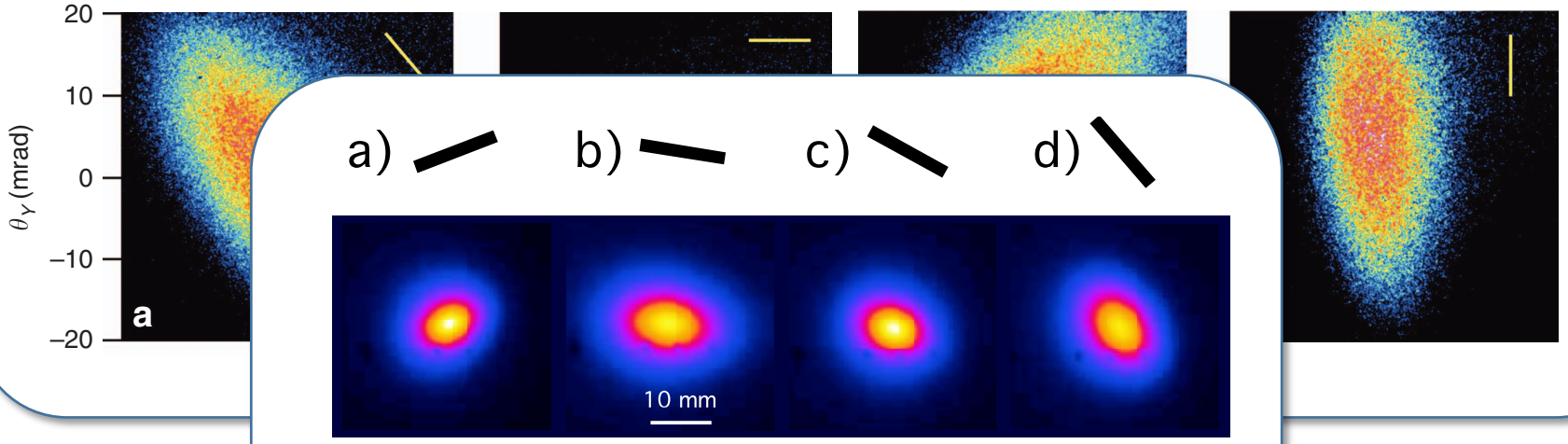

Elliptical electron beams rotate with laser polarization

SPD Mangles *et al*, Phys Rev Lett 96, 215001 (2006)

X-ray

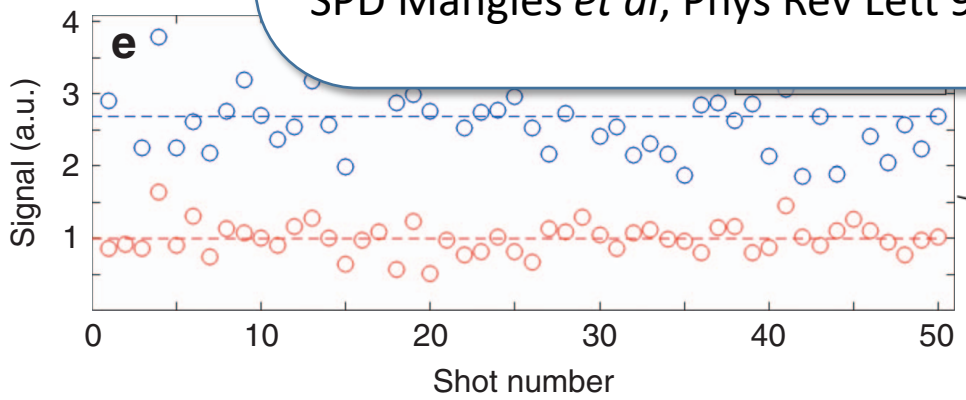

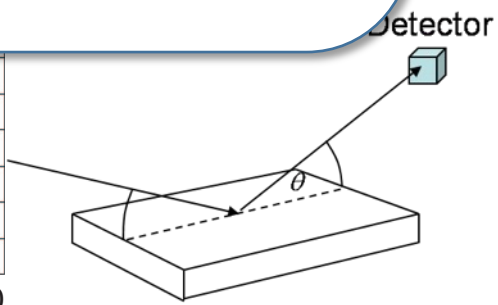

A Döpp *et al*, Light: Science and Application 6, e17086 (2017)

loa

LUND UNIVERSITY

Spectral characterization using Ross filters

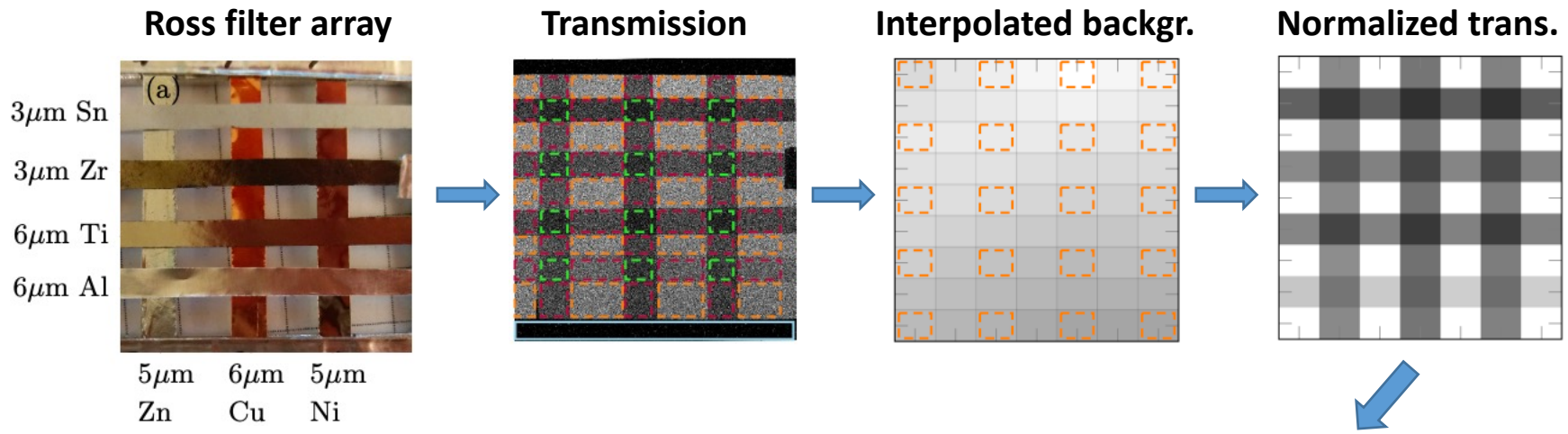

$$\Lambda^2(E_c) = \sum_i \left(T(F_i, E_c) - T_{CCD}(F_i)\right)^2$$

calculated measured

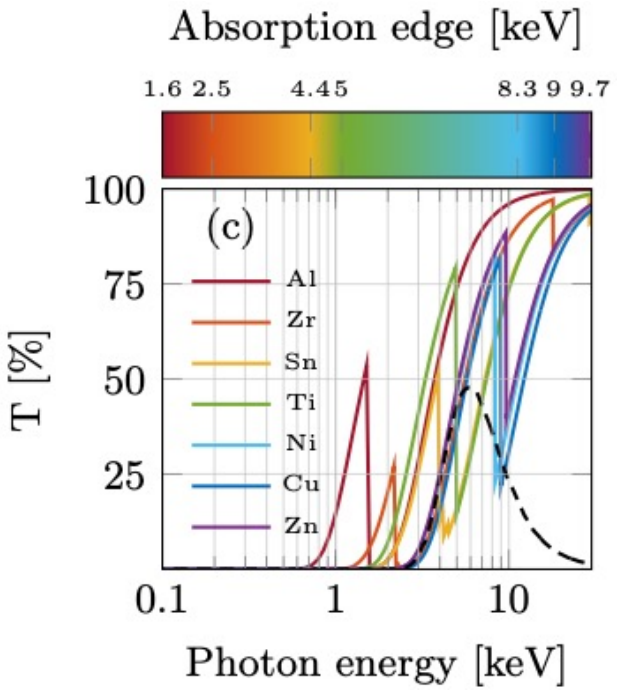

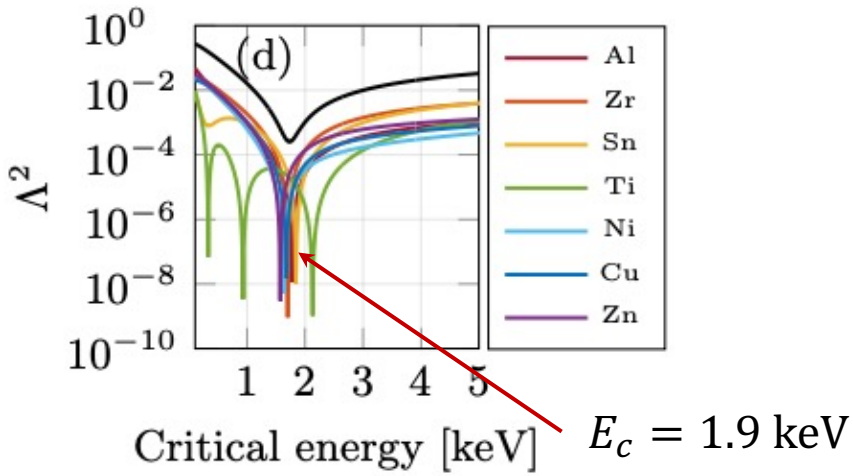

I Gallardo Gonzales, PhD Thesis, 2018

Source characterization using Ross filters

Critical energy: 2-3 keV

Flux: 1-2·10^{11} photons/sr

Divergence: 30 × 40 mrad

$4 \cdot 10^9$ photons

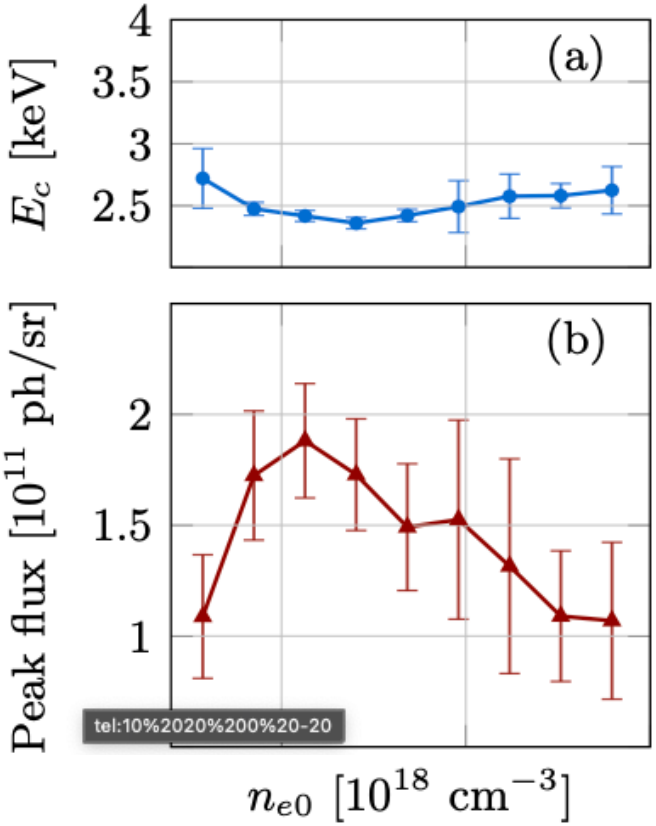

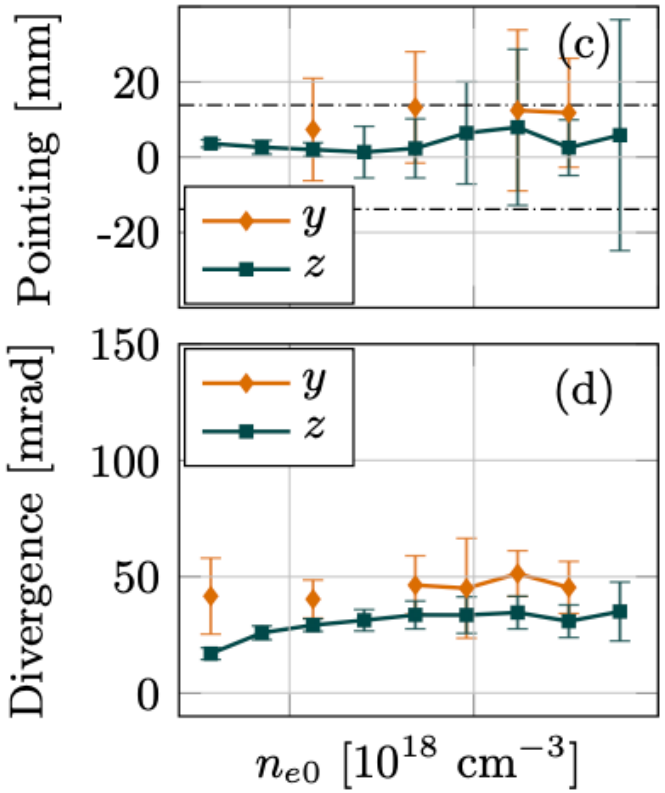

I Gallardo Gonzales, PhD Thesis, 2018

Betatron as a diagnostic for LWFA electrons

25 µm tungsten wires

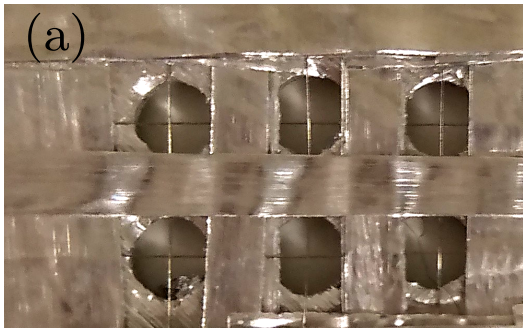

Wire shadow on CCD

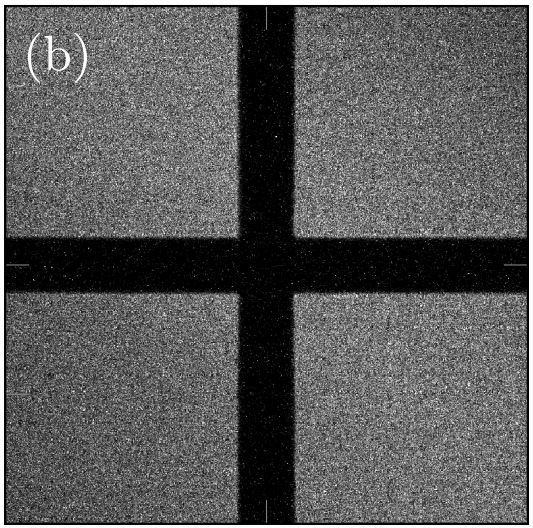

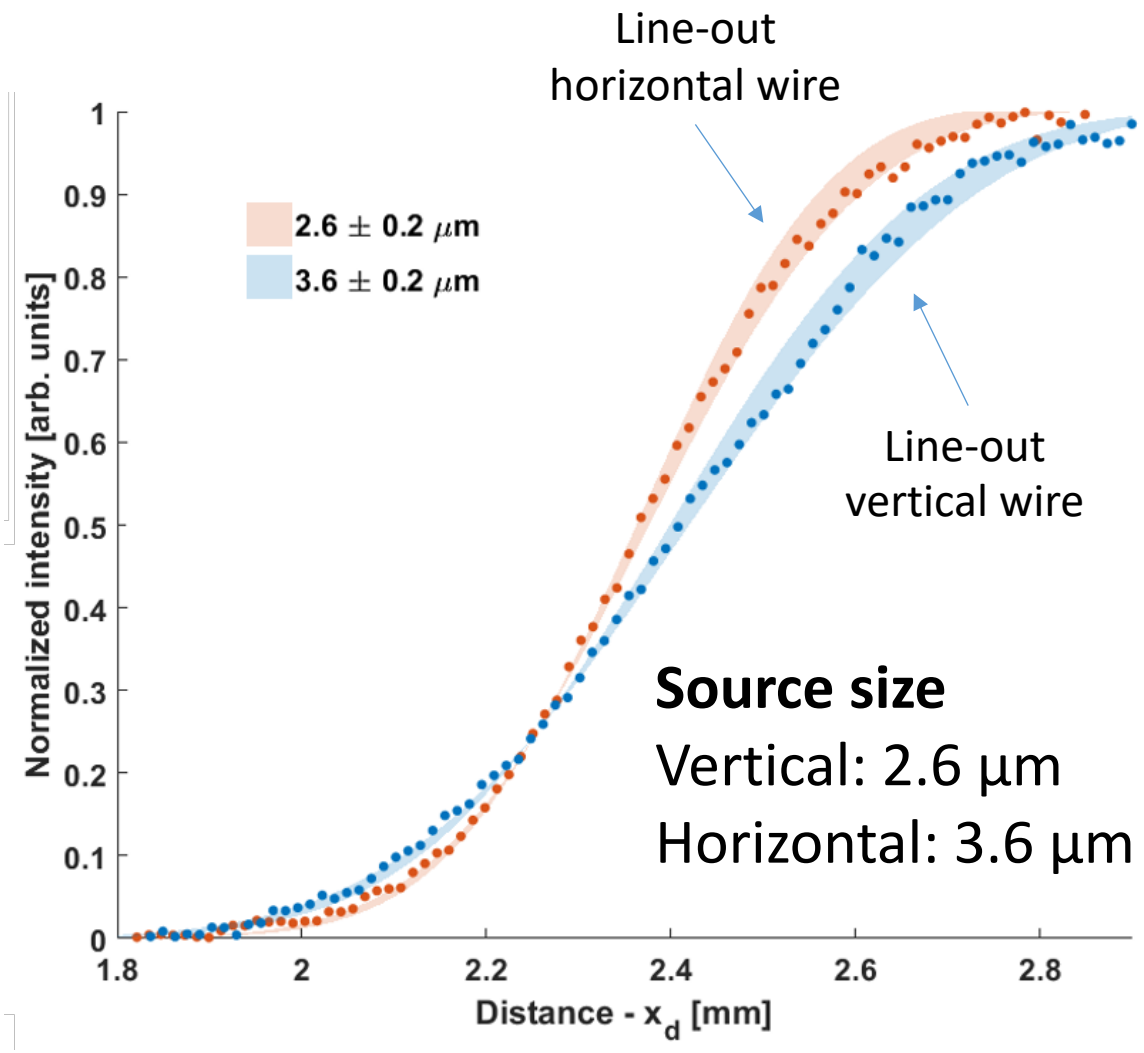

K Svendsen, PhD Thesis, 2022

Betatron as diagnostic of LWFA

$$E_c = \frac{3\hbar}{2c}\gamma^3\omega_\beta^2 r_\beta \qquad \omega_\beta = \frac{\omega_p}{\sqrt{2\gamma}}$$

- X-ray spectrum measured by single photon counting technique
- Simultaneous measurements of electron- and X-ray spectrum
- Allows measurement of the electron beam size (oscillation amplitude)

Source size measurements

X-ray spectrum: $r_\beta = 0.9 \pm 0.3\ \mu m$

Fresnel diffraction: $r_\beta = 1.8 \pm 0.3\ \mu m$

PIC simulation: $r_\beta = 1.5 \pm 0.2\ \mu m$

Single-shot X-ray spectrum

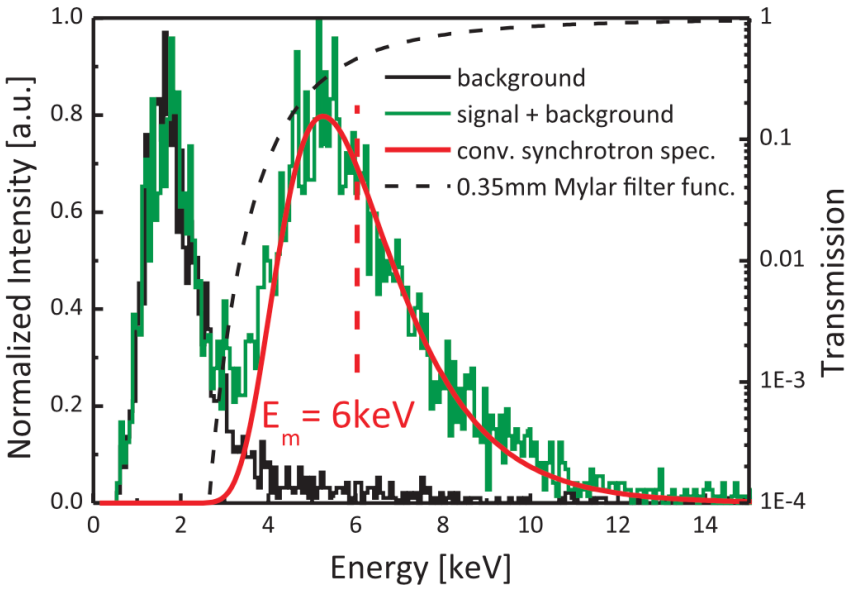

Shadow of 10 µm wire

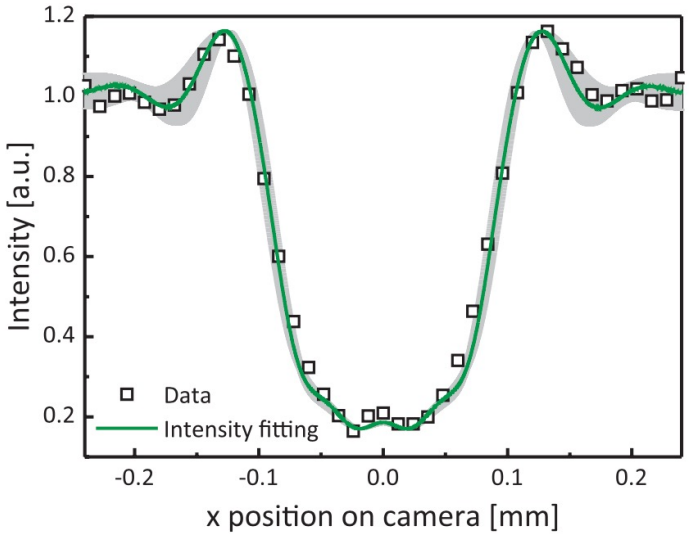

M Schnell *et al*, PRL **108**, 075001 (2012)

Phase-contrast imaging

Propagation-based phase-contrast imaging

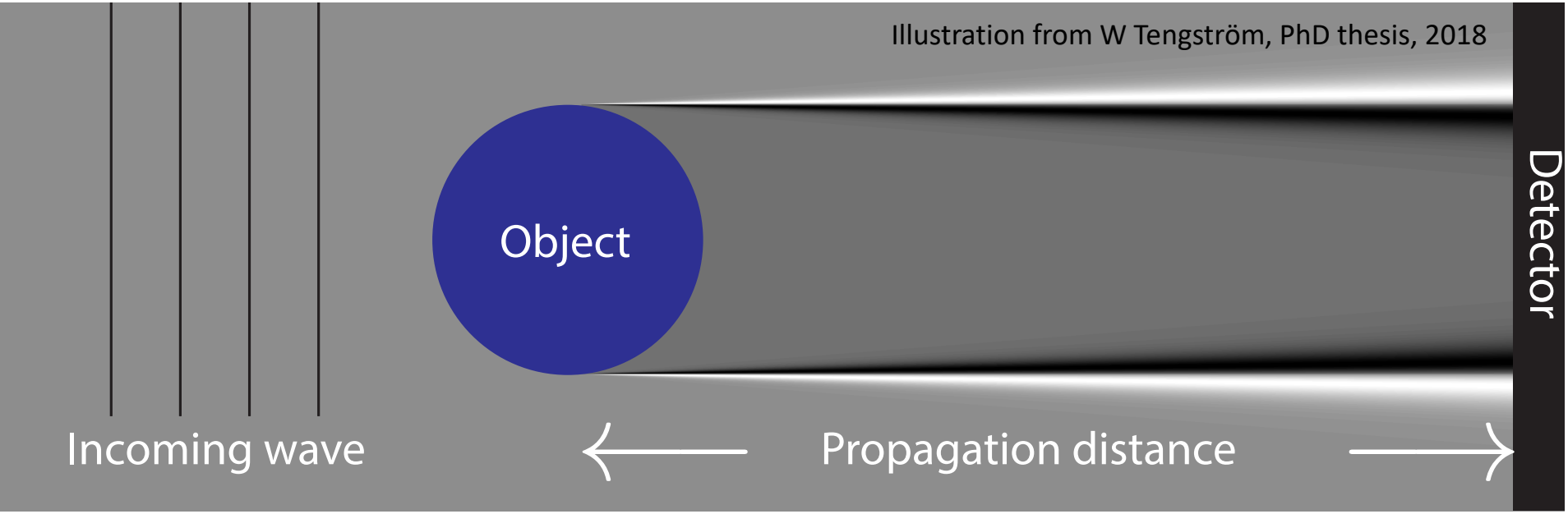

Relies on changes in the refractive index

Ideal for low-absorbing samples

Projected thickness is obtained using algorithms

Requires high spatial coherence -> small source size

Setup for phase-contrast imaging

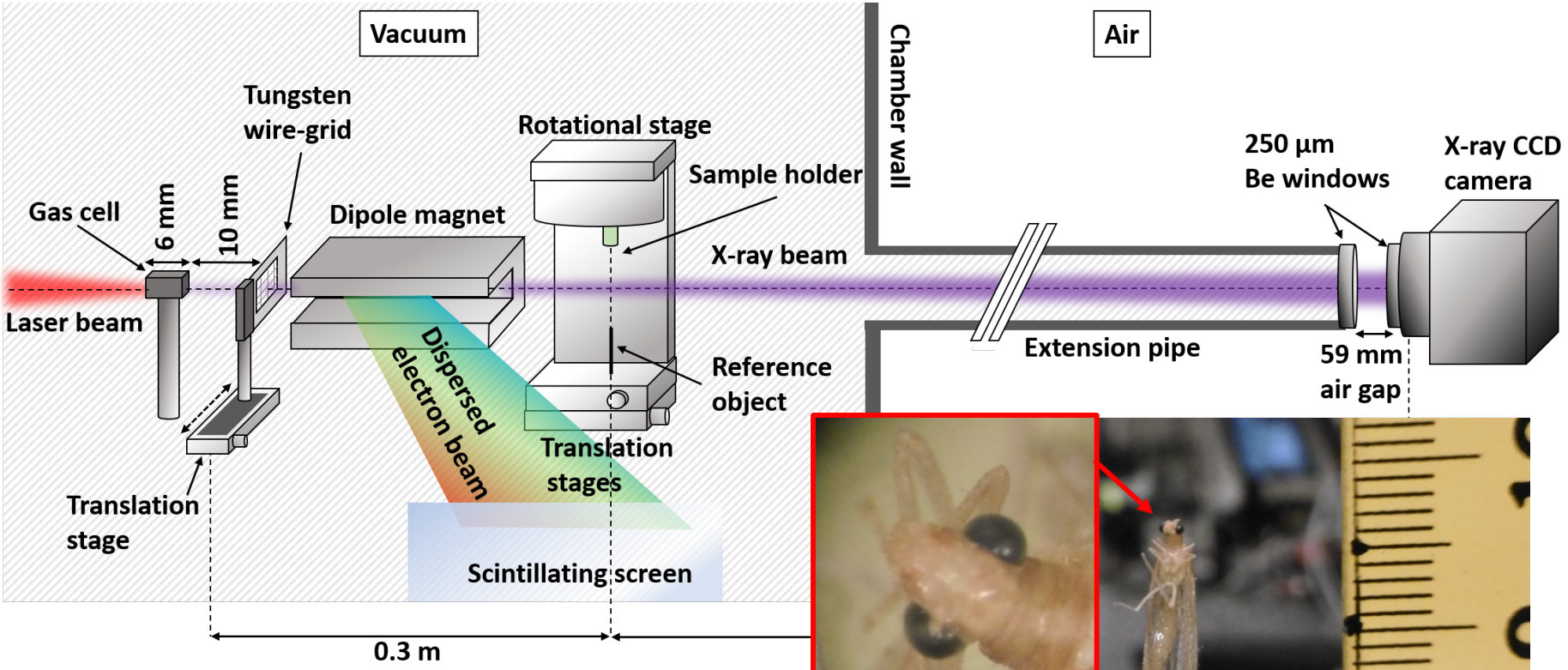

Kristoffer did the experiment

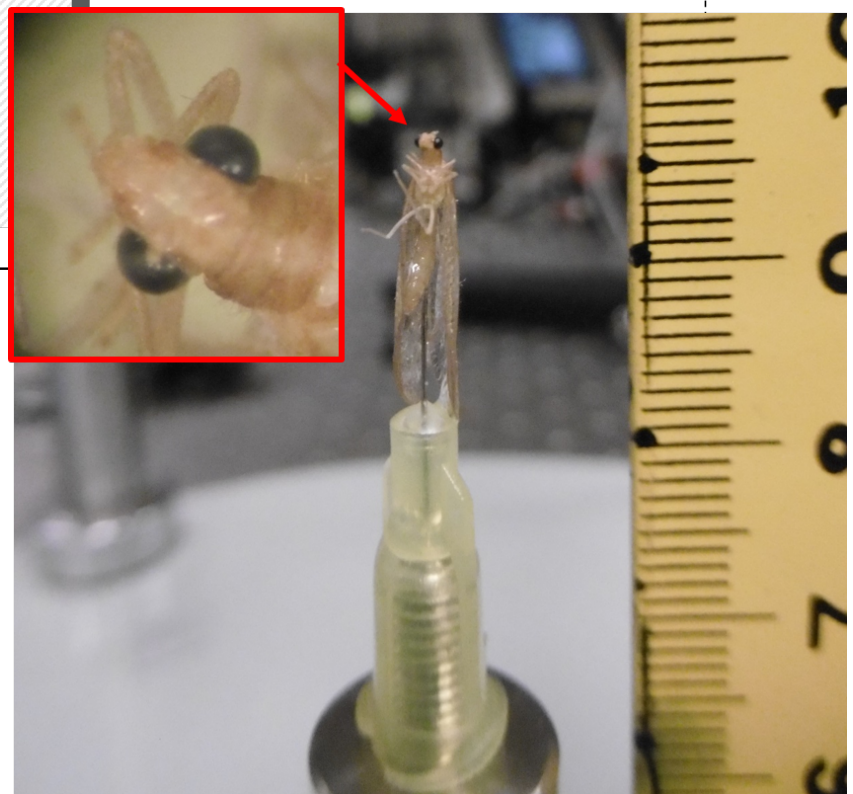

Phase-contrast tomography

Phase-contrast image

Phase-contrast image

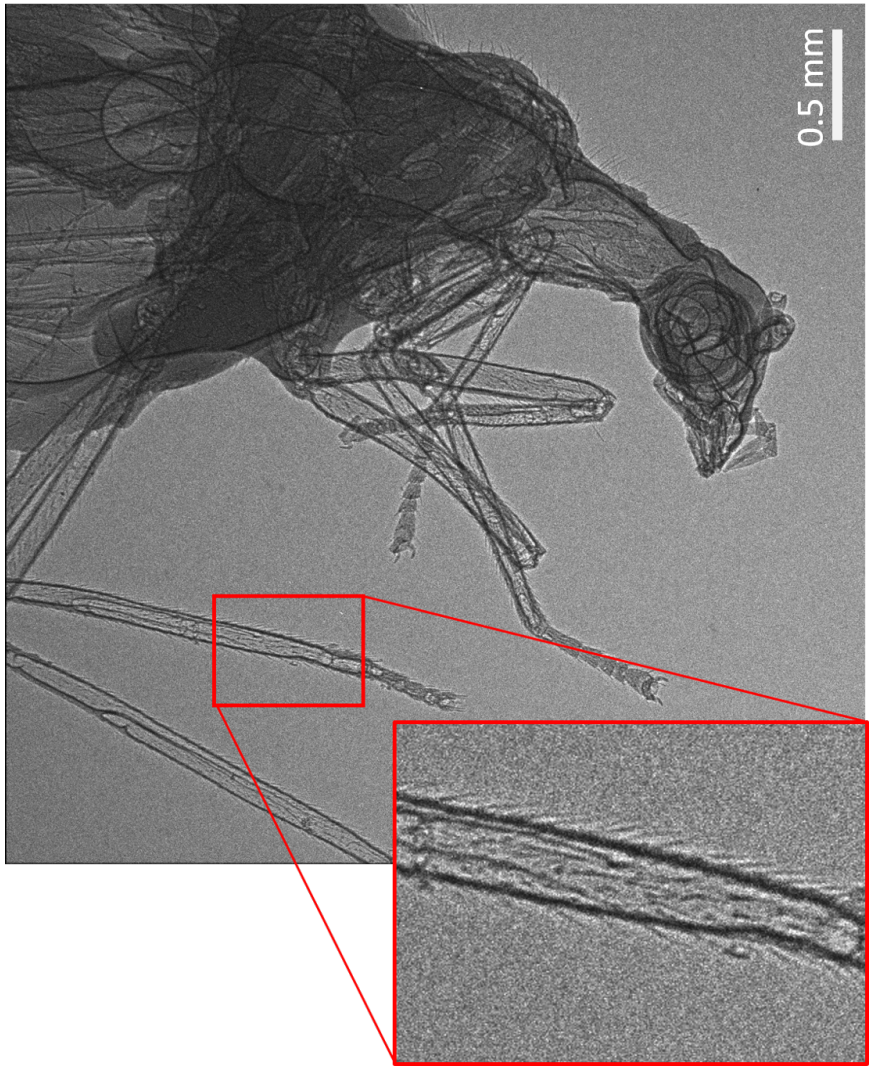

Projected thickness

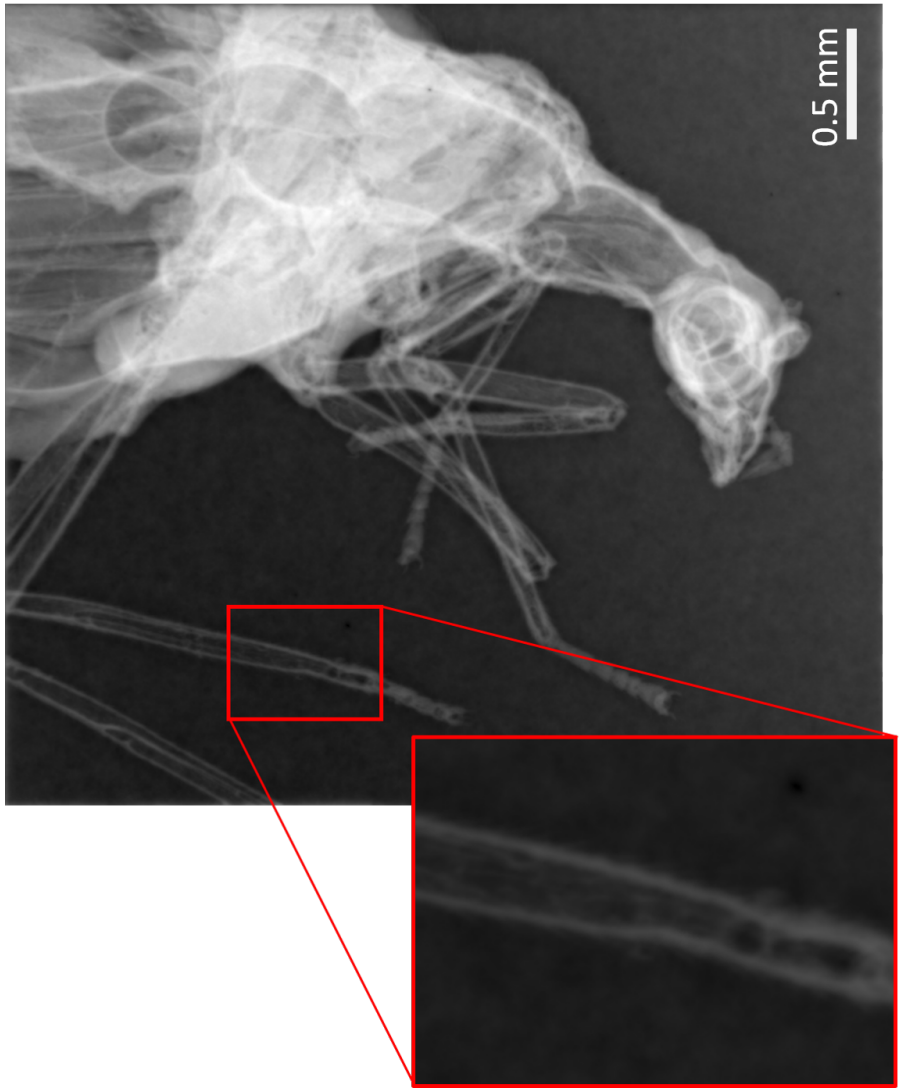

3D rendering

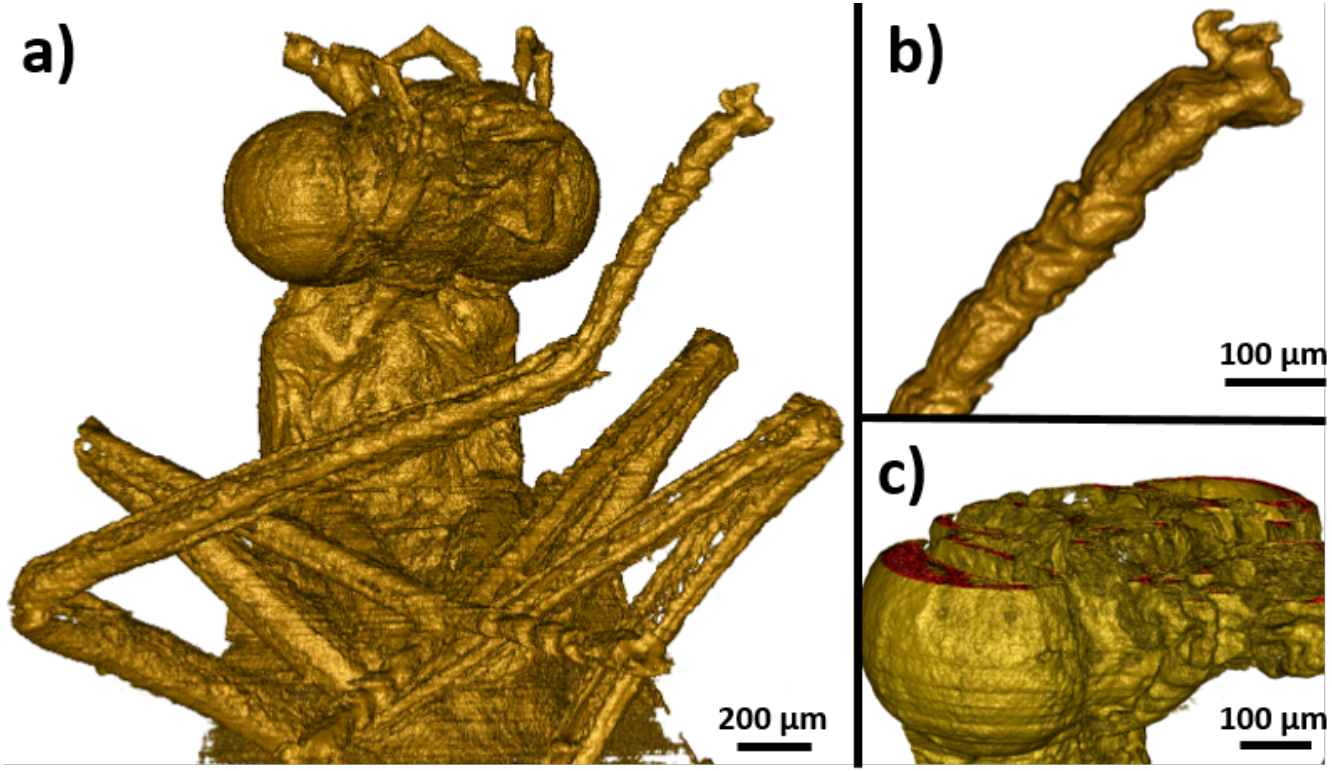

10 µm structures can be resolved in tomogram

K. Svendsen *et al*, Optics Express **26**, 33930 (2018)

Tomography for medical purposes

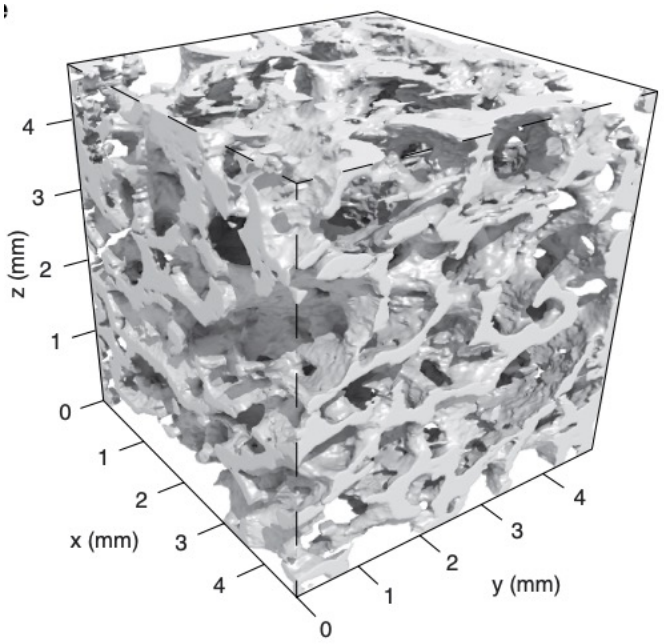

Tomographic reconstruction of trabecular bone sample
J M Cole *et al*, Sci Rep **5** (2015)

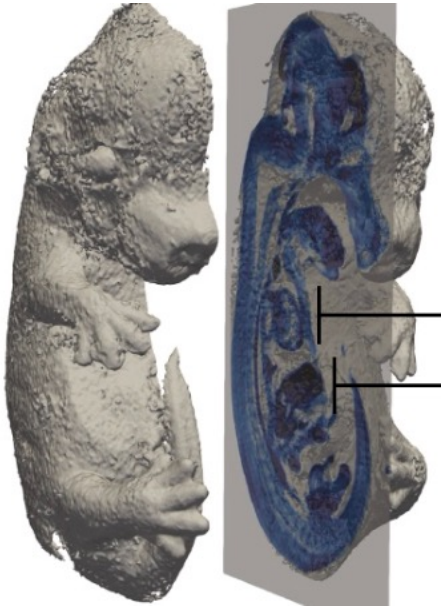

High-resolution μCT of a mouse embryo
J M Cole *et al*, PNAS **115** (2018)

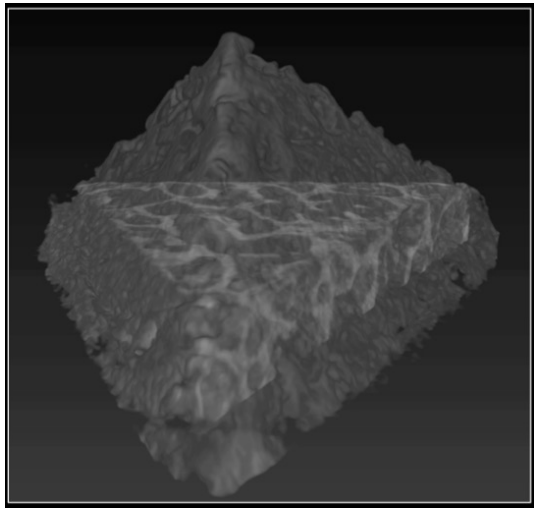

Quick micro-tomography
A Döpp *et al*, Optica **5** (2018)

Spray applications

Internal Combustion Engines Applications: Diesel and GDI sprays

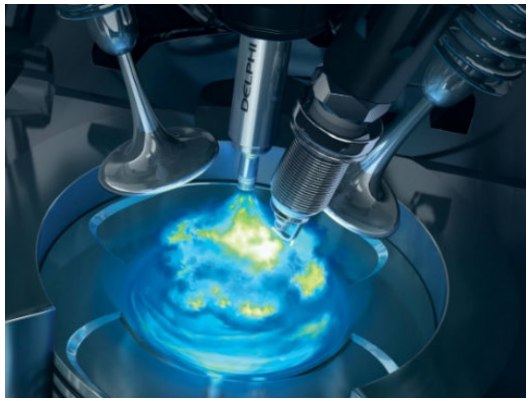


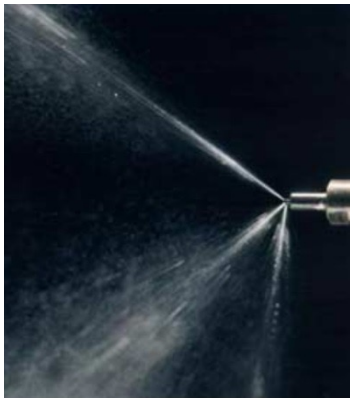
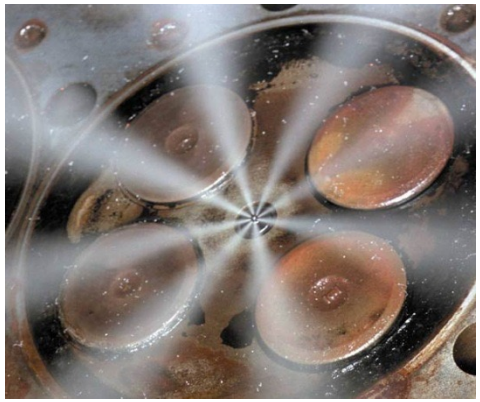

Gas Turbines Applications: Aero Engines

Spray imaging with laser plasma accelerator

Understanding breakup and atomization of sprays is essential for improving e.g. engine efficiencies.

Challenges Fast dynamics (ns to µs)
Highly scattering media
Multiple jets in the same spray

Approach **Mass flow:** X-ray imaging
Atomization: 2-photon LIF

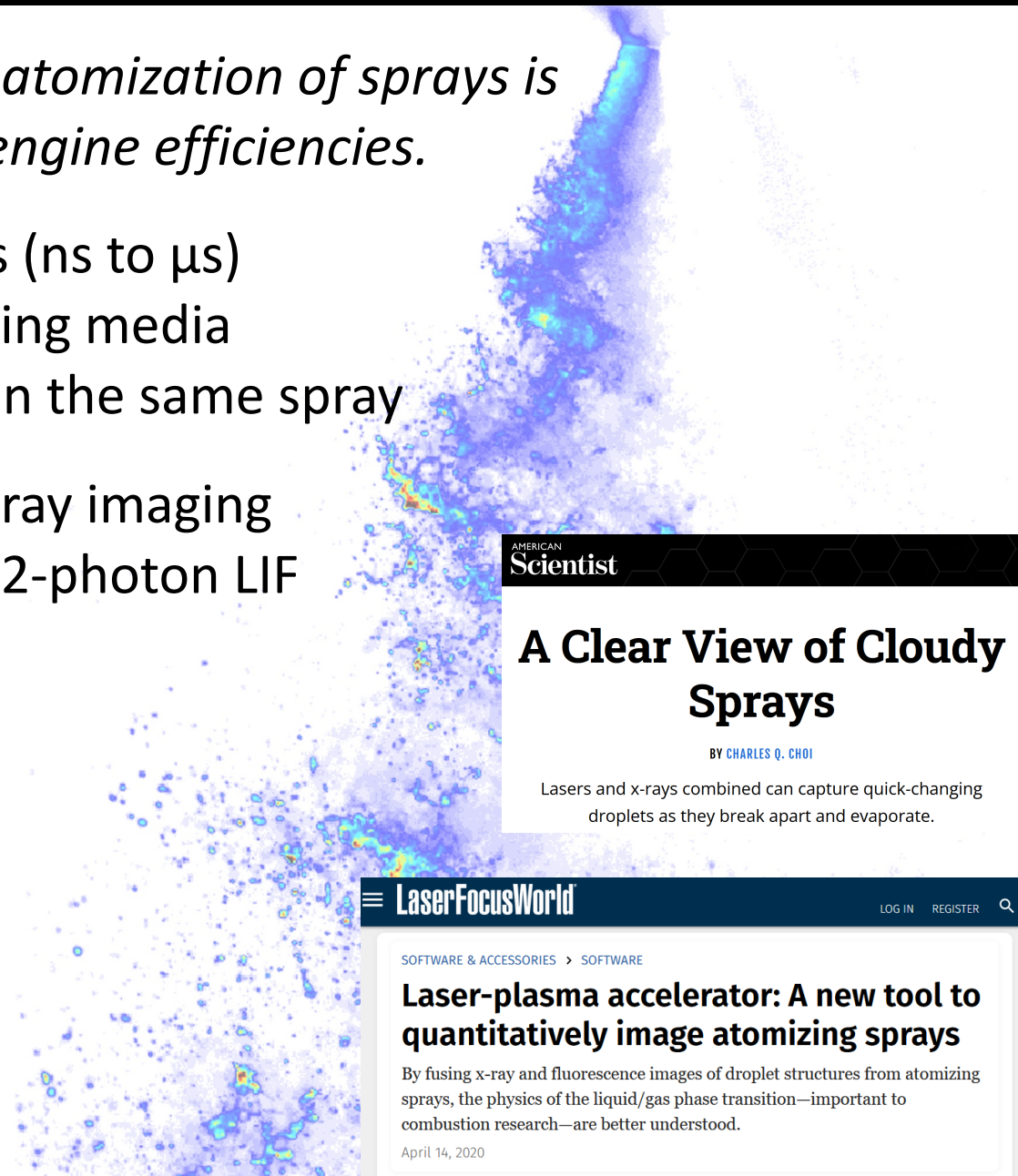

AMERICAN Scientist

A Clear View of Cloudy Sprays

BY CHARLES Q. CHOI

Lasers and x-rays combined can capture quick-changing droplets as they break apart and evaporate.

LaserFocusWorld LOG IN REGISTER

SOFTWARE & ACCESSORIES › SOFTWARE

Laser-plasma accelerator: A new tool to quantitatively image atomizing sprays

By fusing x-ray and fluorescence images of droplet structures from atomizing sprays, the physics of the liquid/gas phase transition—important to combustion research—are better understood.

April 14, 2020

Atomizing sprays

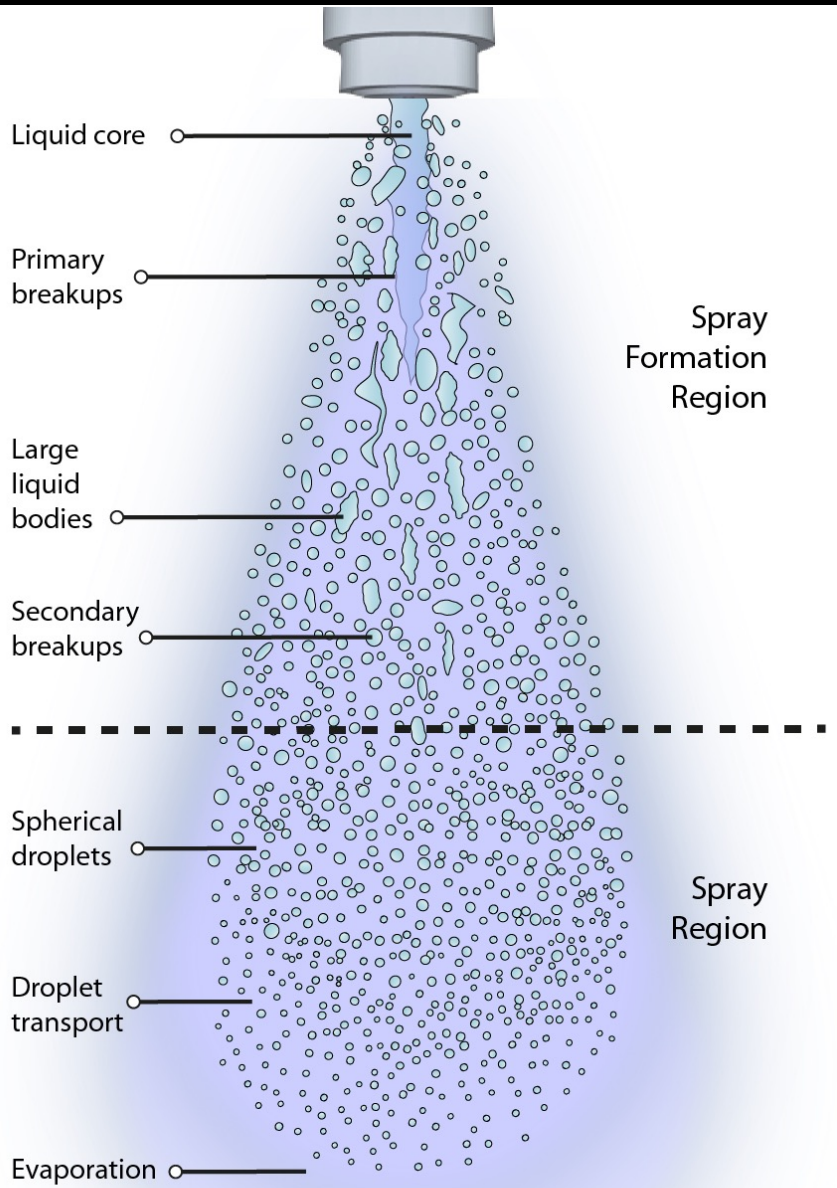

Atomizing sprays

Optical Depth

$$I_t = I_i \cdot \exp(-OD)$$

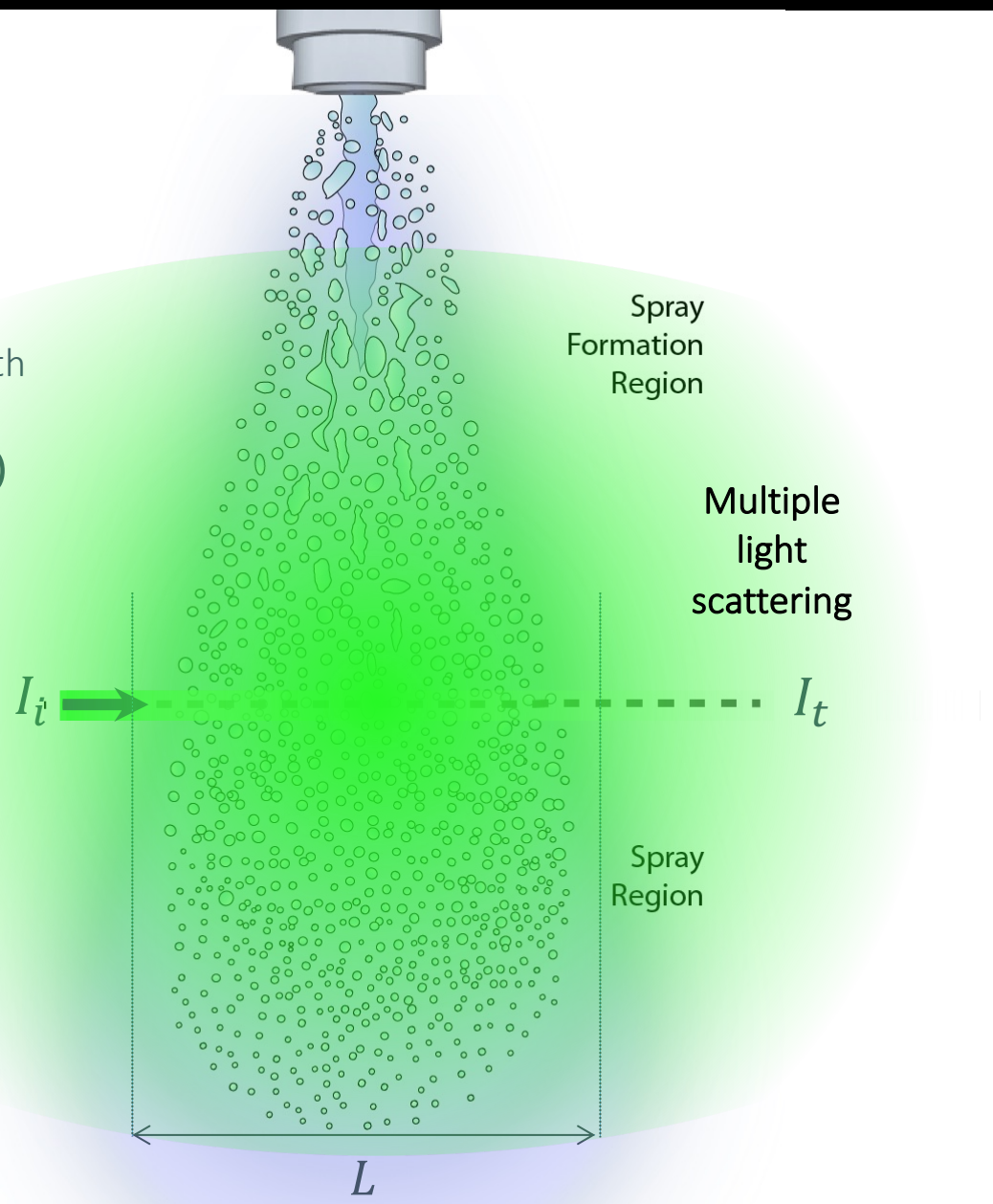

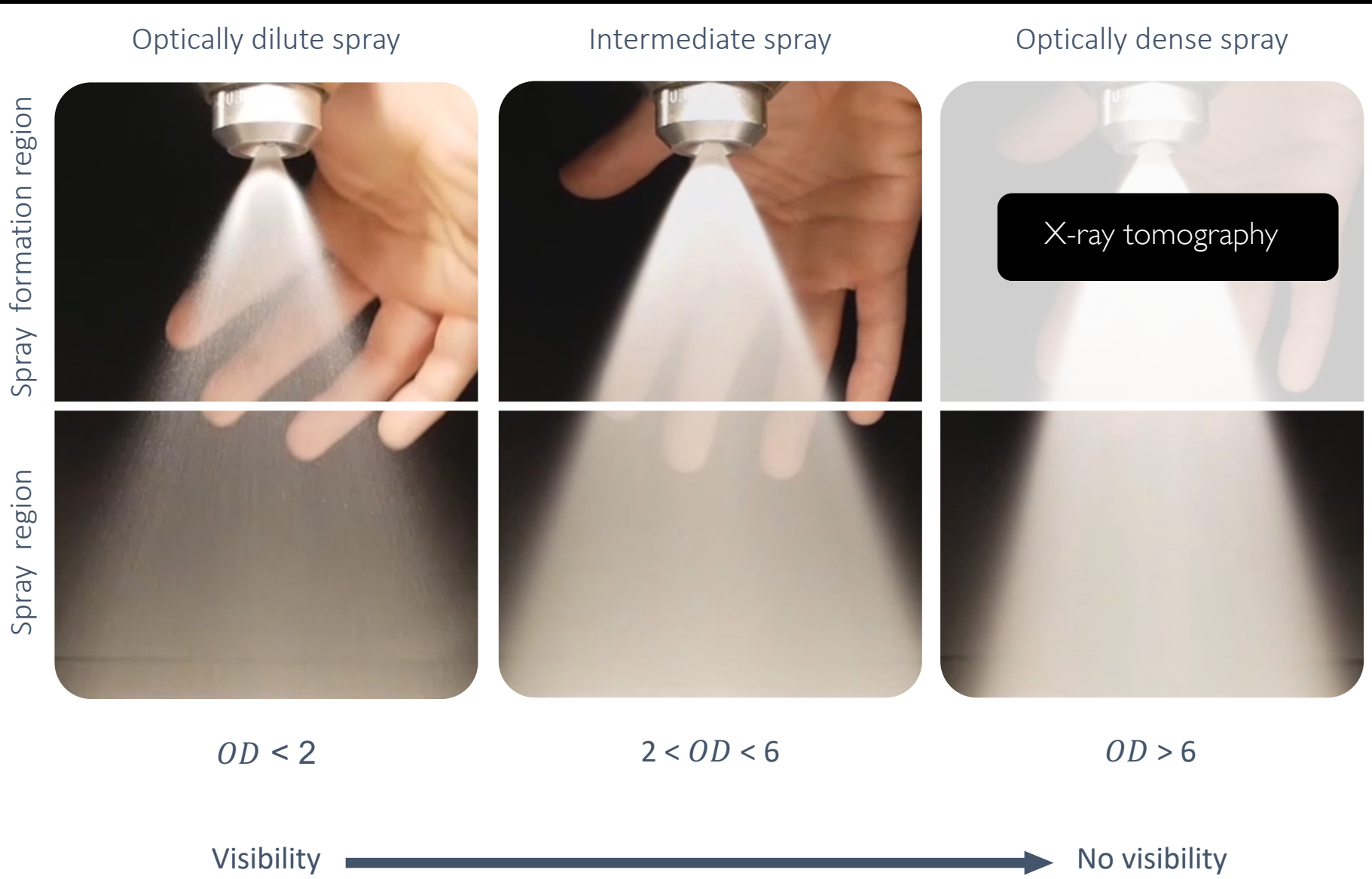
Optically dilute spray
Intermediate spray
Optically dense spray
Spray formation region
Spray region
X-ray tomography
$OD < 2$
$2 < OD < 6$
$OD > 6$
Visibility
No visibility

Experimental setup

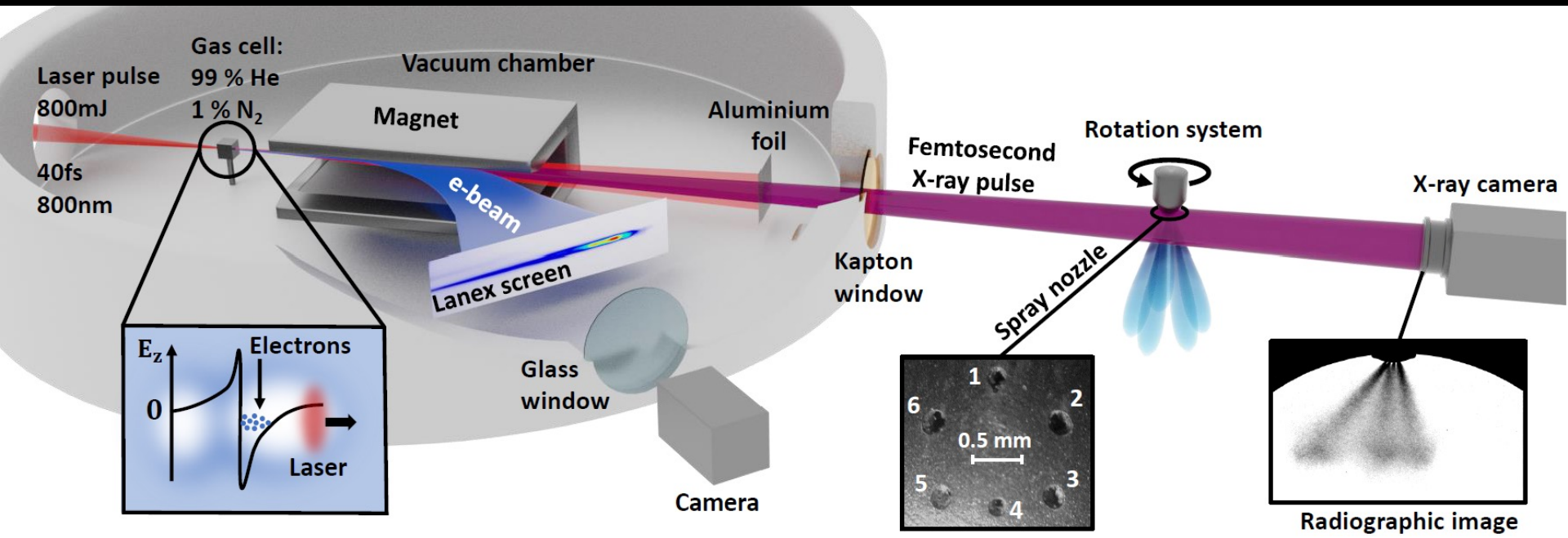

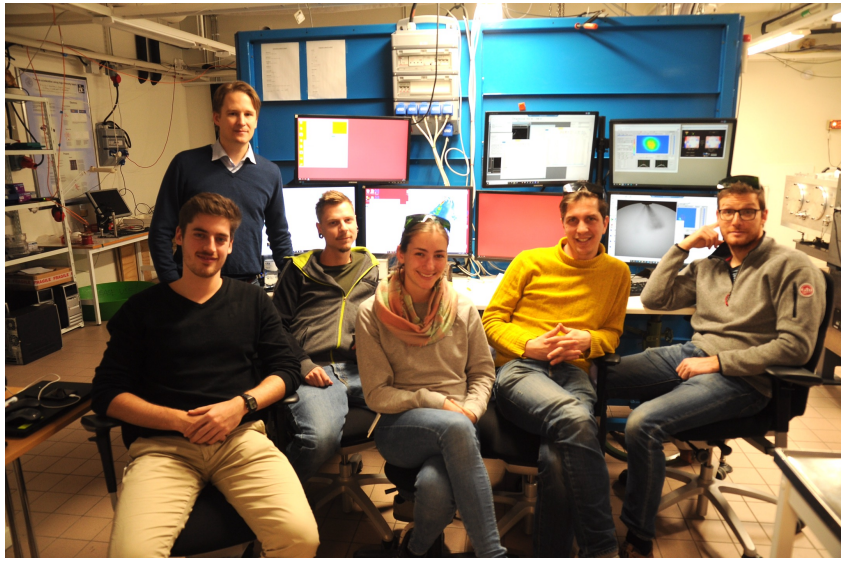

X-ray absorption

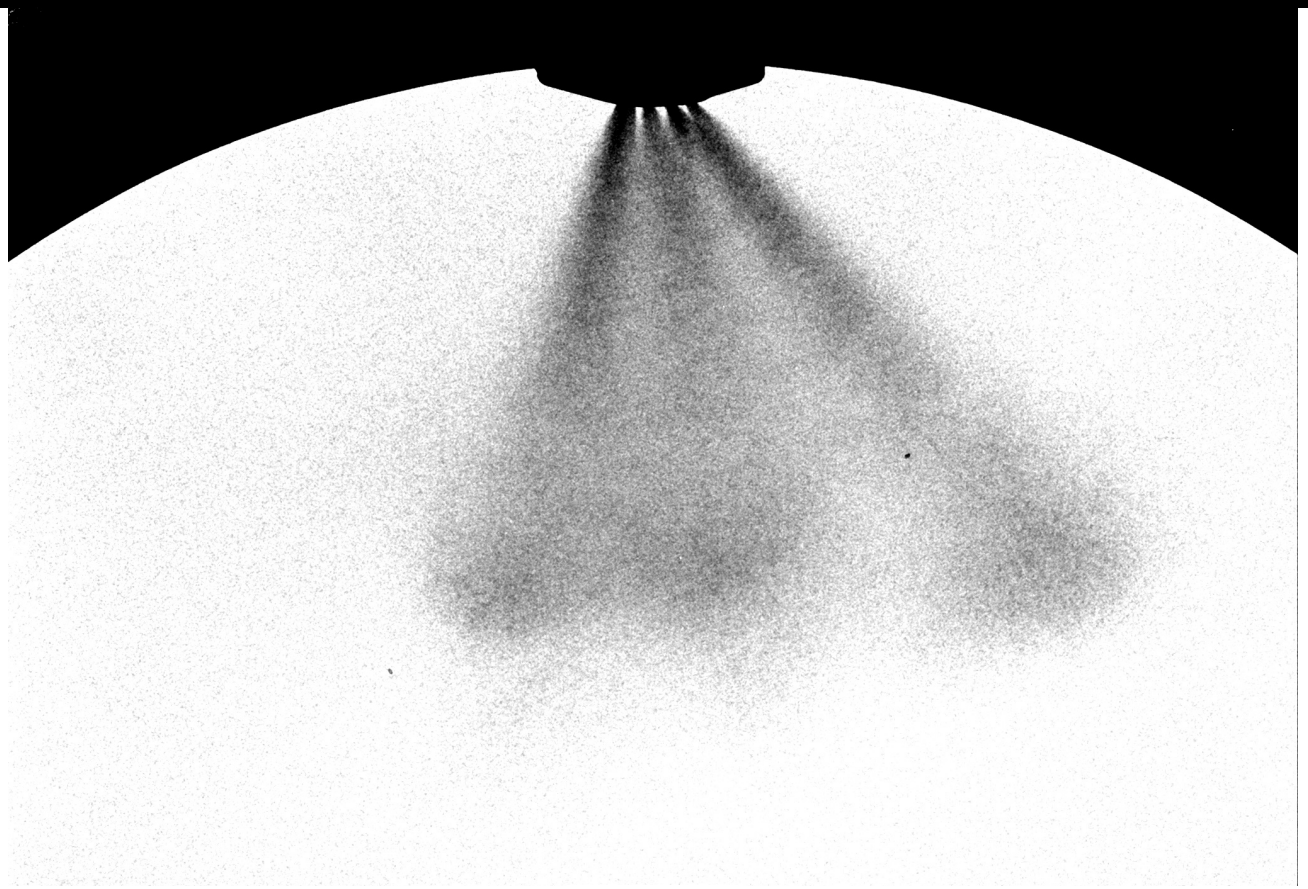

80°

Transient spray tomography

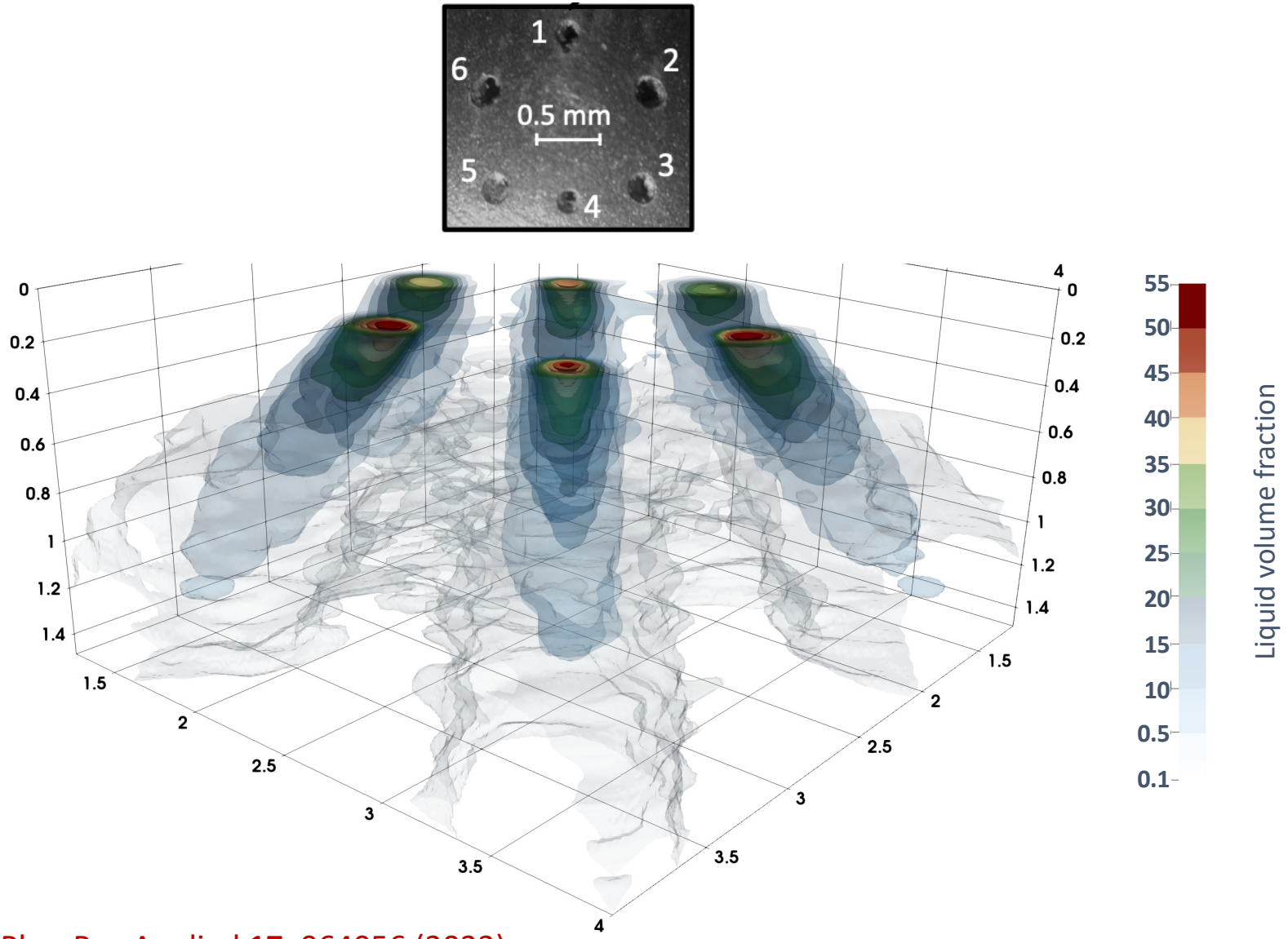

D. Guenot *et al*, Phys Rev Applied **17**, 064056 (2022)

H. Ulrich *et al*, Phys of Fluids **34**, 083305 (2022)

Combining X-rays and flourescence

2-photon laser-induced flourescence

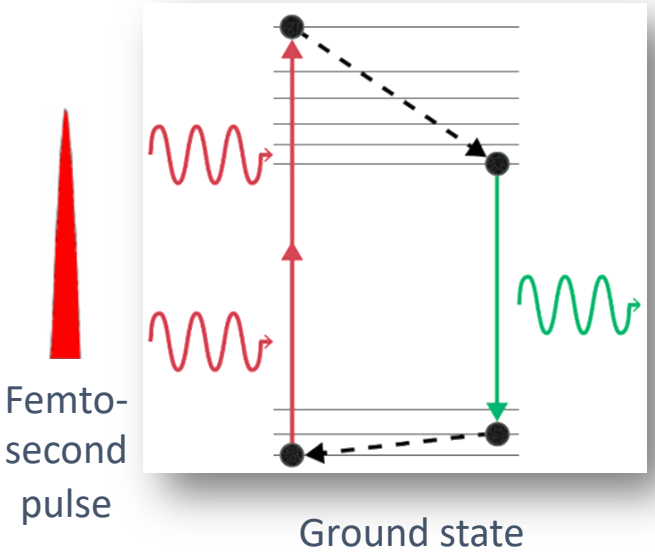

Technique developed by
Edouard Berrocal (Lund University)

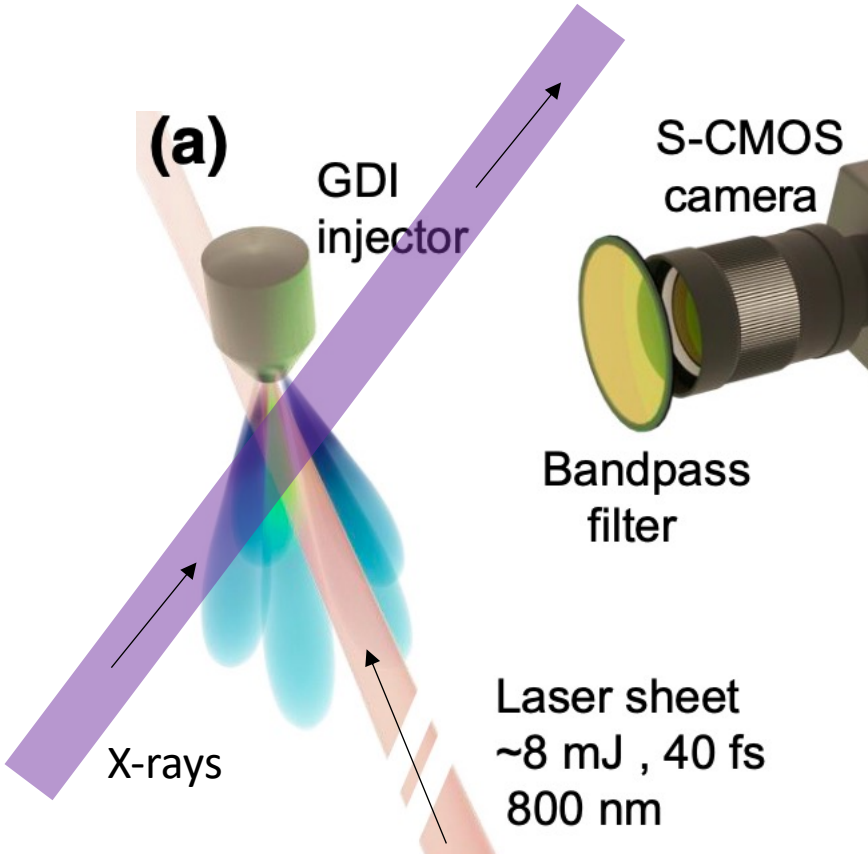

Simultaneous recordings

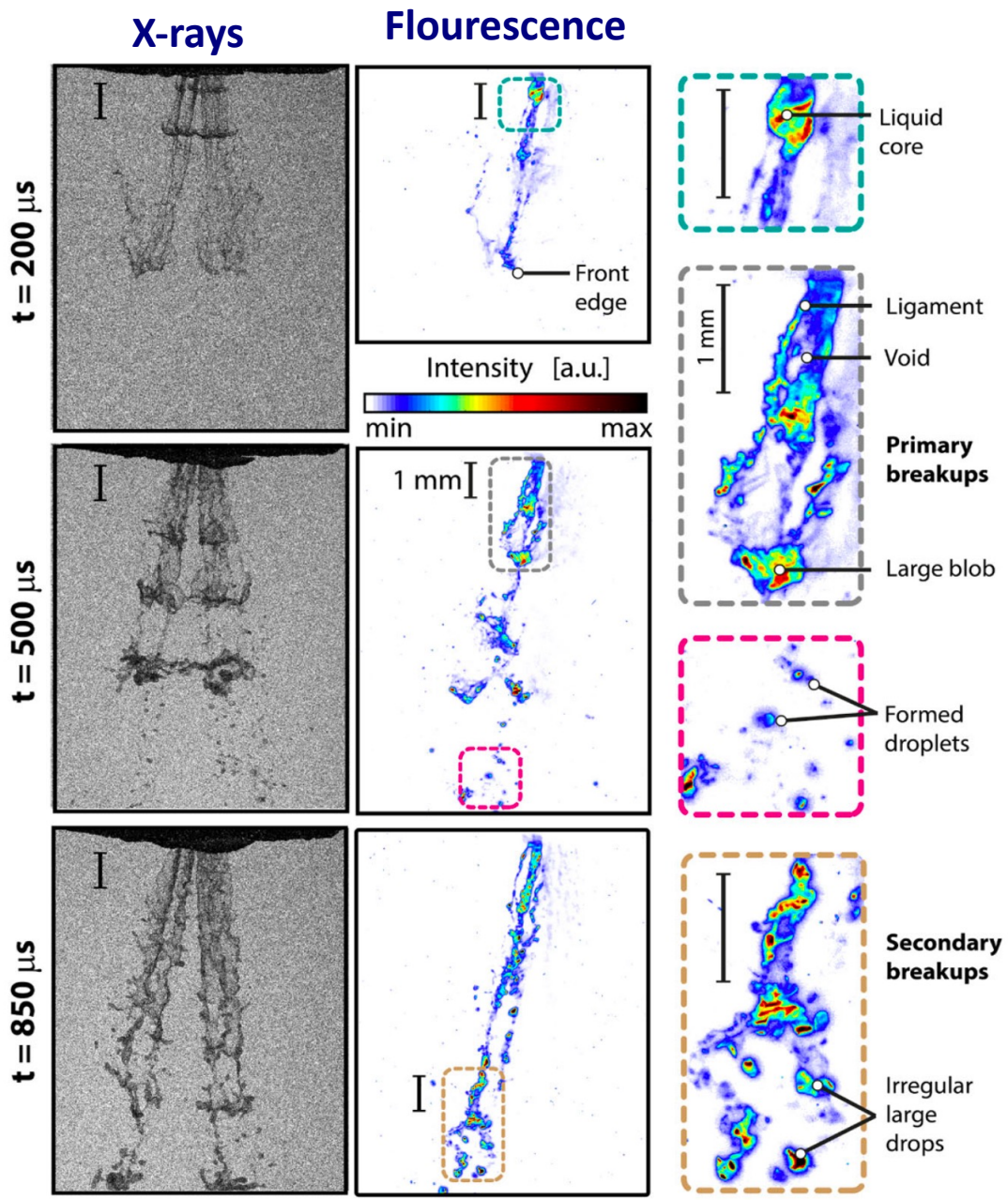

Diego Guenot *et al*,
Optica **7**, 131-134 (2020)

Outline

Laser-accelerated electron beams for radiotherapy

Betatron X-rays for imaging and spectroscopy

Other light sources based on plasma accelerators

Probing warm dense matter using XANES

WDM (Warm dense matter) lies between solid and plasma with a temperature of a few 10^4 K. It is a subject of increased interest due to its importance for planetary physics, inertial confinement fusion research, and material science.

XANES (X-ray absorption near-edge structure) is an essential tool to study the electronic and atomic structural properties of matter.

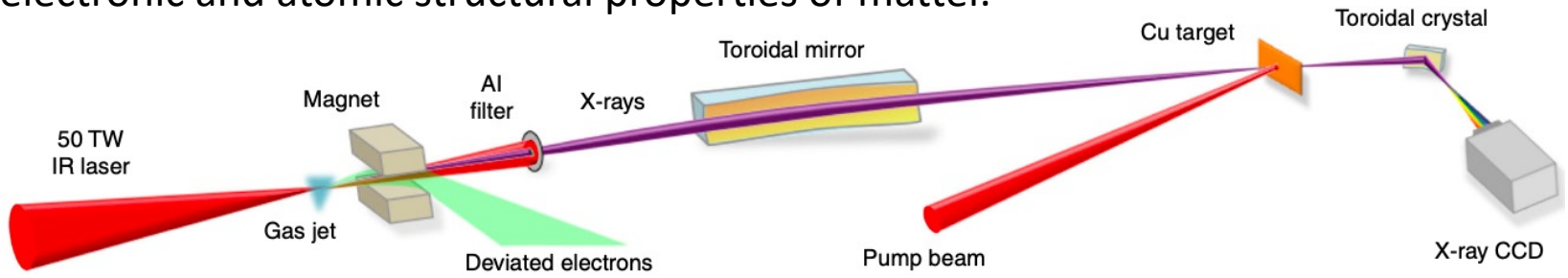

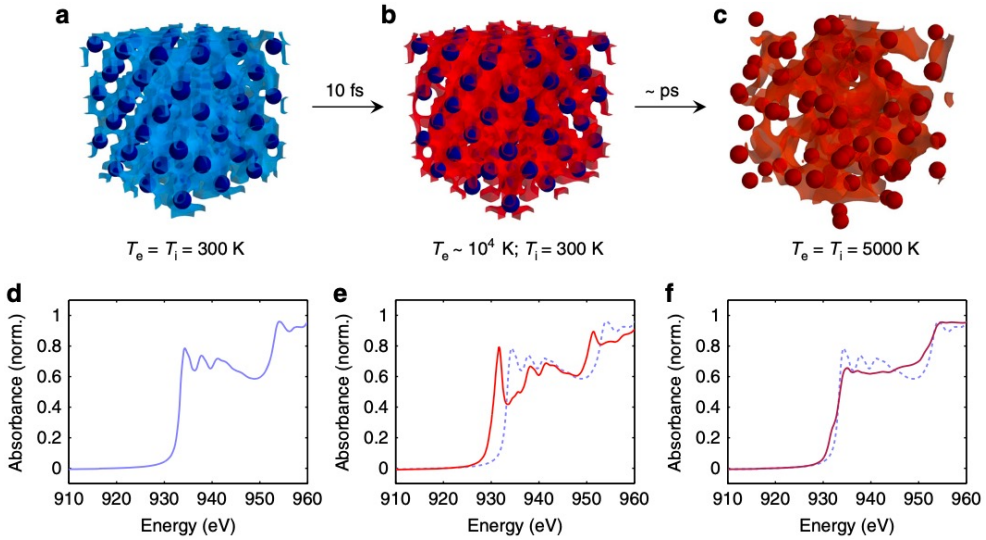

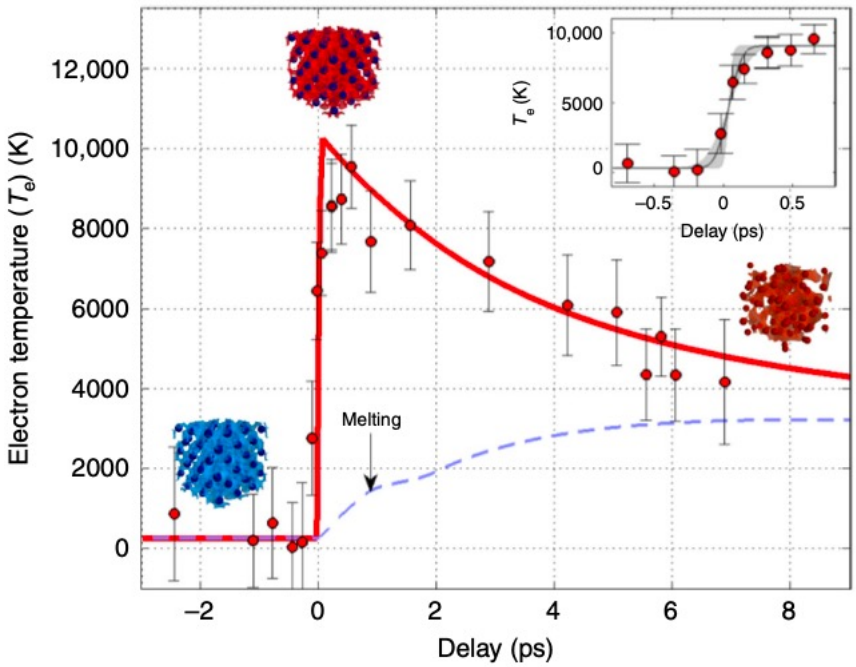

B Mahieu *et al*, Nature Commun **9**, 3276 (2018)

Towards Ultrafast X-ray Spectroscopy

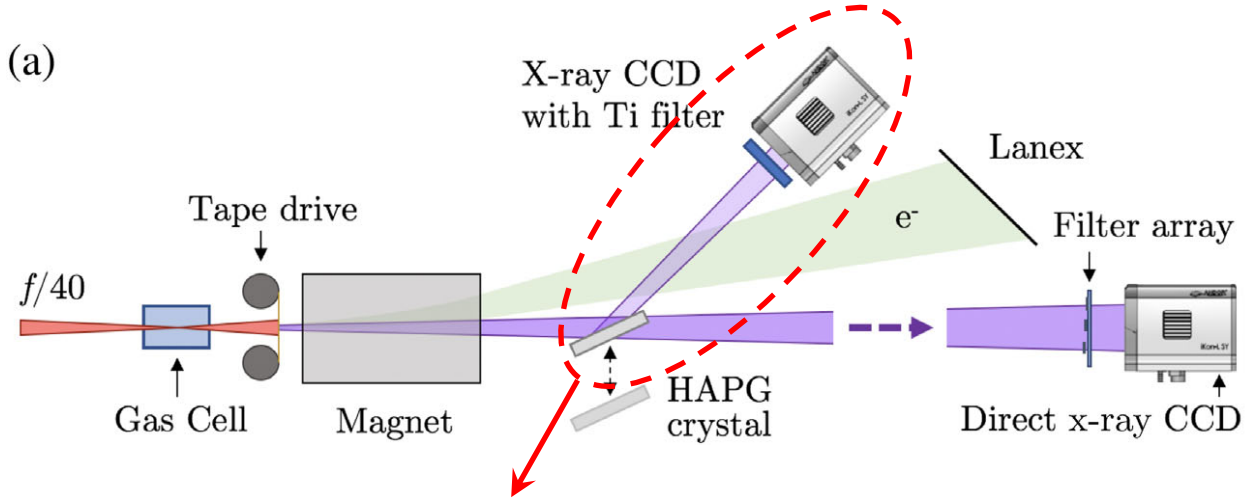

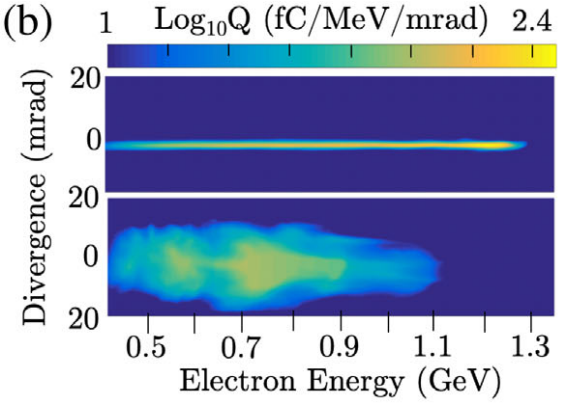

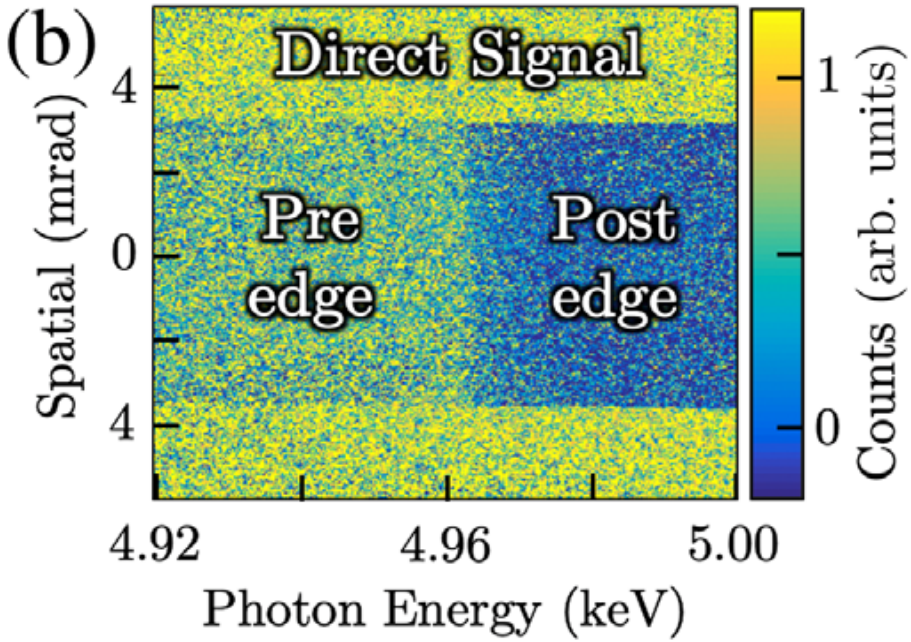

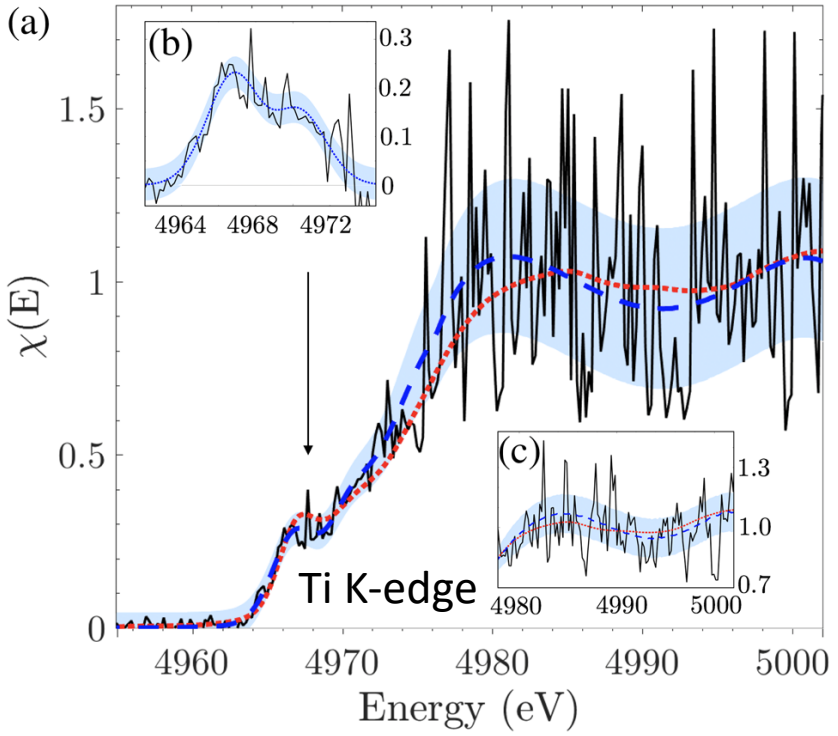

Kettle *et al*, Phys Rev Lett 123, 254801 (2019)

Outline

Laser-accelerated electron beams for radiotherapy

Betatron X-rays for imaging and spectroscopy

Other light sources based on plasma accelerators

Hard X-rays from Compton scattering

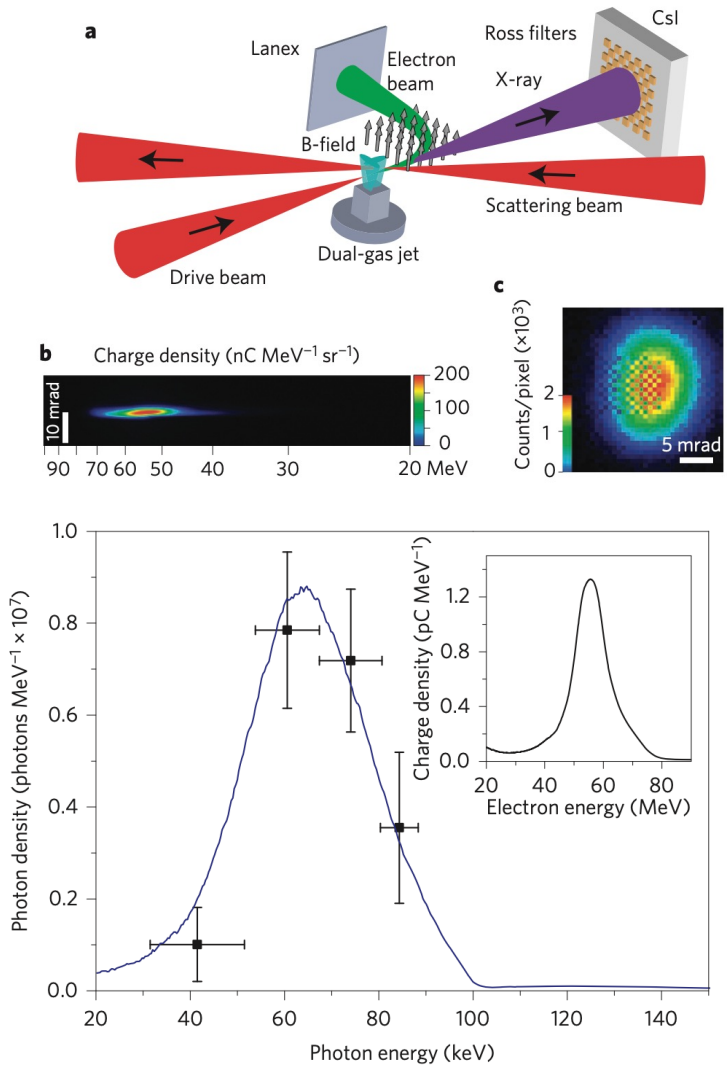

N D Powers *et al*, Nature Photonics **8**, 28–31 (2014)

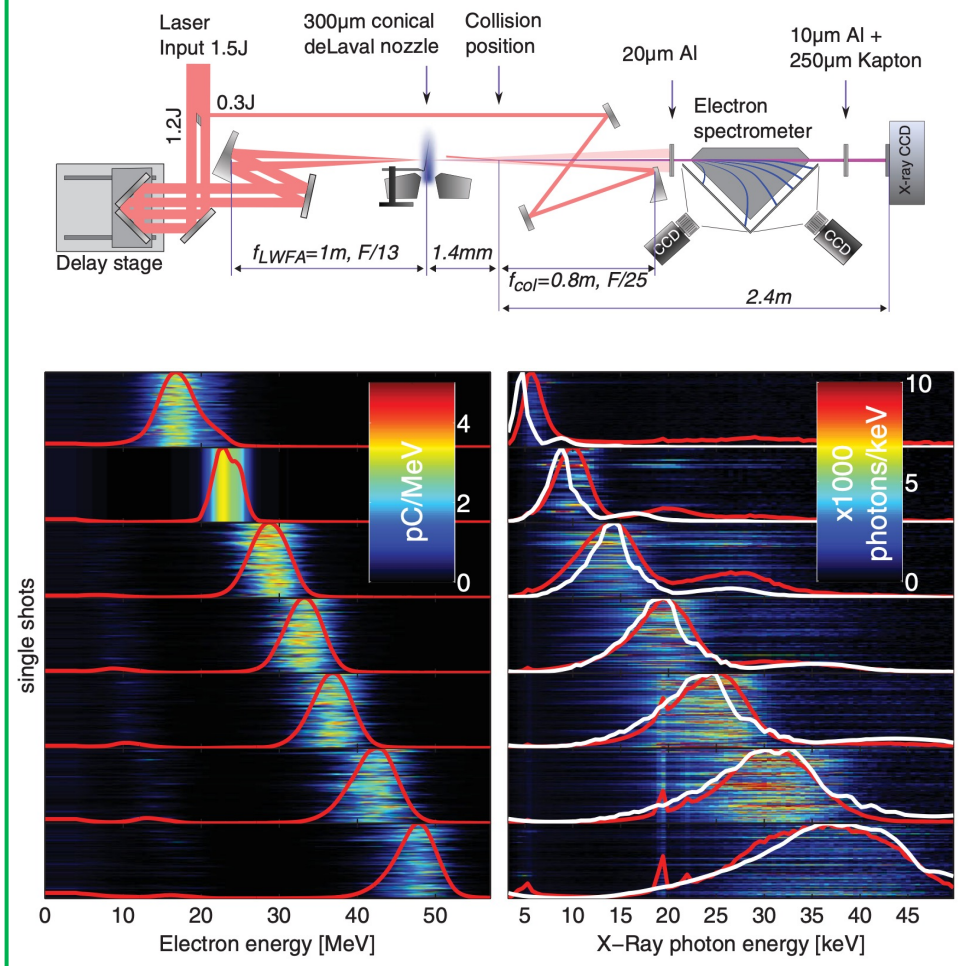

K Khrennikov *et al*, PRL 114, 195003 (2015)

Compton scattering using only one laser beam

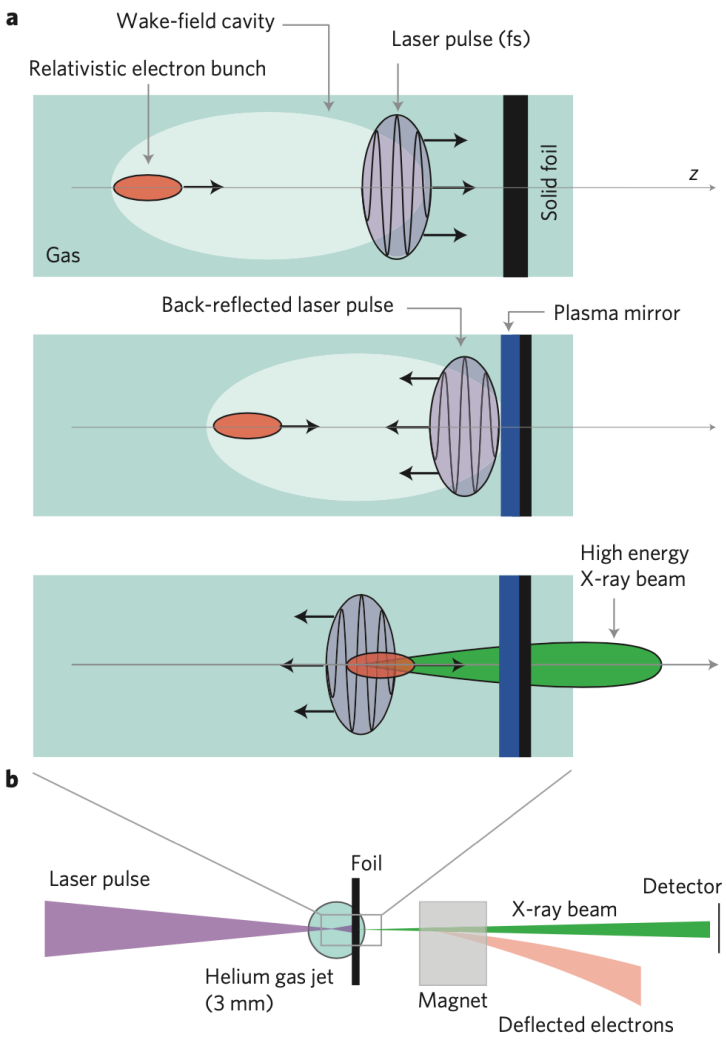

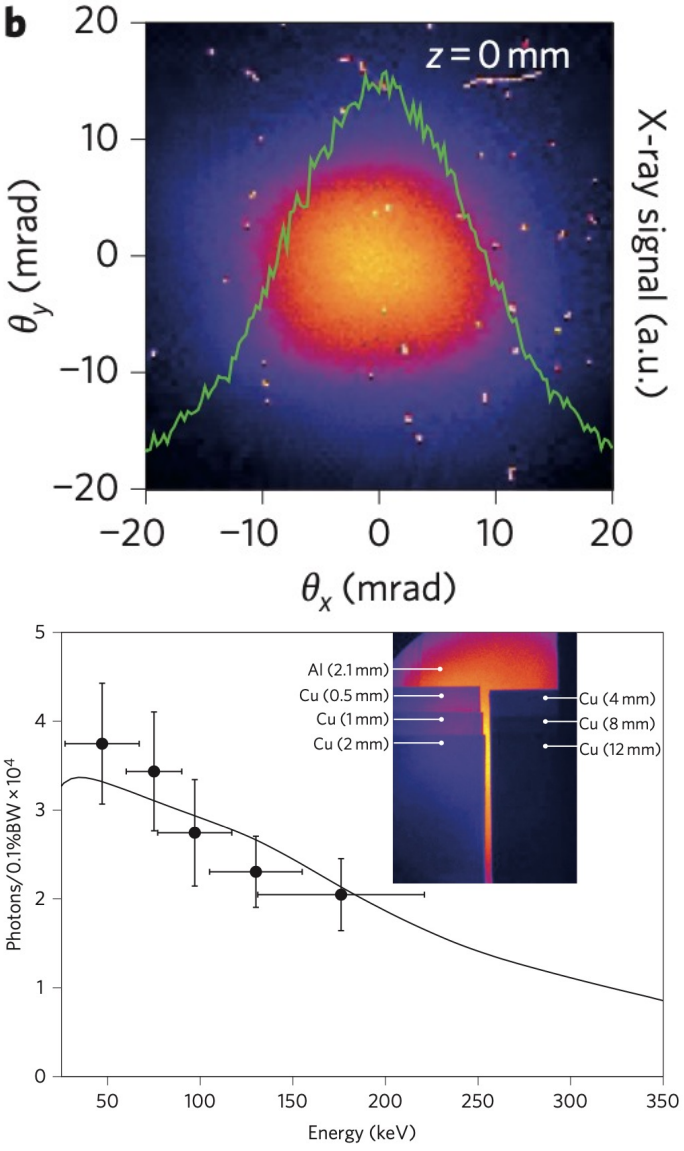

K Ta Phuoc *et al*, Nature Photonics **6**, 308–311 (2012)

Gamma-ray source for radiography

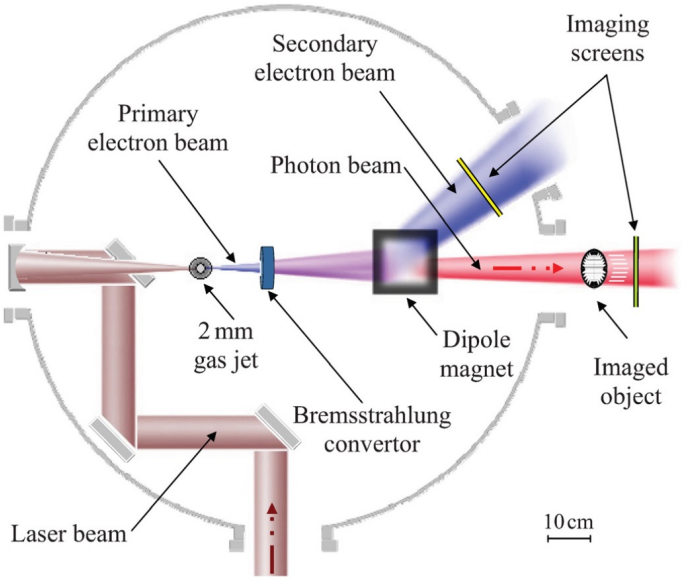

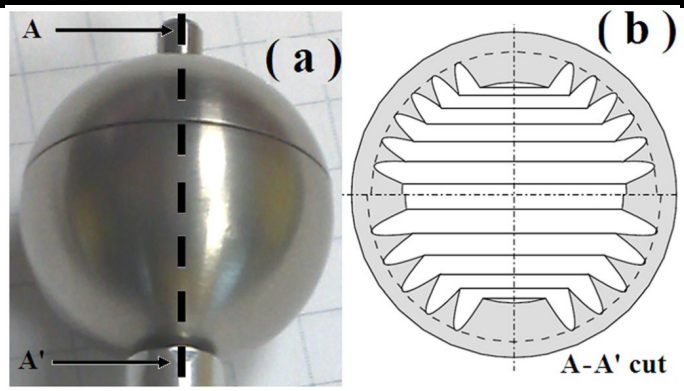

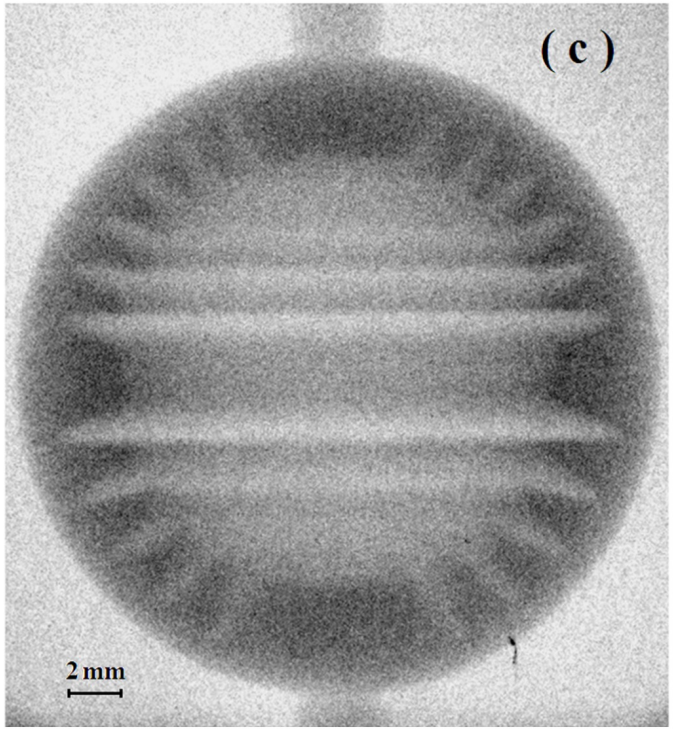

- Laser: 30 TW, 30 fs laser
- Electrons: 100 MeV, 70 pC
- 1 mm tantalum Bremsstrahlung converter
- Image plate detector
- Copper foil enhances gamma detection (converts gamma-rays to low-E electrons)

Radiograph of a dense hollow sphere
(20 mm diameter tungsten)

A Ben-Ismail *et al*, Appl. Phys. Lett. **98**, 264101 (2011)

Laser-driven soft-X-ray undulator source

$$\lambda = \frac{\lambda_u}{2n\gamma^2}\left(1 + \frac{K^2}{2} + \gamma^2\Theta^2\right)$$

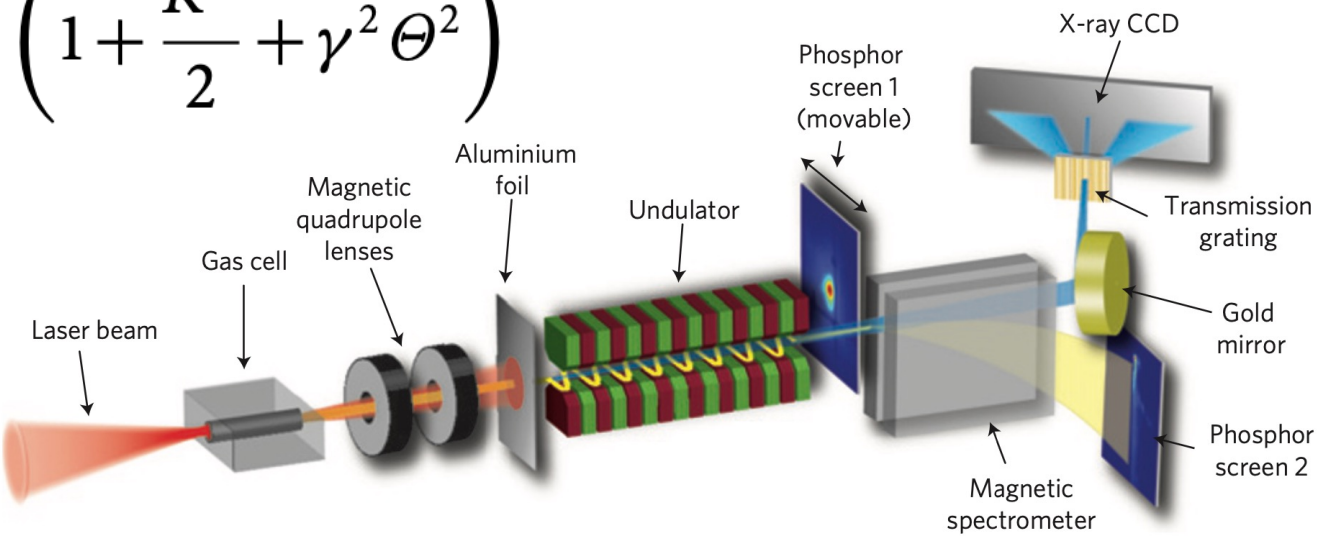

Scaling with observation angle

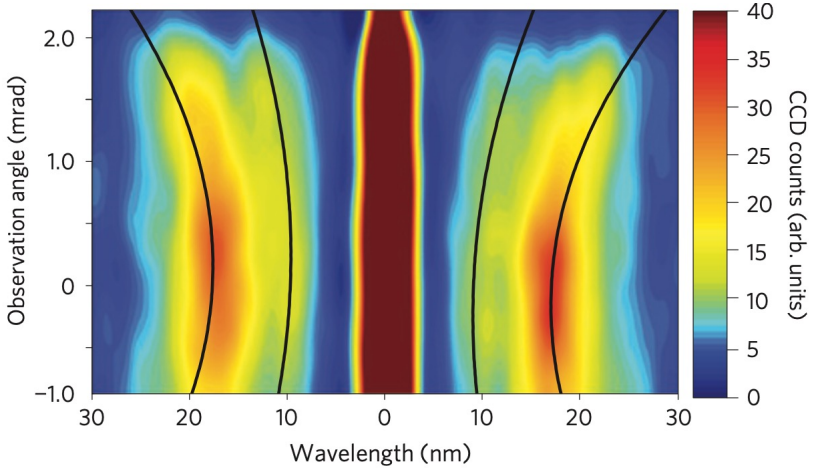

Scaling with electron energy

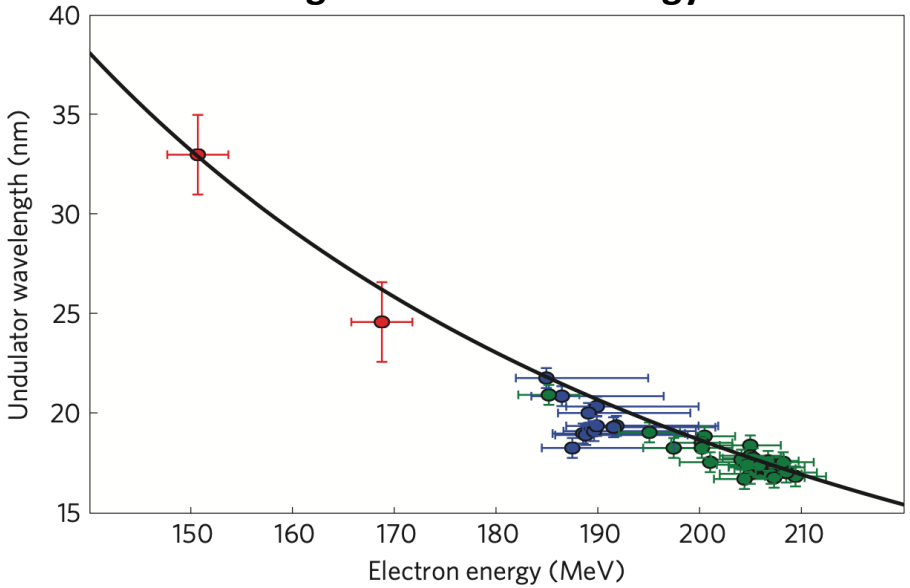

M Fuchs *et al,* Nature Physics **5**, 826–829 (2009)

Coherent radiation from an undulator

Electrons in a bunch passing through an undulator can interact with the radiation produced by other electrons within the bunch so that "microbunches" start to develop, which gives an exponential increase in the radiation intensity with distance along the undulator.

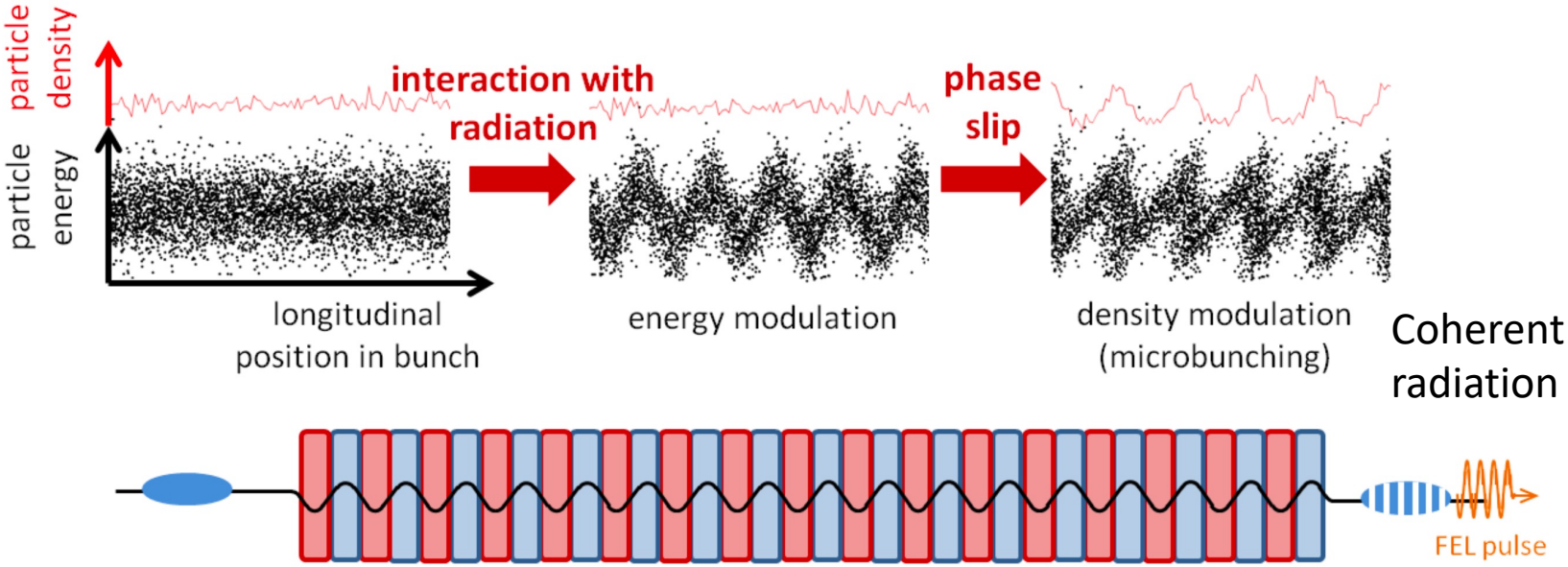

To achieve gain require exceptional electron beams with **simultaneously**

- High peak current (kA)
- Low normalized emittance (<1 mm mrad)
- Low energy spread (<1%)

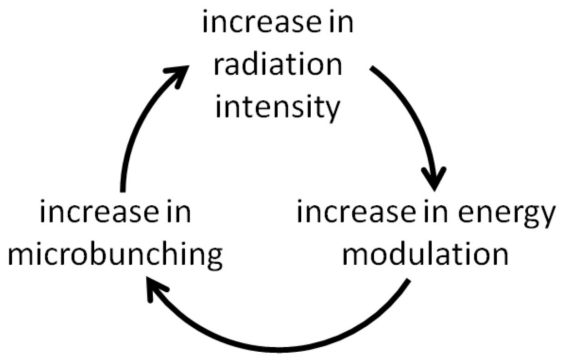

Slide: A Wolski, CAS 2012

Laser-driven FEL

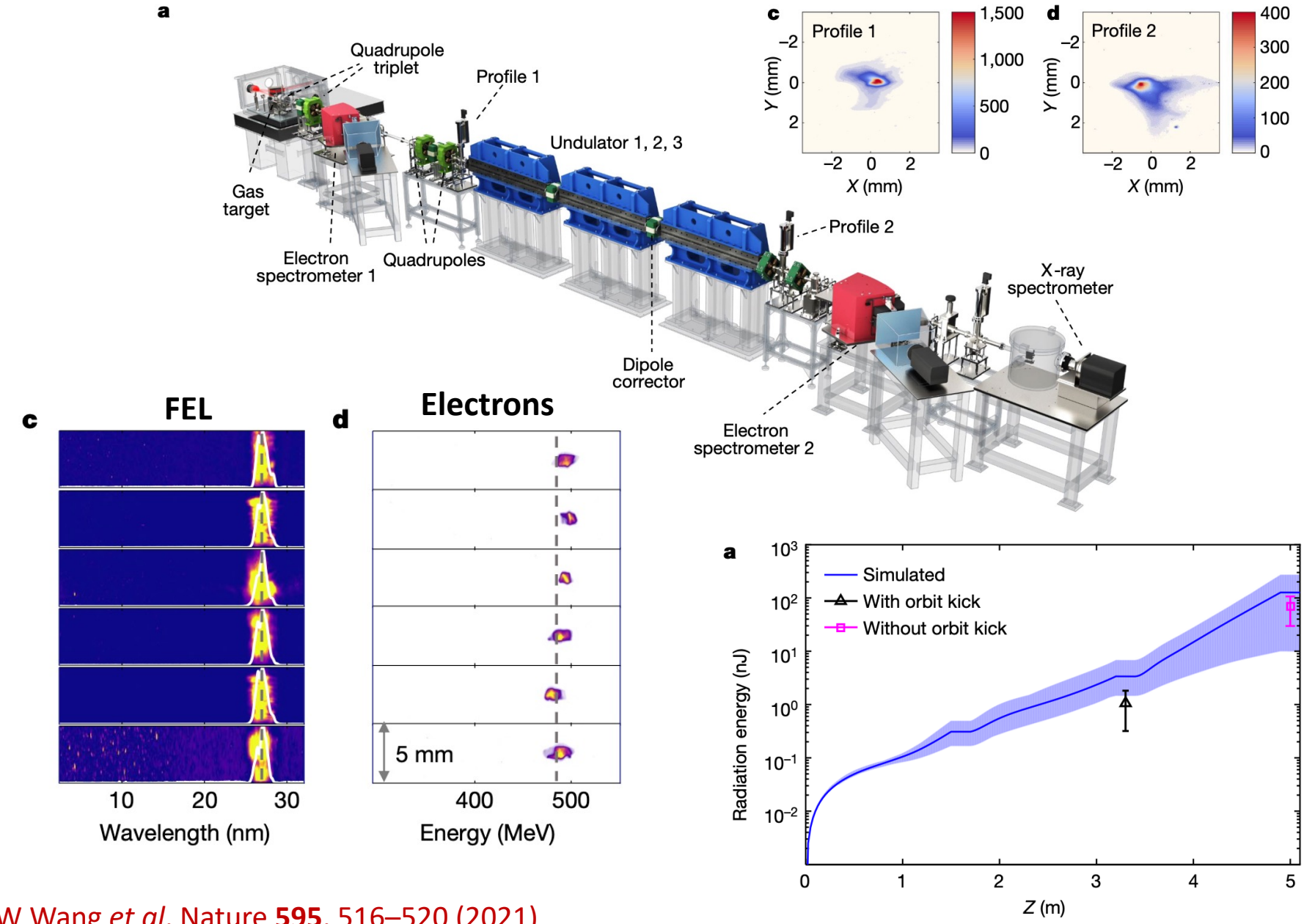

W Wang *et al*, Nature **595**, 516–520 (2021)

Beam-driven FEL

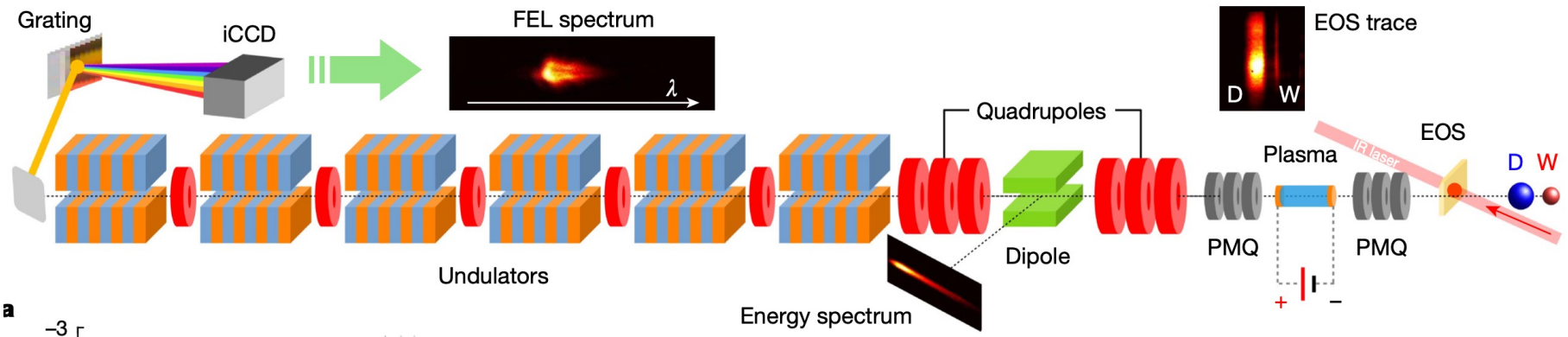

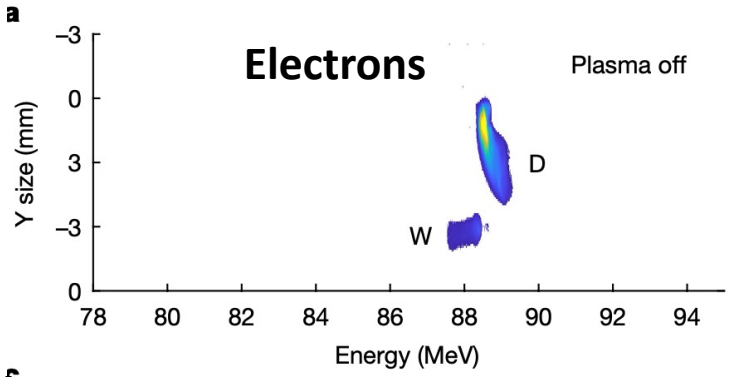

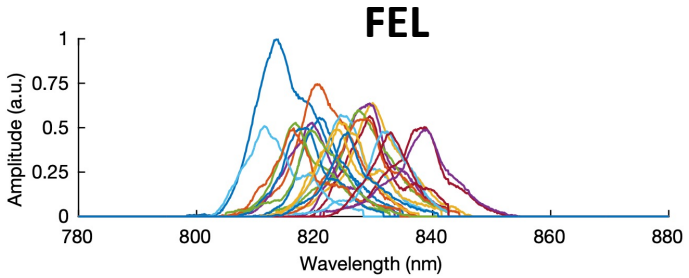

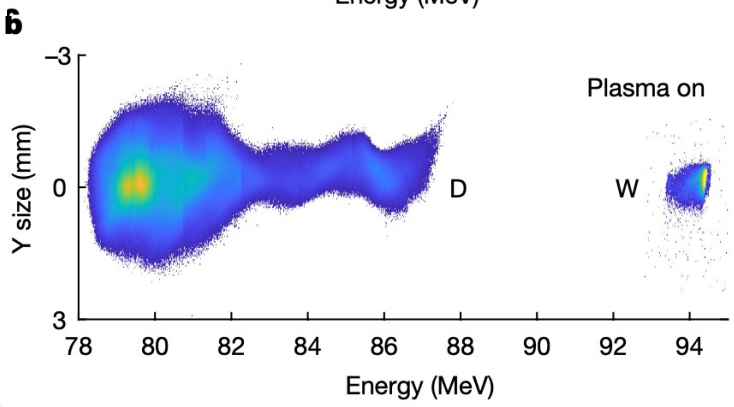

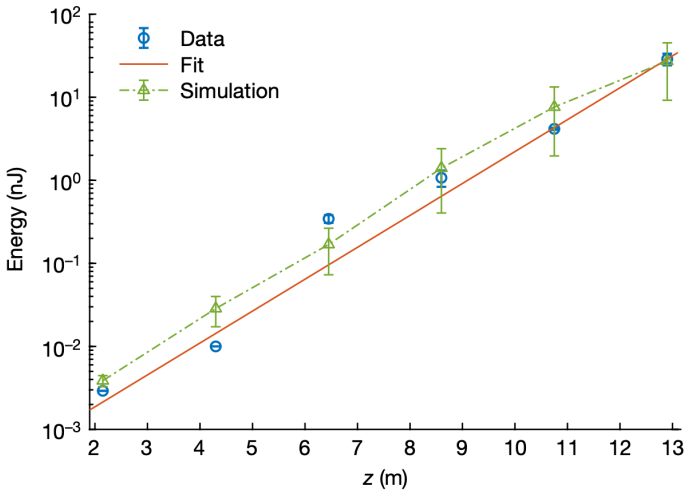

R Pompili *et al*, Nature **605**, 659–662 (2022)

Seeded FEL

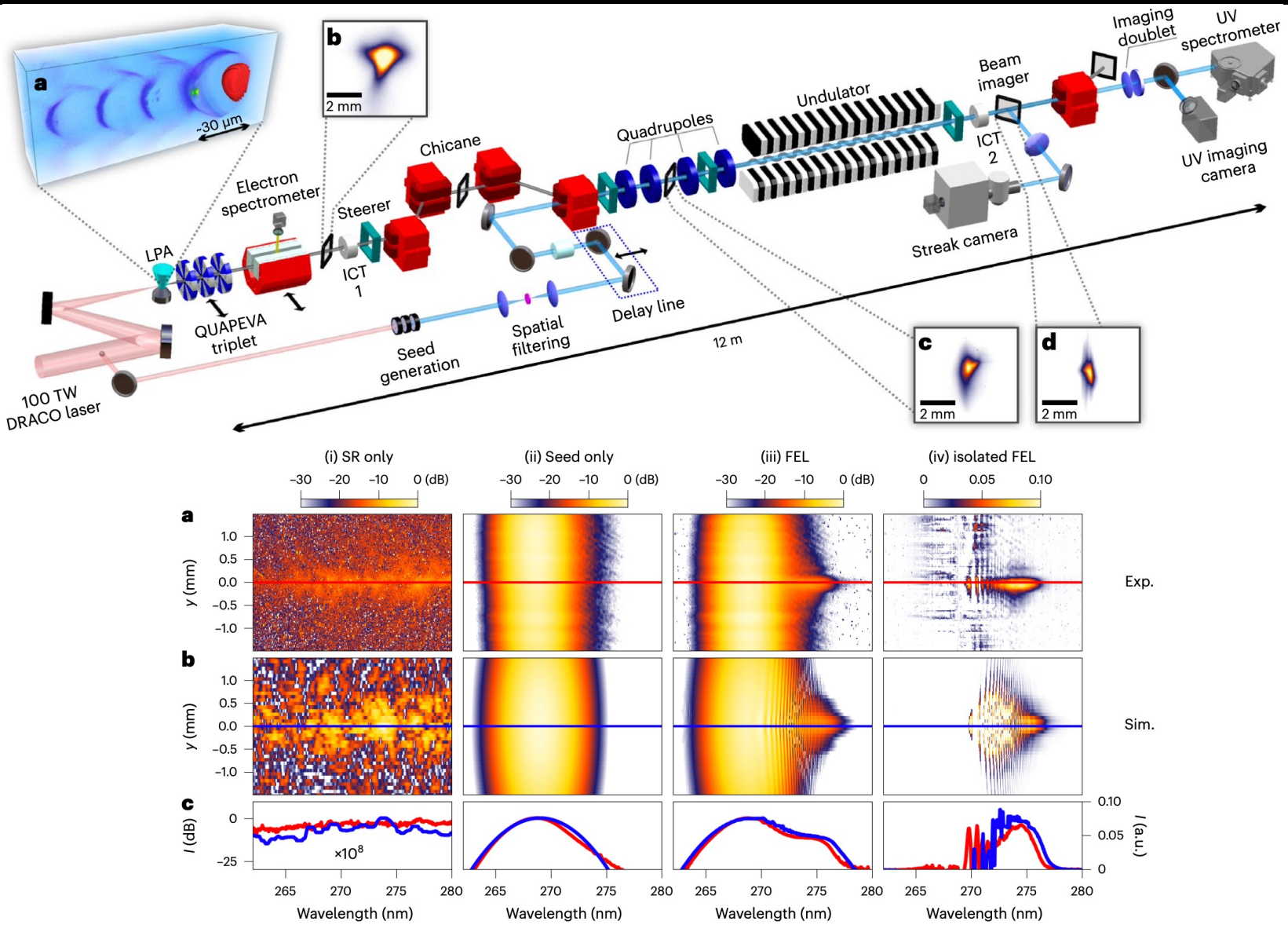

M Labat *et al*, Nature Photonics **17**, 150–156 (2023)

Conclusion

High-power lasers needed for plasma acceleration are already available as commercial products, and in **compact setups** suitable for space-limited environments **in industrial or hospital settings**.

This is the **perfect time** to identify key areas where compact laser-plasma accelerators can have a **deep societal impact.**

Congratulations for joining at this perfect time!